



AGN population studies with gamma-rays

Edivaldo Moura Santos
Instituto de Física - USP

Overview

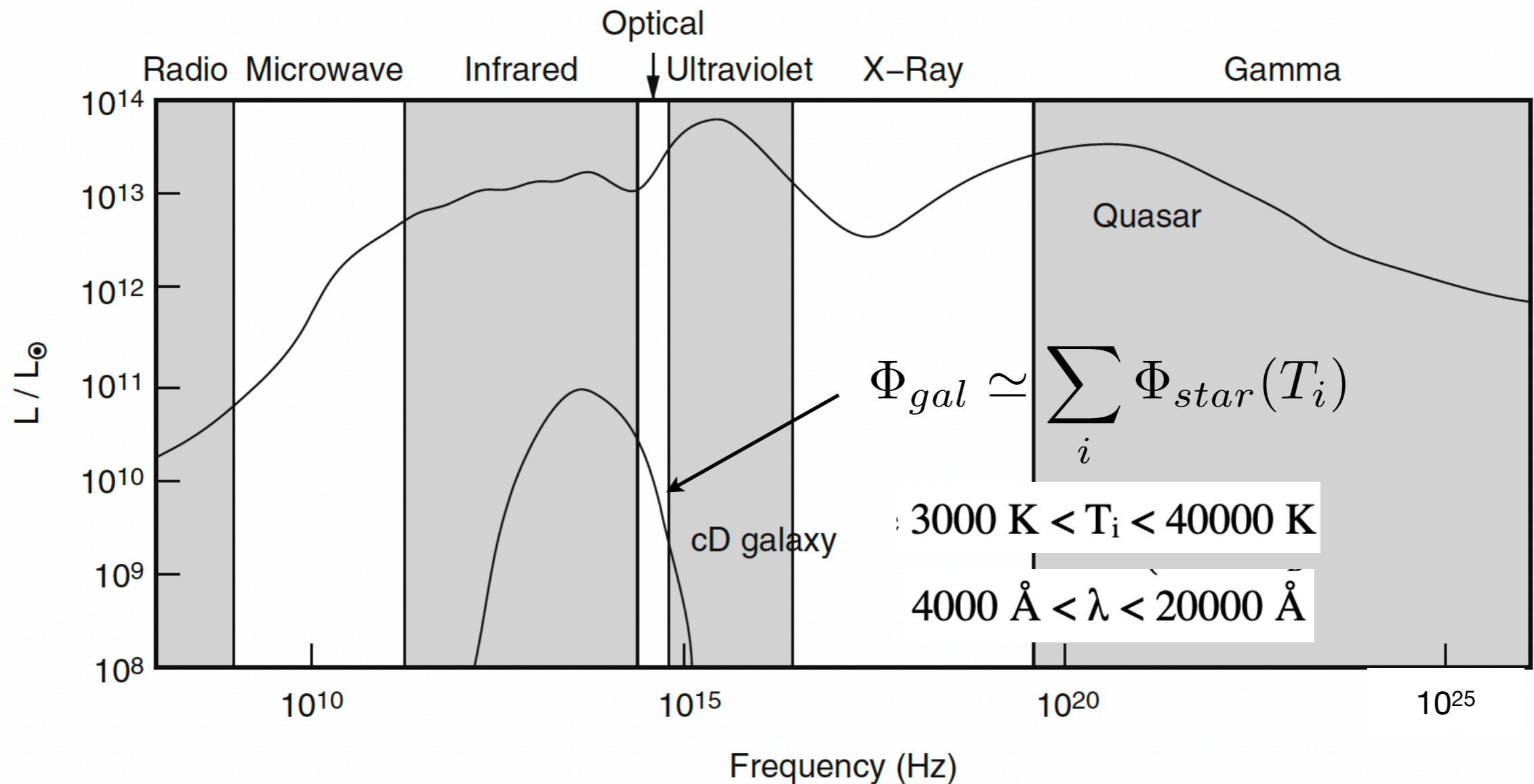
- AGN versus normal galaxies
- Blazar emission at the GeV scale and status of the GLF
- Blazar emission at the TeV energy scale
- Accounting for absorption effects in the GeV-TeV
- What about the PeV scale?
- CTA extragalactic survey
- Summary

A few questions

- How do AGNs are distributed in redshift and luminosity (GLF)?
- How do AGNs properties evolve with redshift
- What is their contribution to the isotropic gamma-ray background (IGRB)?
- What is the best (unbiased) way to probe parameters of the AGN GLF?
- What do we know so far about the GLF?
- What is likely to be the extragalactic sky seem by CTA in the near future?
- How well will CTA determine parameters of blazar GLF?
- Can we go beyond phenomenological GLF parameterizations?

AGN x normal galaxies

- Some galaxies present a much broader spectrum, with significant emission essentially in the whole electromagnetic spectrum, from radio all the way to X-rays and even γ -rays.

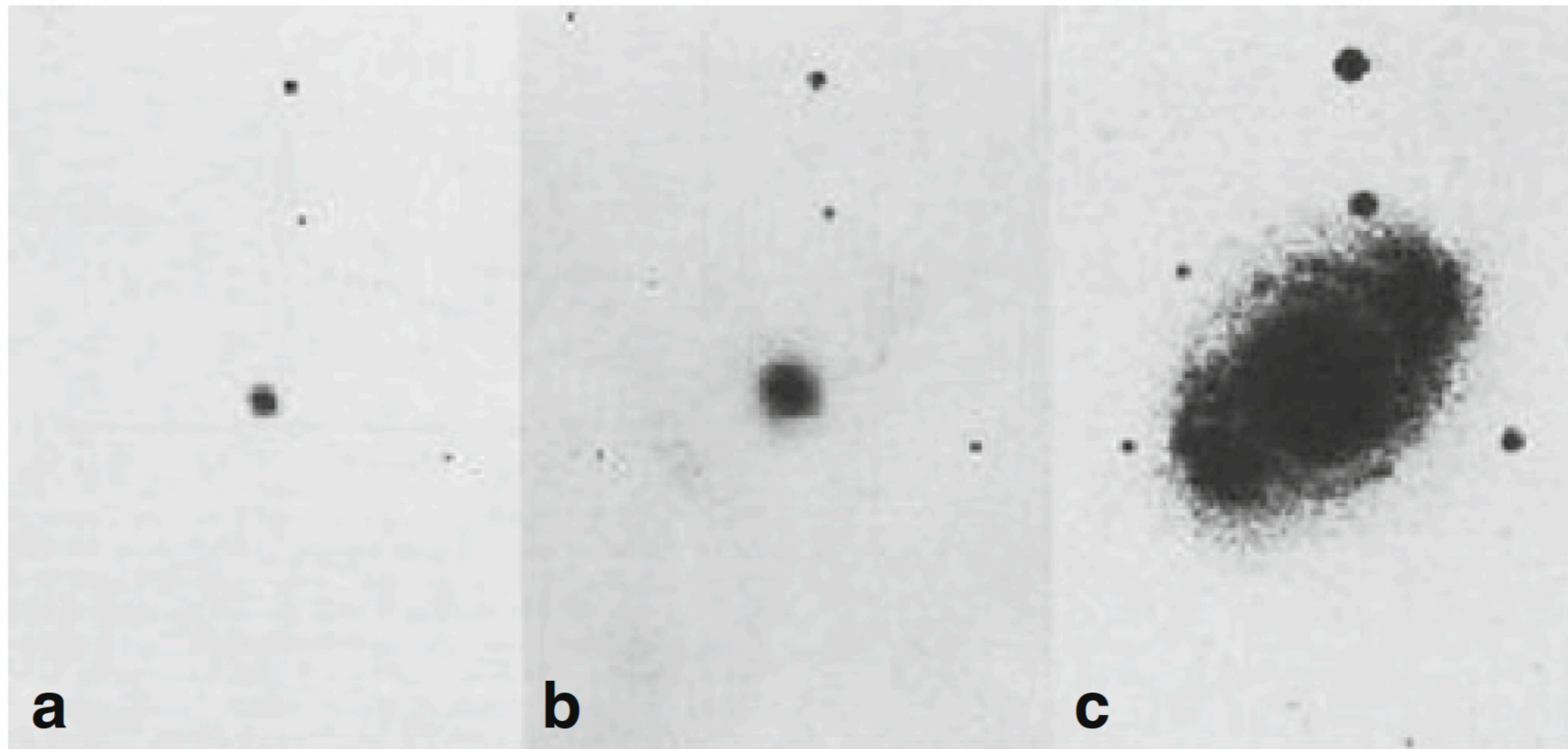


- Their luminosity is much higher than normal galaxies: $L_{AGN} \gtrsim 10^3 L_{gal}$
- From the shape of the spectrum, we can see that the emission process is mostly non-thermal.

Active Galactic Nuclei (AGN)

- We nowadays know that the emission in these galaxies comes from a very small region (<1 pc) at the center of the galaxy called the active galactic nucleus (AGN).

Seyfert galaxy NGC4151



Exposure time



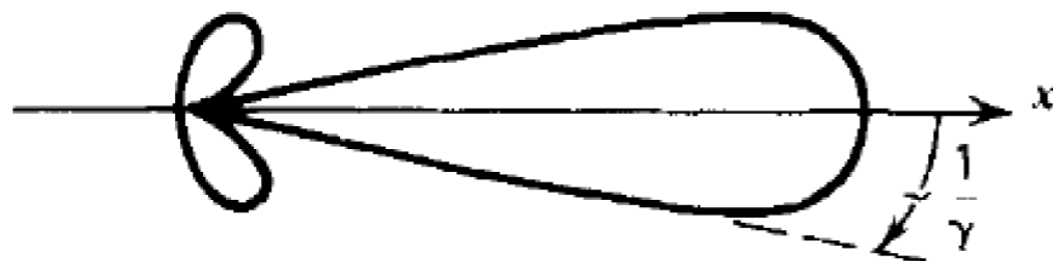
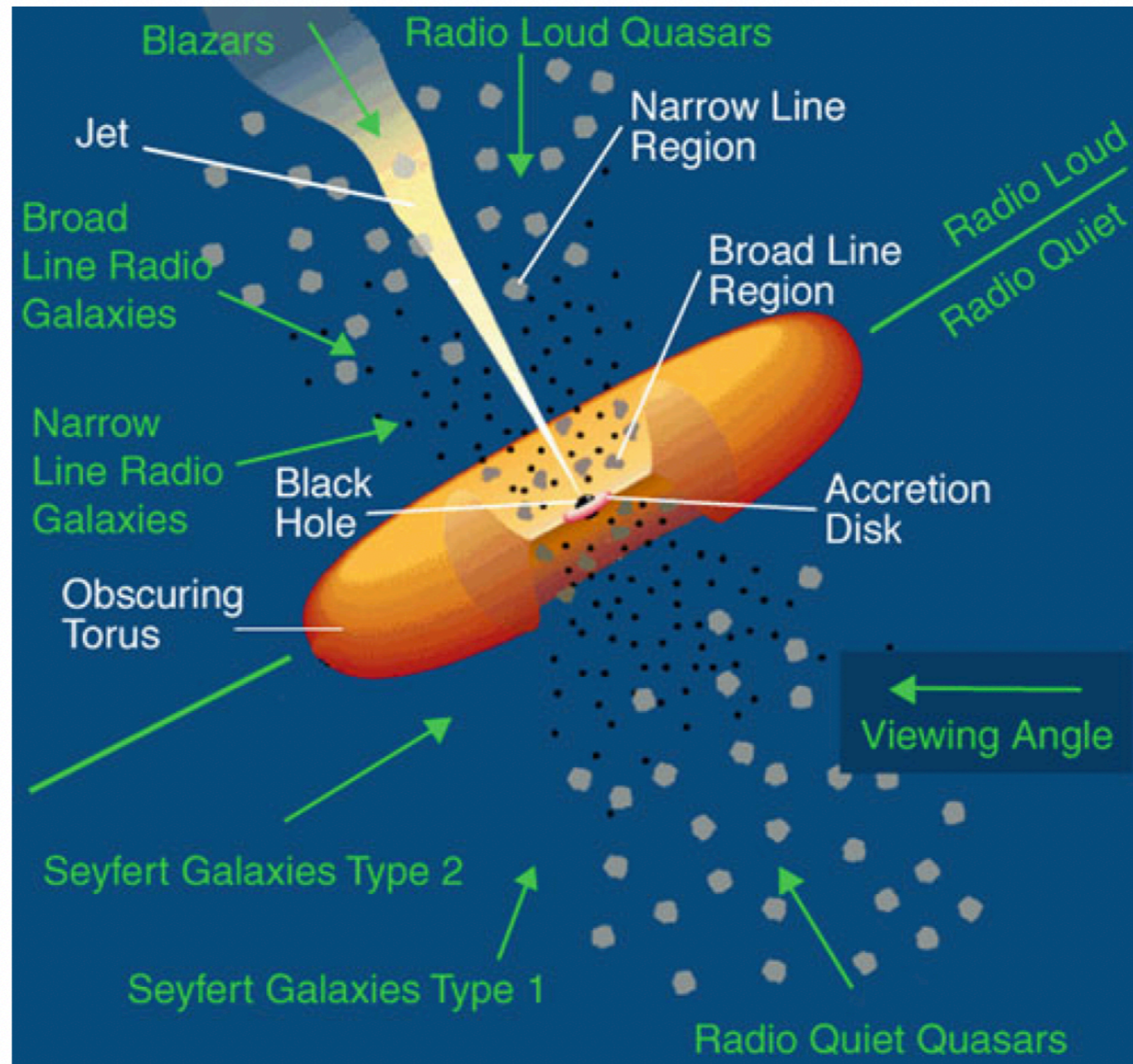
- At low exposure times, only the central part of the galaxy is detectable. Only at high exposure times, the rest of the galaxy becomes visible (emission is dominated by the nucleus!)

Summarized properties

Table 5.1 Overview of the classification of active galactic nuclei

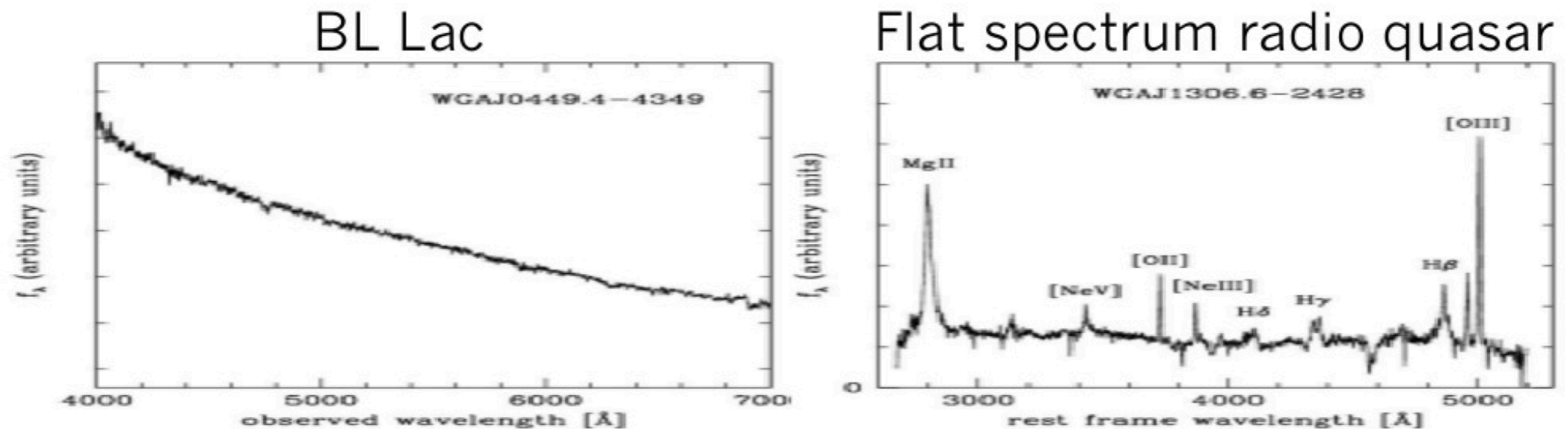
	Normal galaxy	Radio galaxy	Seyfert galaxy	Quasar	Blazar
Example	Milky Way	M87, Cygnus A	NGC 4151	3C273	BL Lac, 3C279
Galaxy type	Spiral	Elliptical, Irregular	Spiral	Irregular	Elliptical?
L_{AGN}/L_{\odot}	$< 10^4$	10^6-10^8	10^8-10^{11}	$10^{11}-10^{14}$	$10^{11}-10^{14}$
M_{BH}/M_{\odot}	4×10^6	3×10^9	10^6-10^9	10^6-10^9	10^6-10^9
Radio emission	Weak	Core, jets, lobes	Only $\approx 5\%$ radio-loud	Only $\approx 5\%$ radio-loud	Strong, Short-time variable
X-ray emission	Weak	Strong	Strong	Strong	Strong
Gamma emission	Weak	Weak	Medium	Strong	Strong

AGN unified model



$$I_{lab} = \frac{1}{[\gamma(1 - \beta \cos \phi)]^3} I_{RF}$$

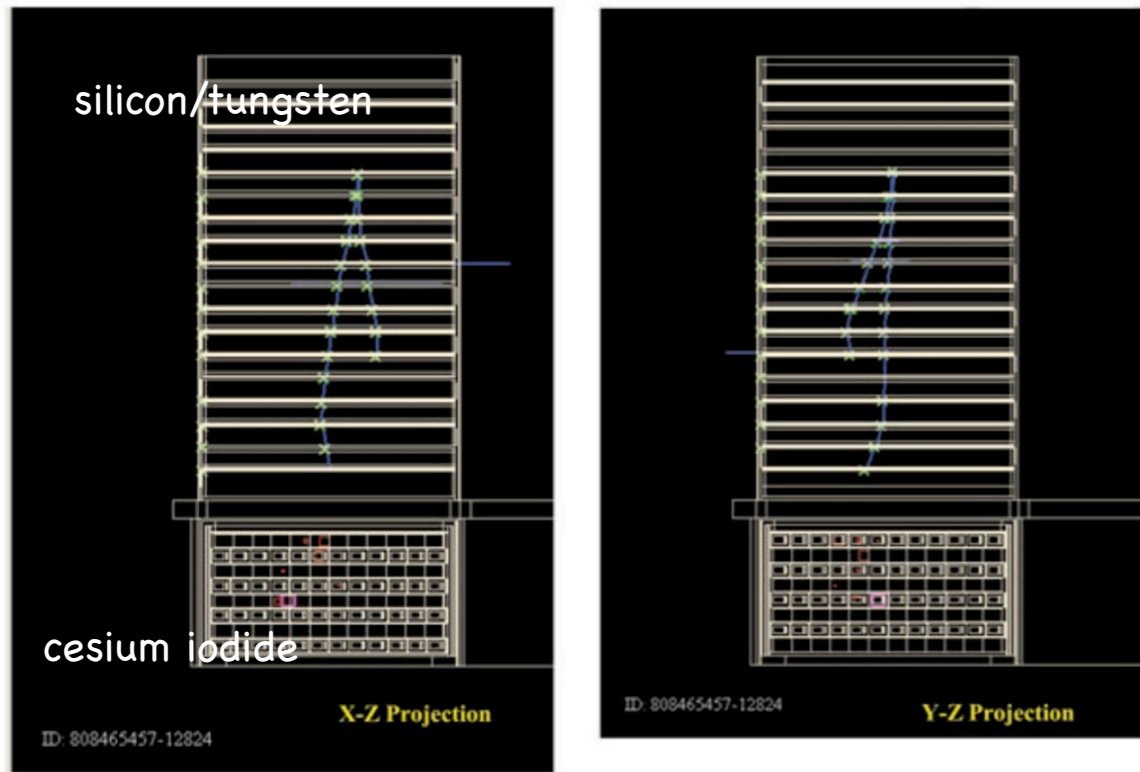
BL Lac and FSRQ in the optical



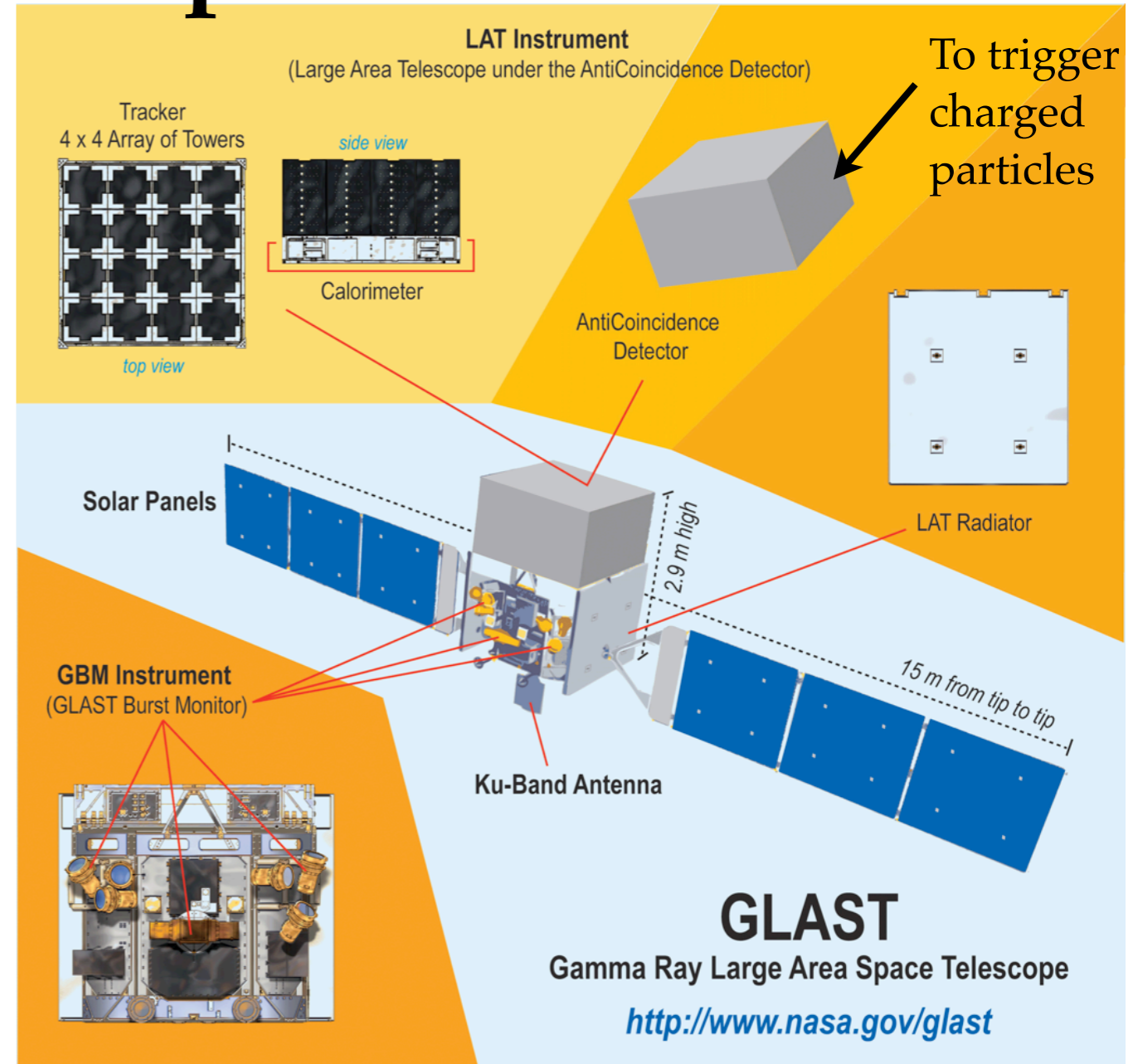
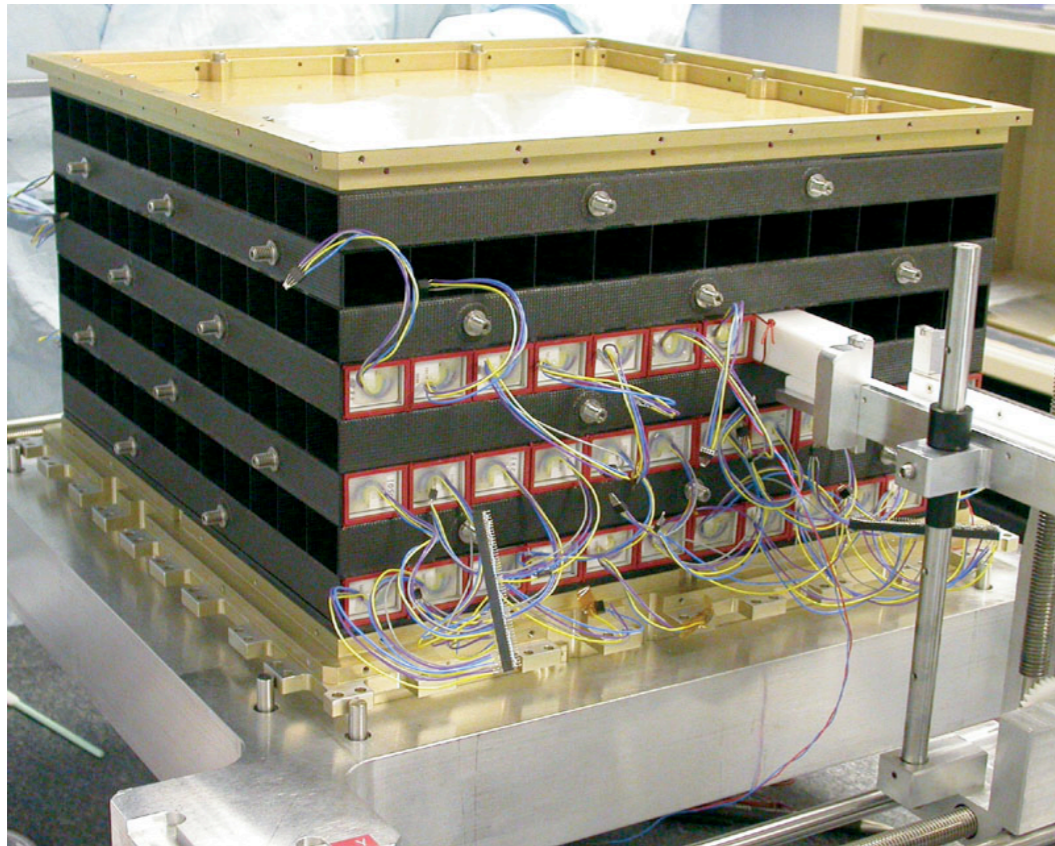
- Blazars have their jets pointed close to the line of sight.
- Most common extragalactic sources emitting gamma-rays.
- Highly variable emission.
- Lack of emission/absorption optical lines for BL Lac means redshifts are hard to determine ($\sim 50\%$ of Fermi's BL Lac lack z).
- Data seems to indicate a positive cosmic evolution for FSRQ up to some cutoff redshift.
- Due to the lack of redshift determinations, evolution of BL Lacs is unclear.

Blazar emission in the GeV scale and the status of the GLF

The Fermi telescope detectors



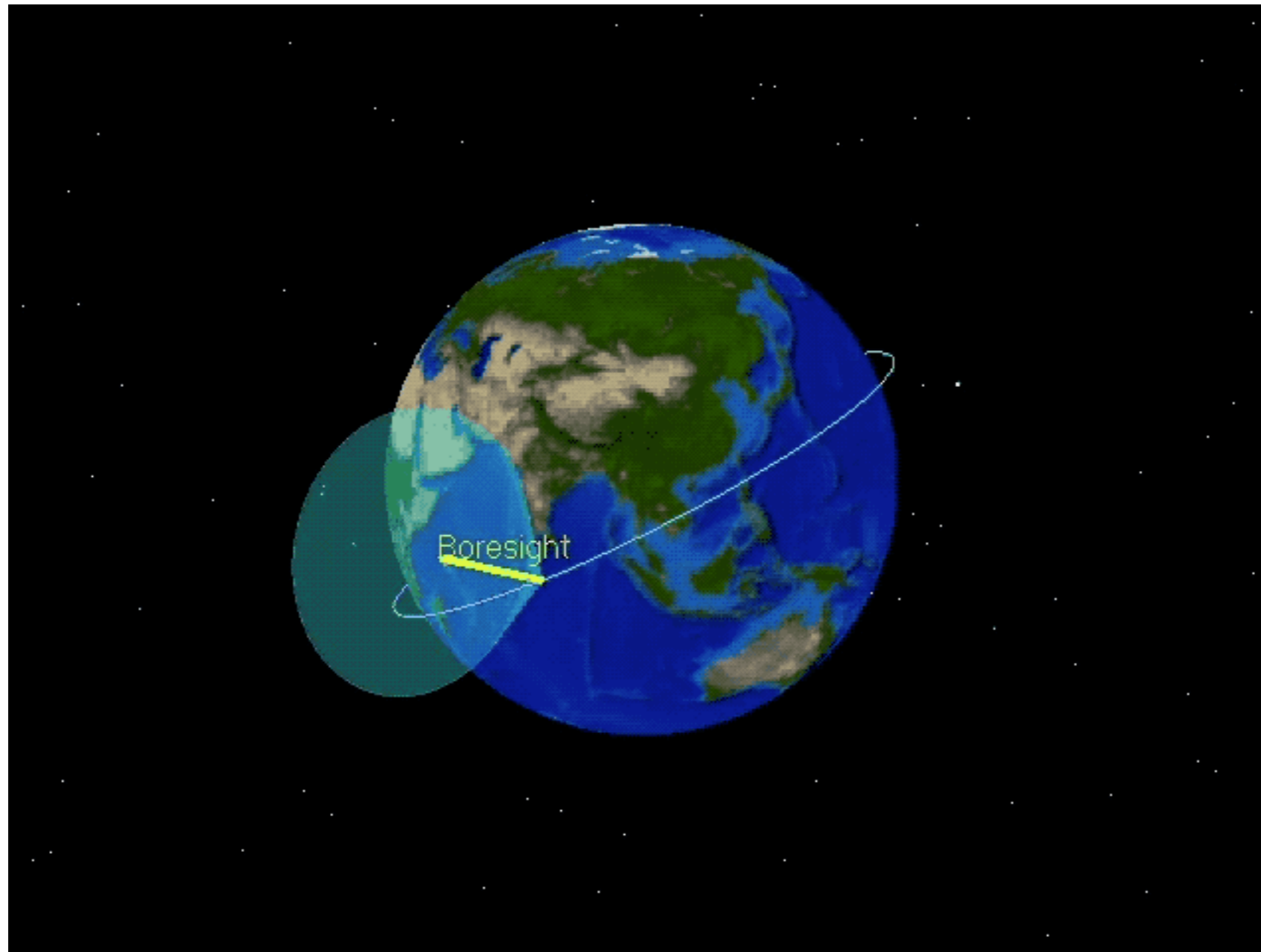
Candidate Gamma-ray Event in 1st LAT Flight Tower



$$20 \text{ MeV} < E_{\gamma} < 300 \text{ GeV}$$

- Photon direction reconstruction through e^+ / e^- tracks
- Calorimetric energy measurement

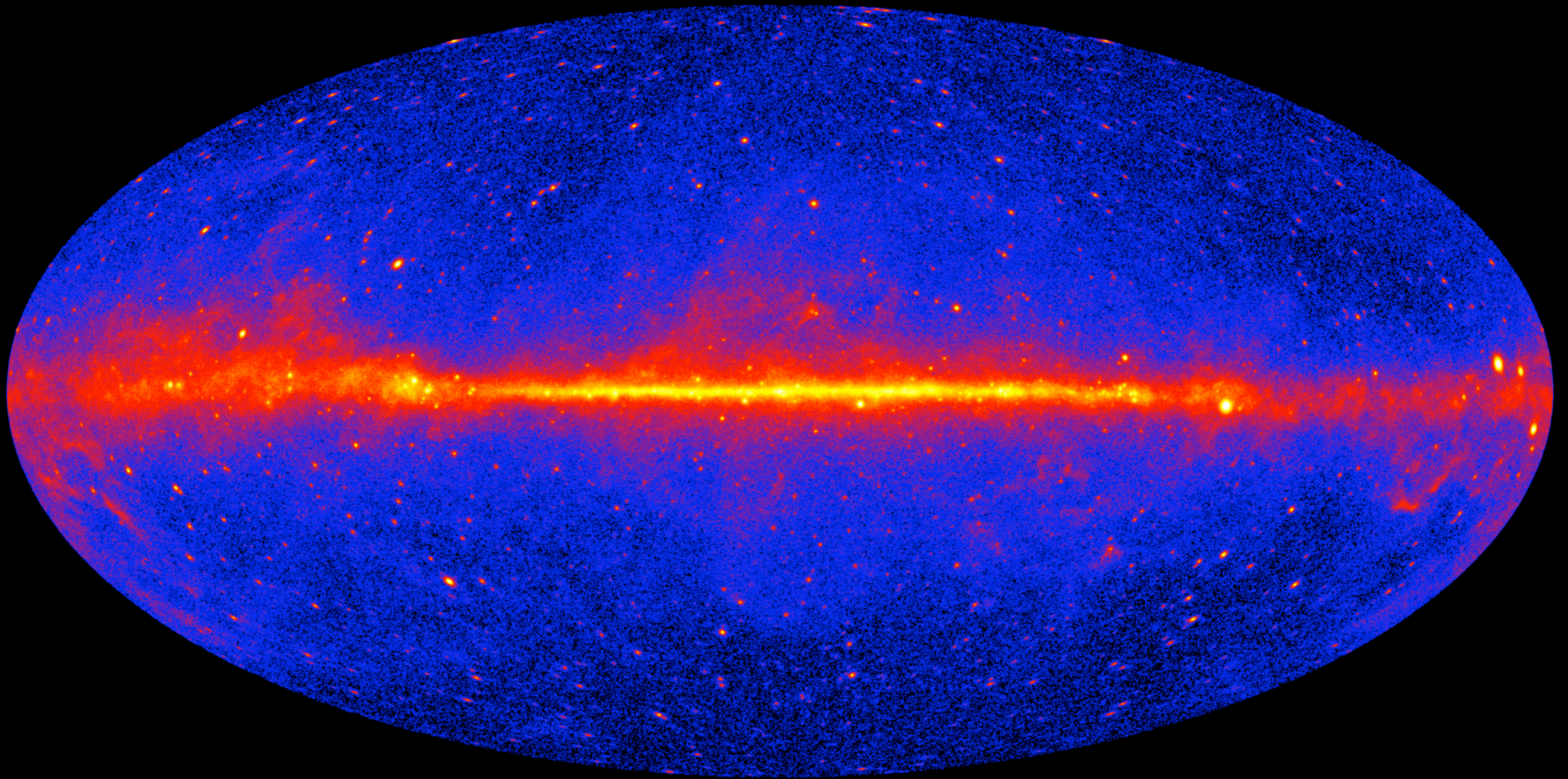
Fermi sky scan strategy



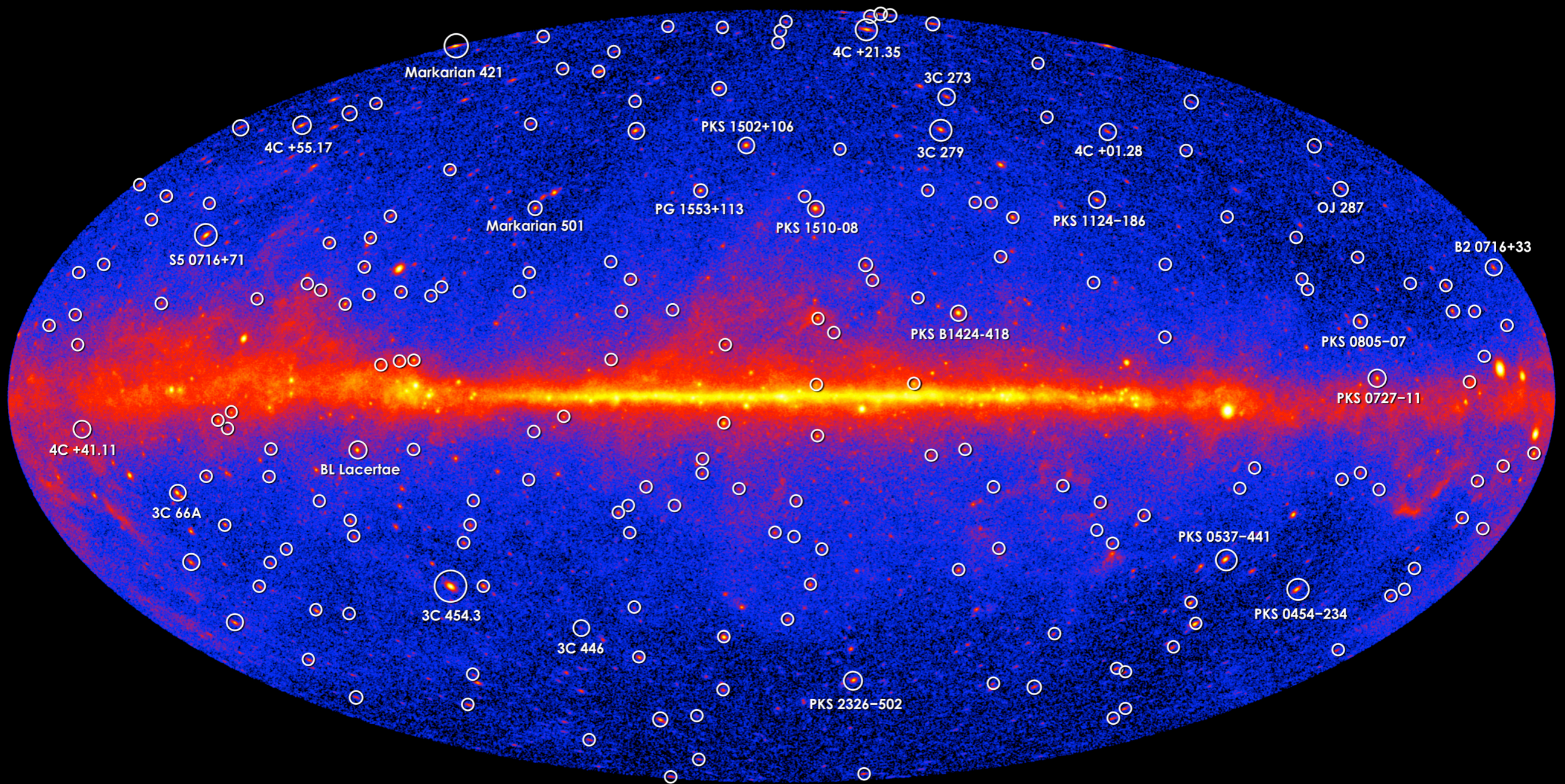
Fermi scans across one hemisphere of the sky for one orbit, then rocks to the other hemisphere to scan for the second orbit.

Excellent scan strategy for AGN population studies (highly uniform sky coverage)

Fermi-LAT all sky map



Blazars detected by Fermi



Modeling the γ -ray AGN luminosity function (GLF)

- **Modification over the so called pure luminosity evolution GLF to better describe first year LAT data (LDDE):**

$$\Phi(L_\gamma, z, \Gamma) = \underbrace{\Phi(L_\gamma, z = 0, \Gamma)}_{\text{GLF @ } z=0} \times \underbrace{e(z, L_\gamma)}_{\text{redshift and luminosity evolution}}$$

GLF @ $z=0$

redshift and luminosity evolution

- **Local behavior:**

$$\Phi(L_\gamma, z = 0, \Gamma) = \frac{A}{\ln(10)L_\gamma} \left[\left(\frac{L_\gamma}{L_*} \right)^{\gamma_1} + \left(\frac{L_\gamma}{L_*} \right)^{\gamma_2} \right]^{-1} e^{-0.5[\Gamma - \mu(L_\gamma)]^2 / \sigma^2}$$

$$\mu(L_\gamma) = \mu^* + \beta[\log(L_\gamma) - 46]$$

- **Luminosity dependent redshift evolution:**

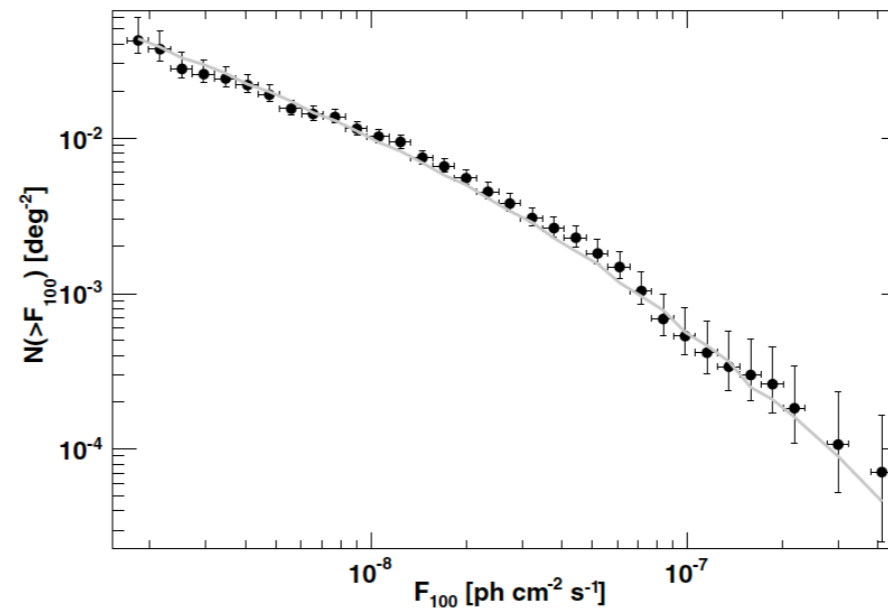
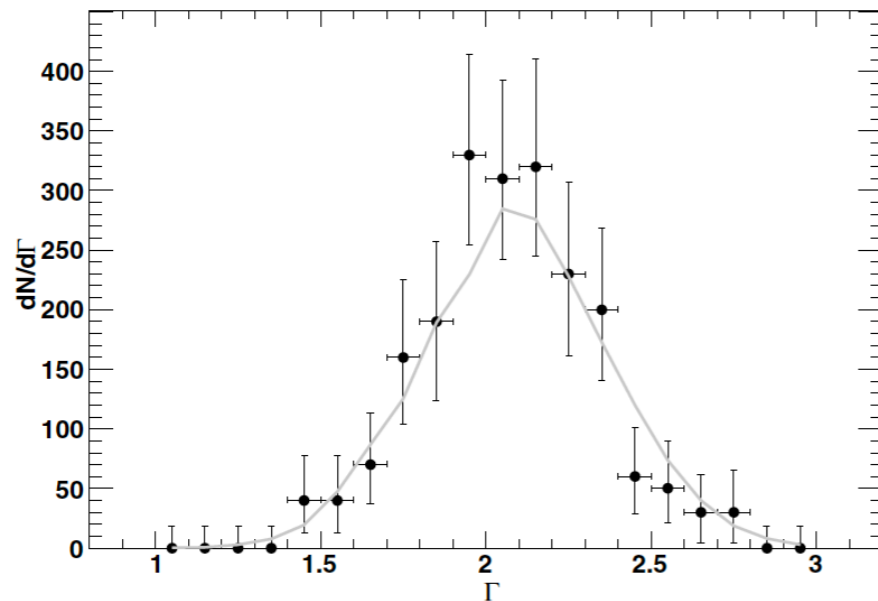
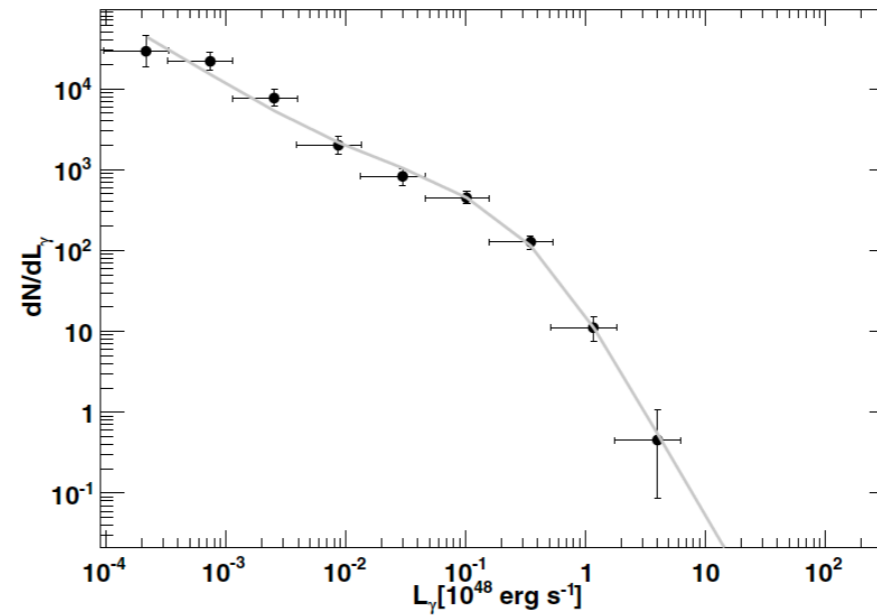
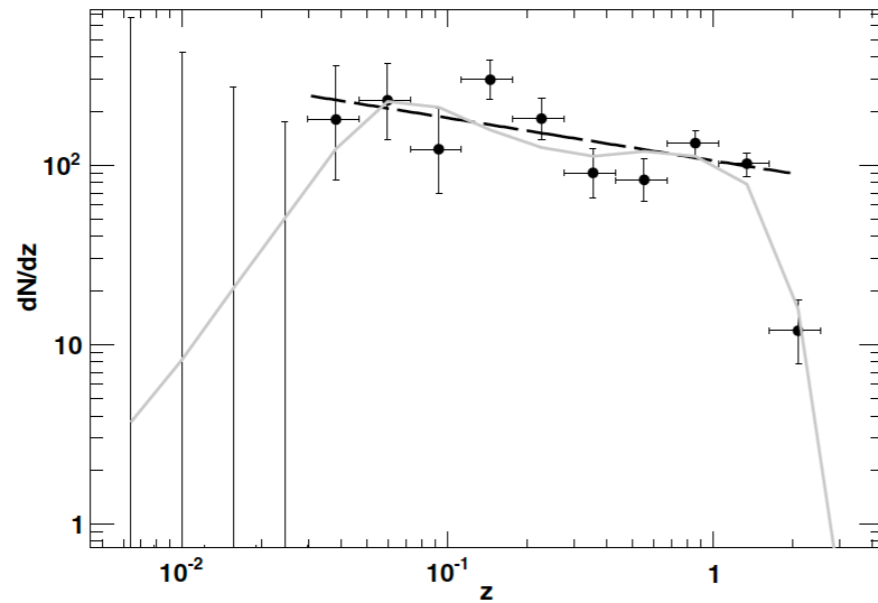
$$e(z, L_\gamma) = \left[\left(\frac{1+z}{1+z_c(L_\gamma)} \right)^{-p_1(L_\gamma)} + \left(\frac{1+z}{1+z_c(L_\gamma)} \right)^{-p_2(L_\gamma)} \right]^{-1}$$

$$p_1(L_\gamma) = p_1^* + \tau(\log(L_\gamma) - 46)$$

$$p_2(L_\gamma) = p_2^* + \delta(\log(L_\gamma) - 46)$$

$$z_c(L_\gamma) = z_c^* (L_\gamma / 10^{48})^\alpha$$

1FGL source counts

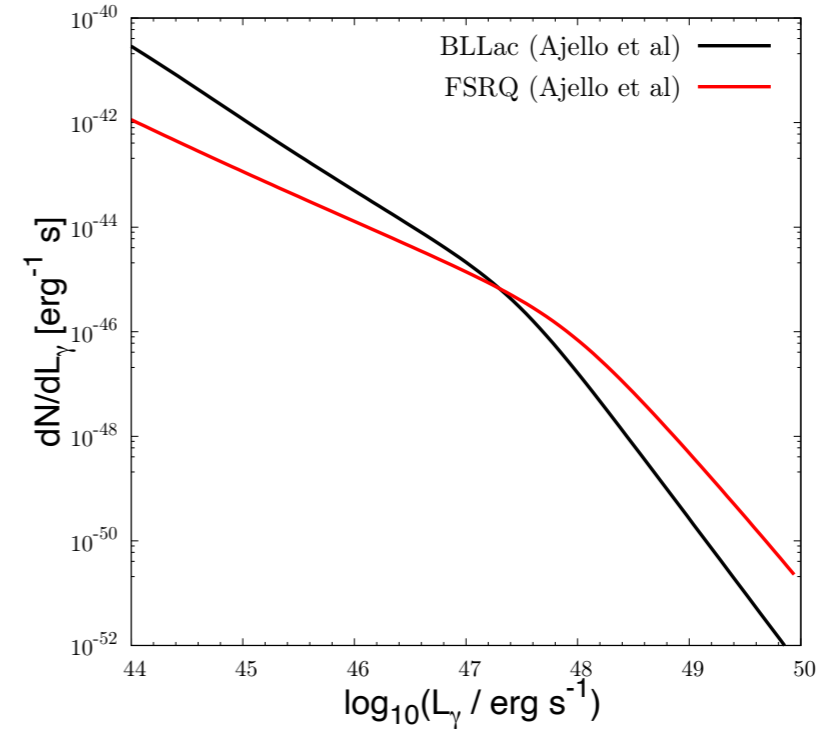
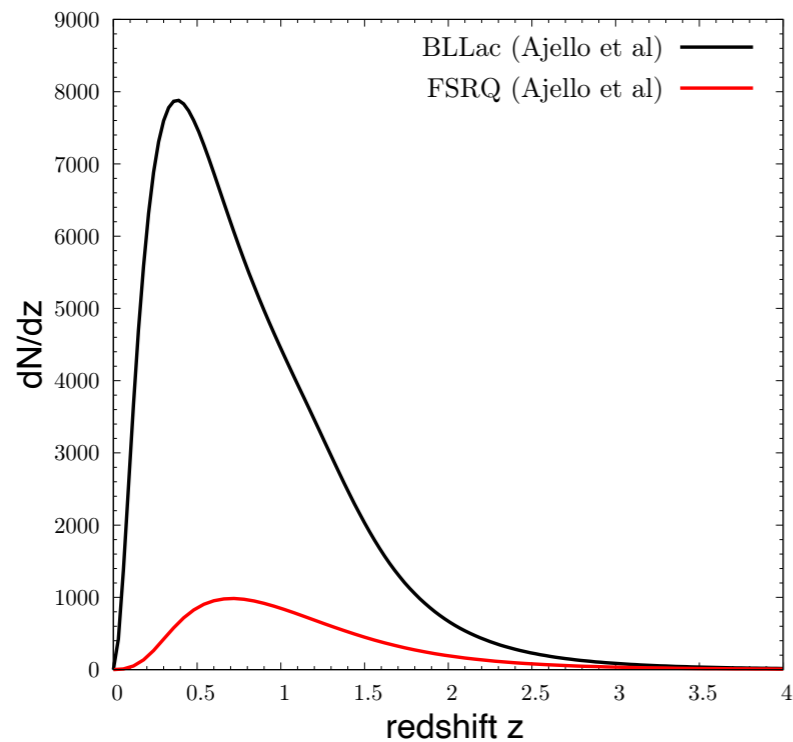


211 BL Lac objects detected by Fermi with $TS > 50$ and $|b| > 15$ deg.

Redshifts or lower/upper limits estimated using photometry/spectroscopy of intervening material or host galaxy

Monte Carlo simulations used to determine and correct for the selection effects.

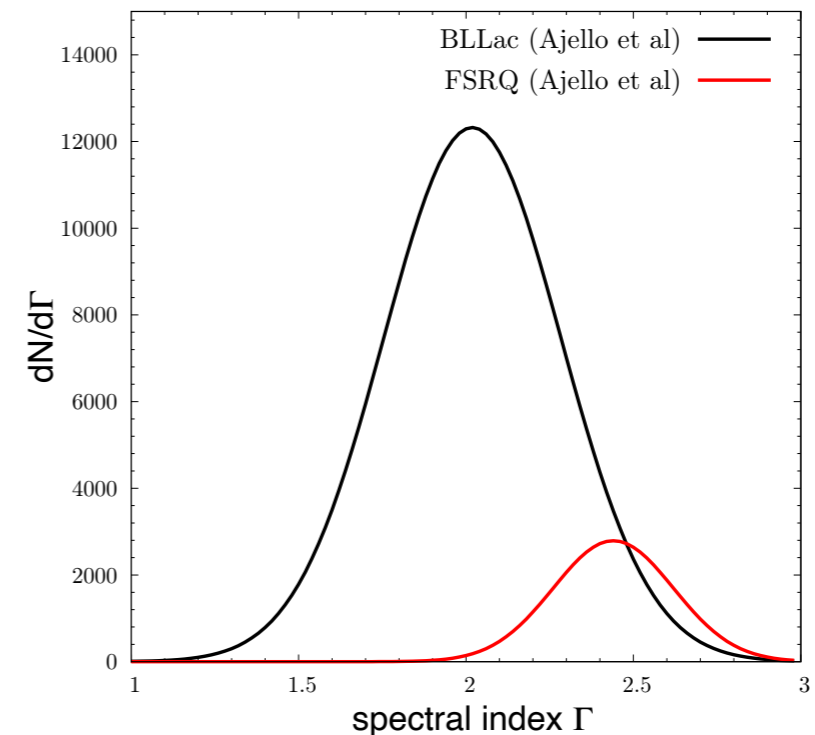
Best-fit GLF properties



According Fermi-LAT 1FGL (>10 GeV):

$$N_{\text{BLLac}} \sim 8000$$

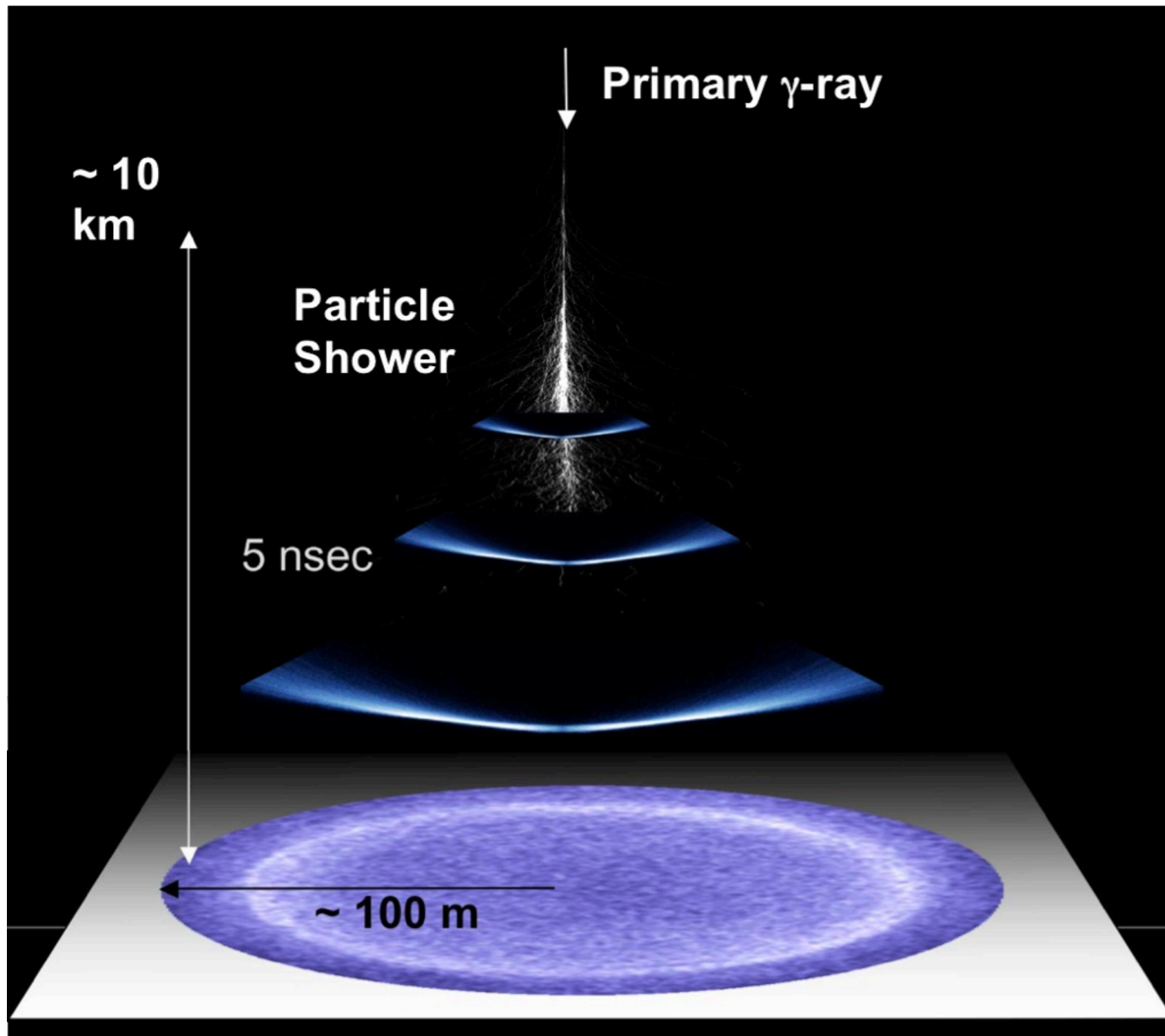
$$N_{\text{FSRQ}} \sim 1100$$



source	A [Gpc $^{-3}$]	γ_1	γ_2	L_* [erg/s]	p_1^*	p_2^*	τ	z_c^*	α	μ^*	β	σ
BL Lac	3.39	0.27	1.86	$10^{47.4472}$	2.24	-7.37	4.92	1.34	0.0453	2.10	0.0646	0.26
FSRQ	3.06	0.21	1.58	$10^{47.9243}$	7.35	-6.51	0.0	1.47	0.21	2.44	0.0	0.18

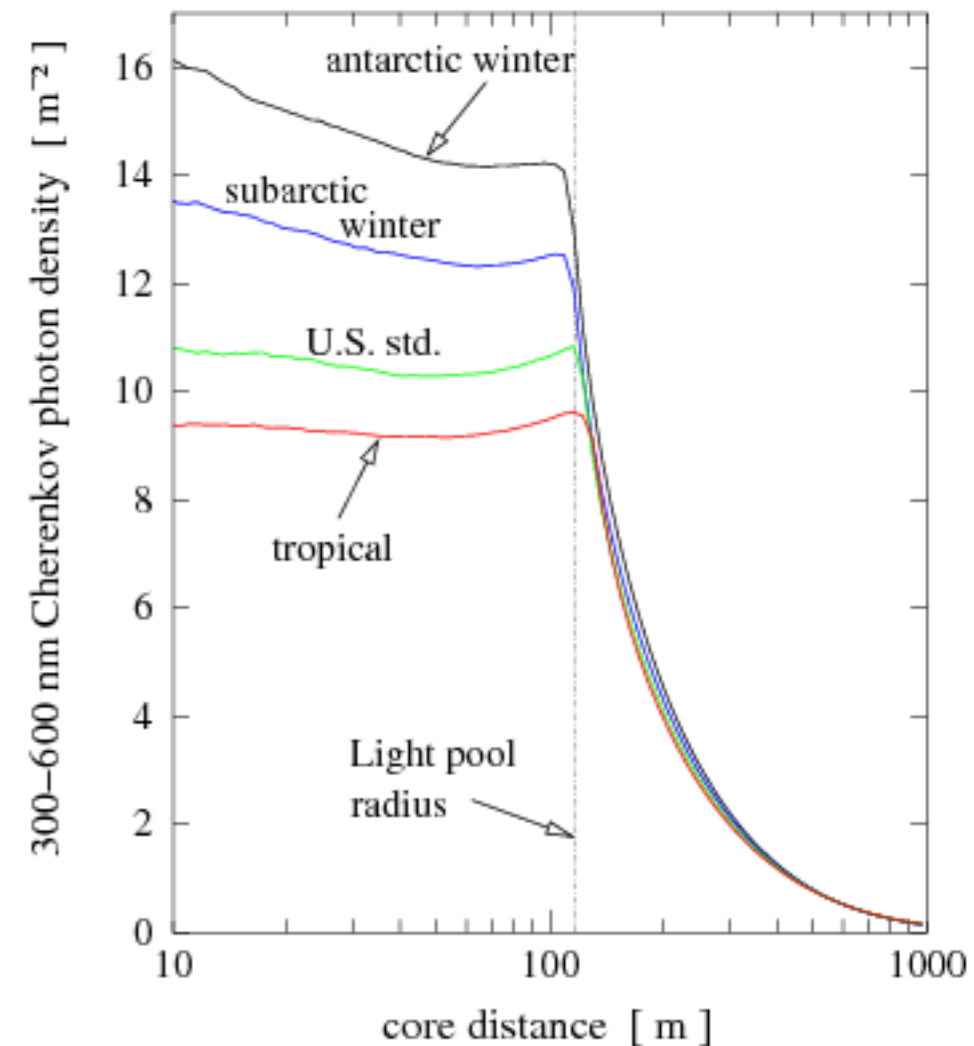
Blazar emission in the TeV scale

IACTs technique



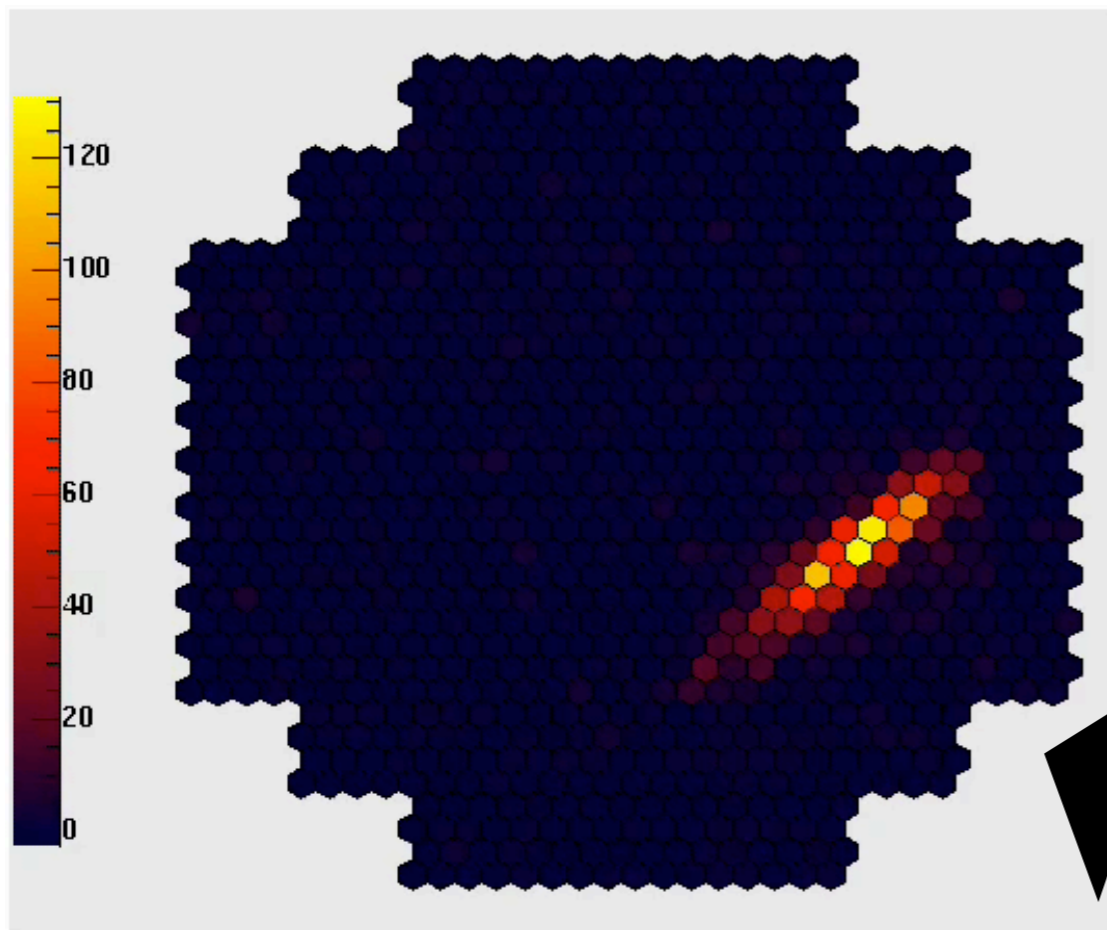
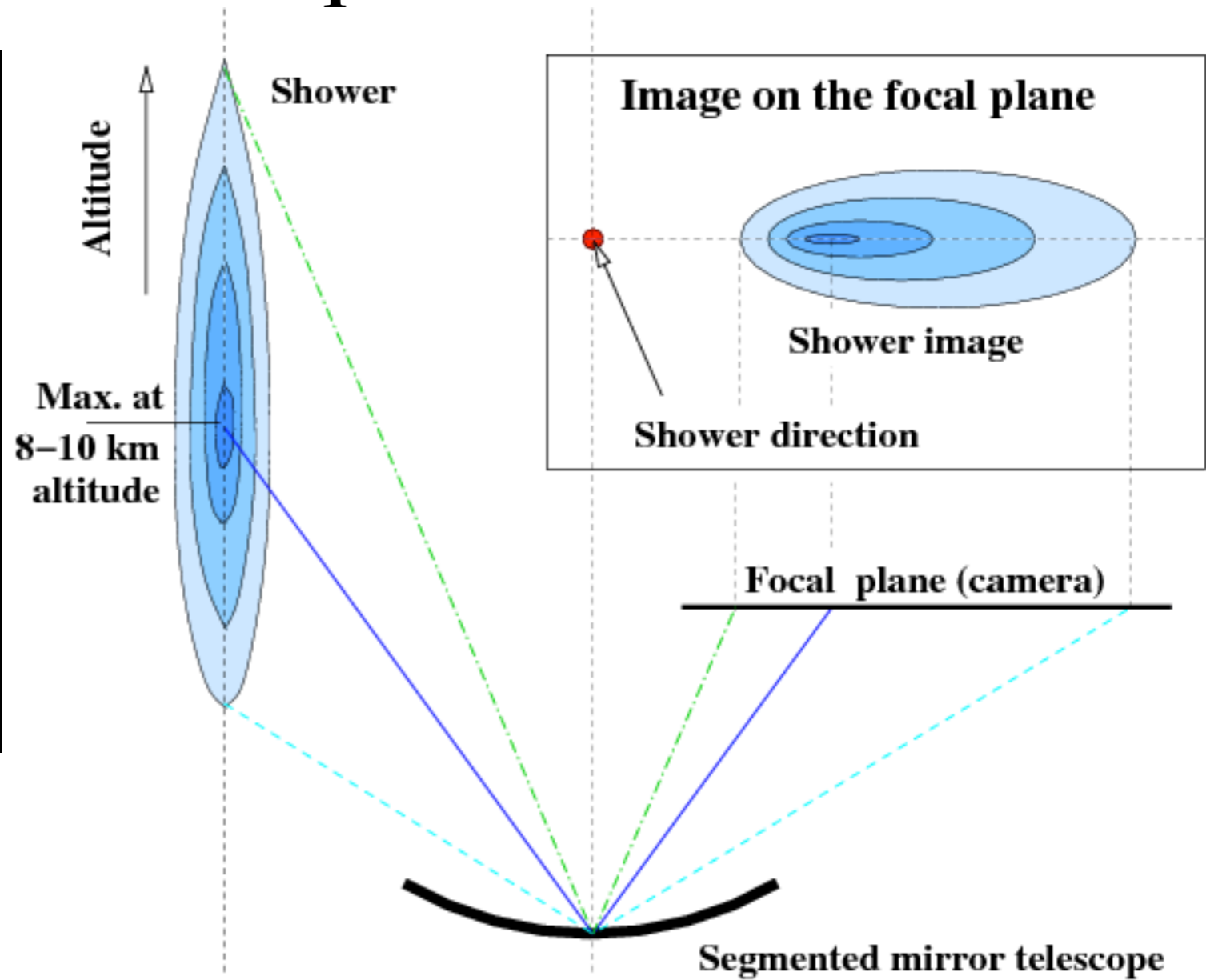
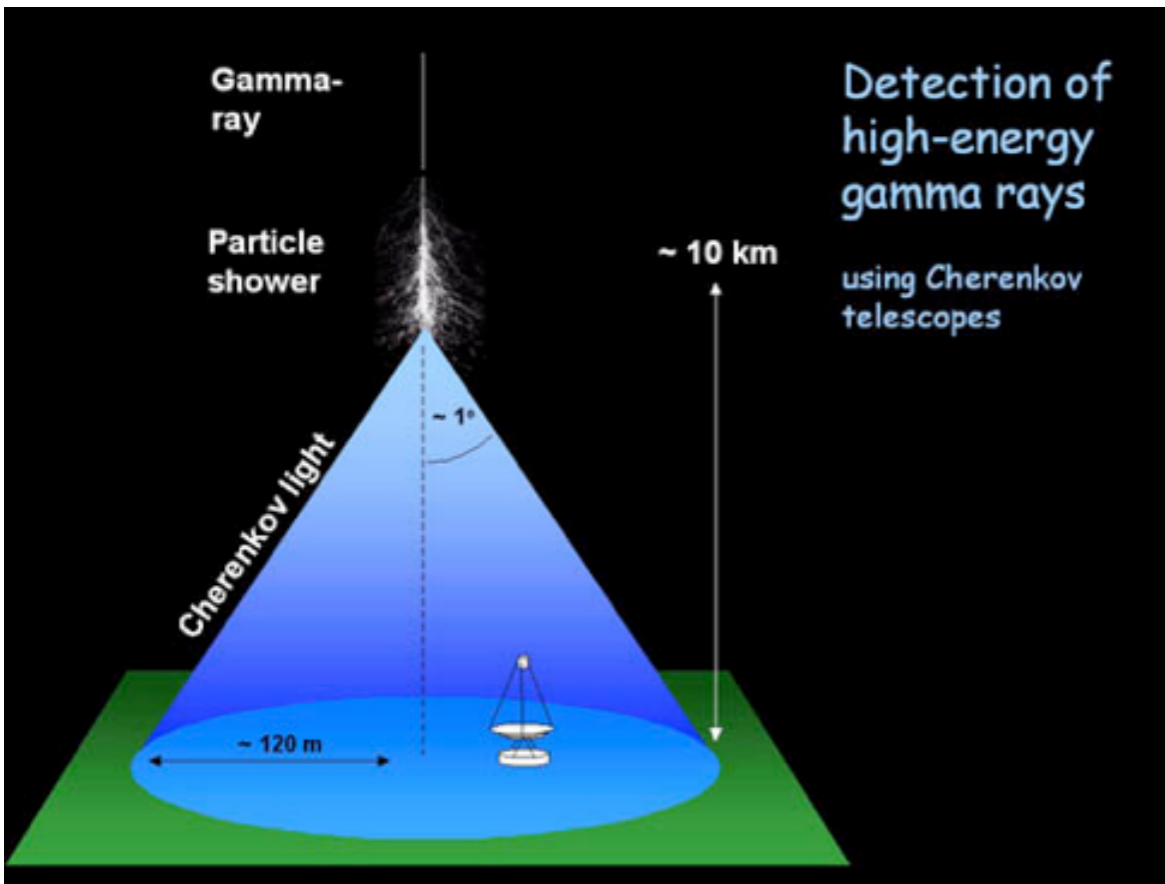
For a 1 TeV primary photon, about $100/\text{m}^2$ Cherenkov photons reach the ground

IACT: Imaging Air Cherenkov Telescope



effective detection area:
 $A_{\text{eff}} \sim \pi(120 \text{ m})^2 \sim 50000 \text{ m}^2$

IACTs technique

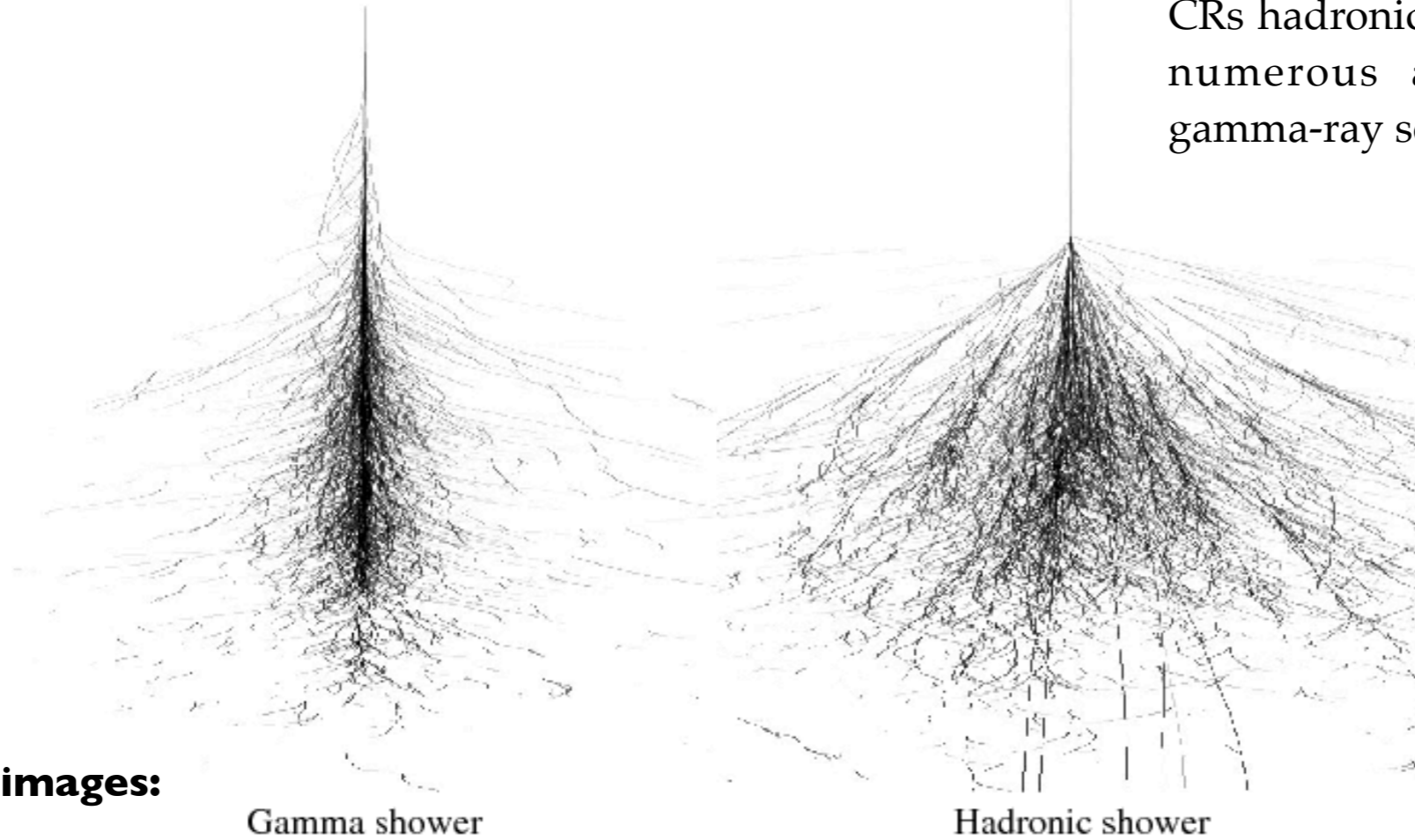


- ~ 5 ns light flash (blue-UV) reach the ground
- only in the last 40 years suitable detectors were developed to capture these signals

projection of shower-mirror intersection onto focal plane camera

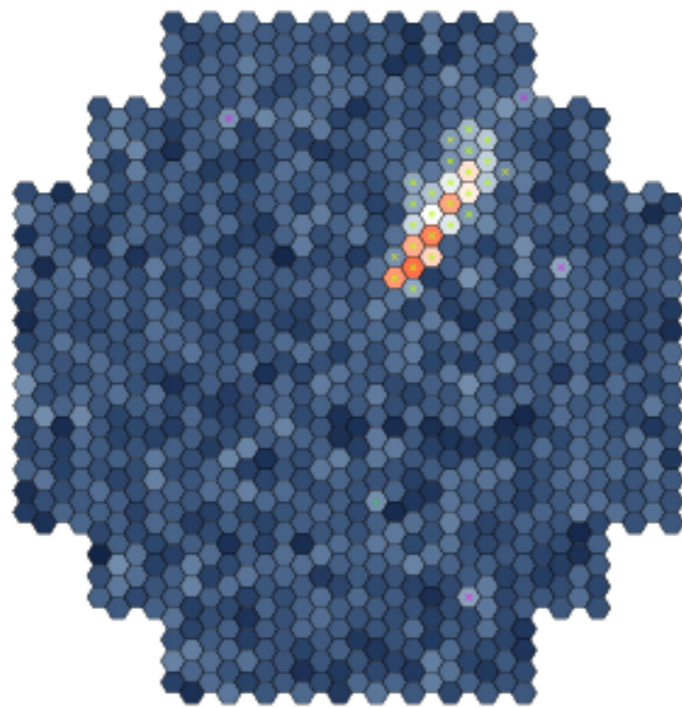
Background rejection: gamma versus hadron

CRs hadronic showers are 1000 times as numerous as the strongest steady gamma-ray source so far detected.



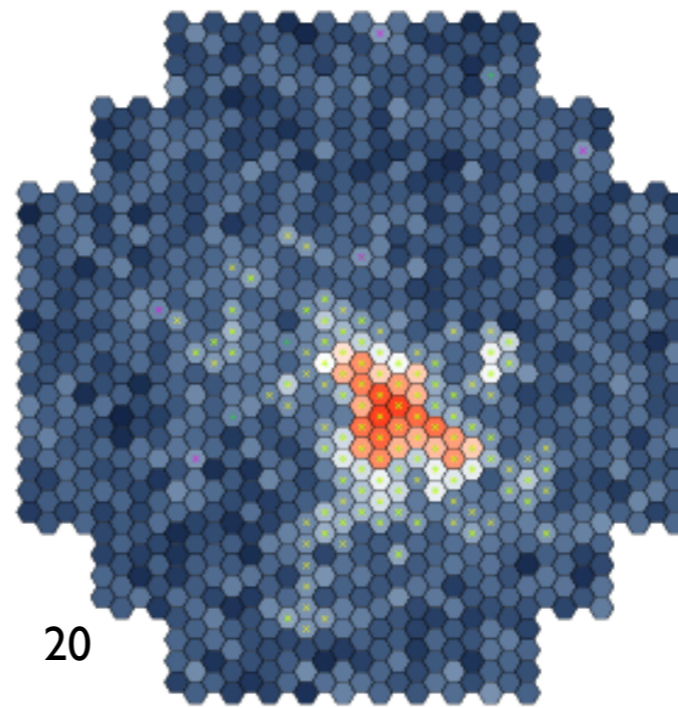
Gamma shower images:

- elongated
- aligned closely with the source position

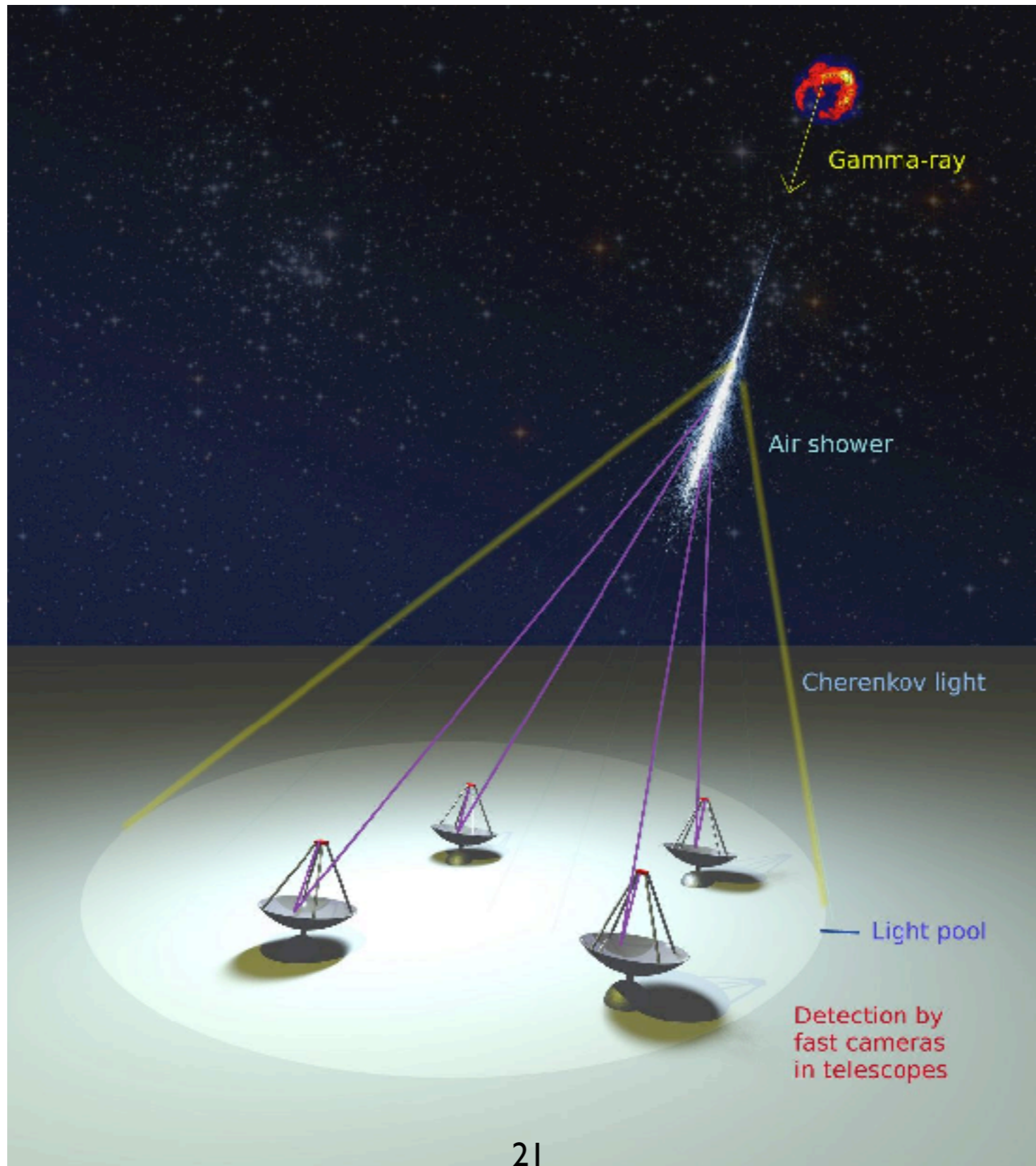


Hadronic shower images:

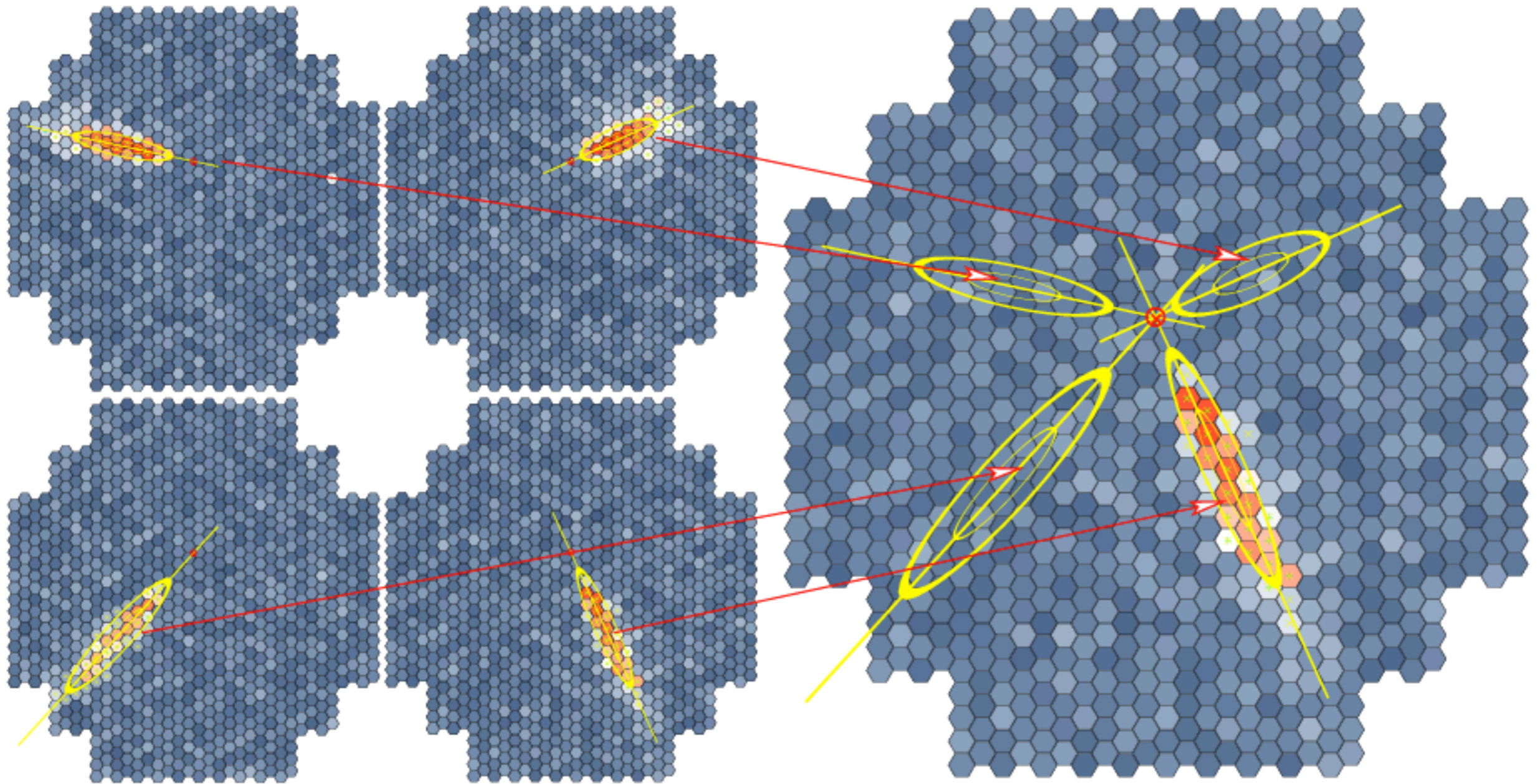
- larger fluctuation (isotropic incidence)
- wider (large pion emission angle in the cascade)
- not aligned with the source



The stereoscopic detection



The stereoscopic detection



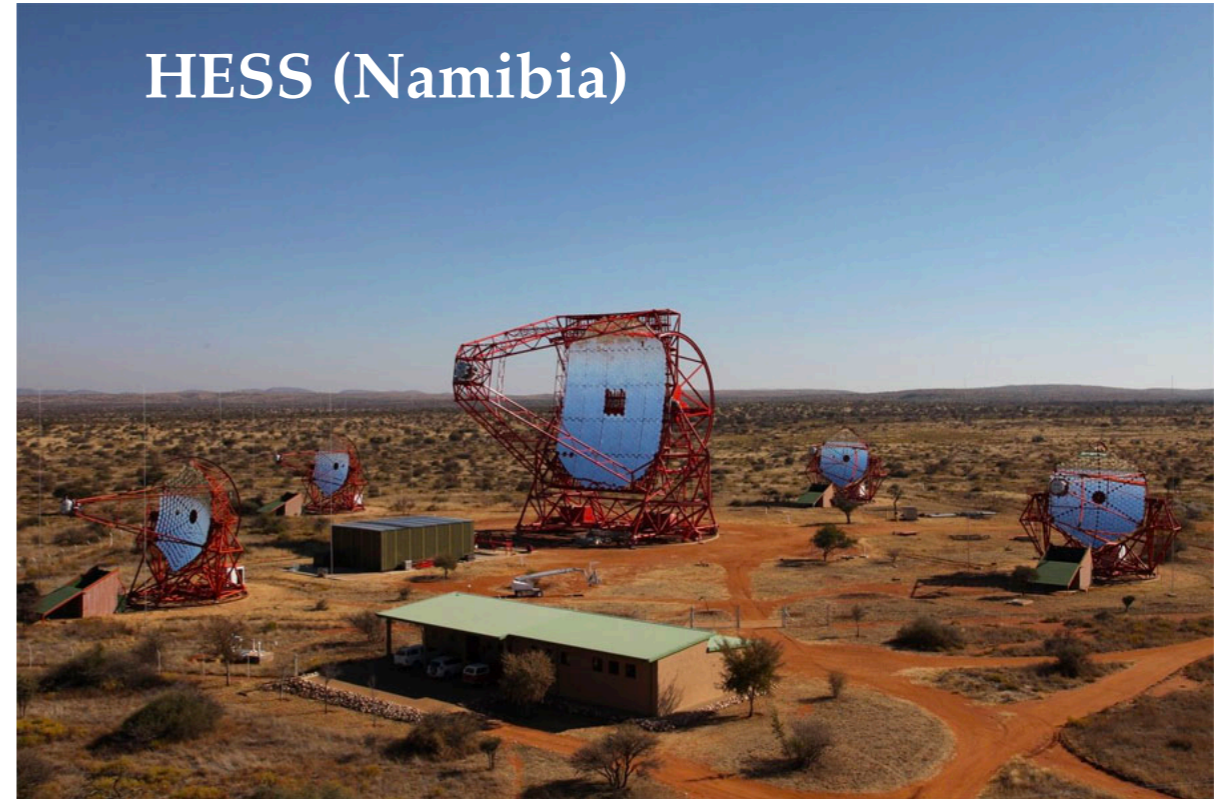
- breakthrough in the area: further background reduction due to cosmic rays
- improved angular resolution

Current generation of IACTs

MAGIC (Canary Islands)



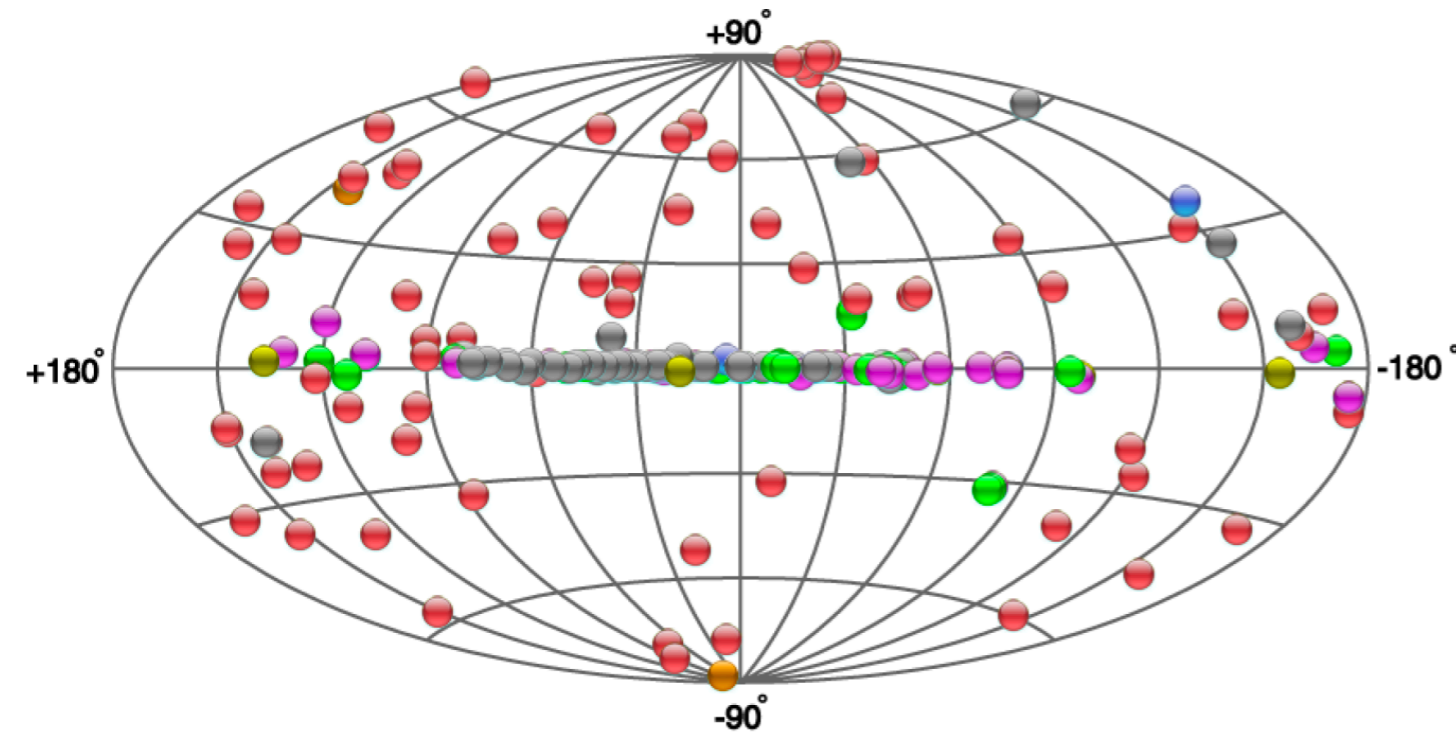
HESS (Namibia)



VERITAS (Arizona)

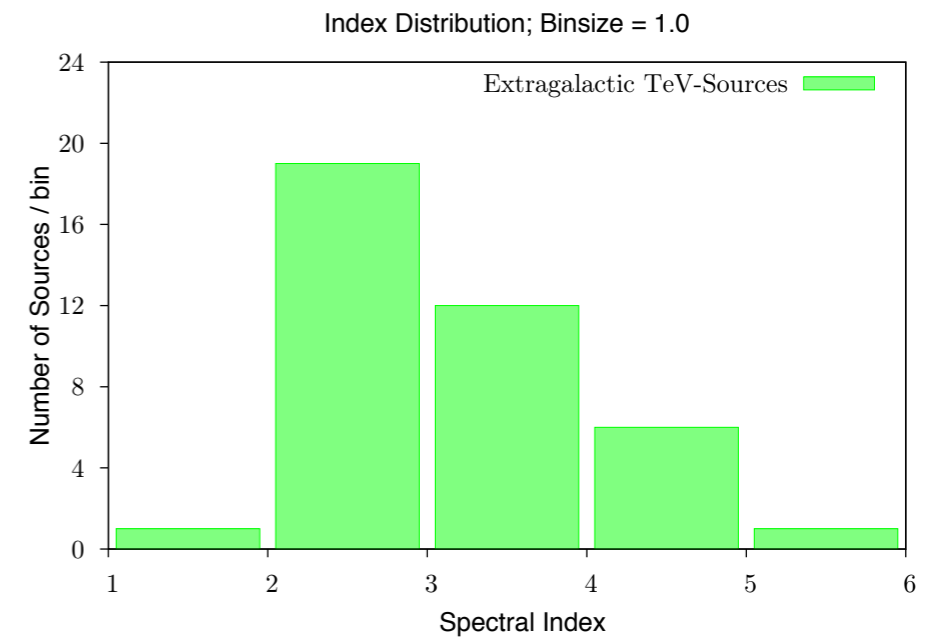
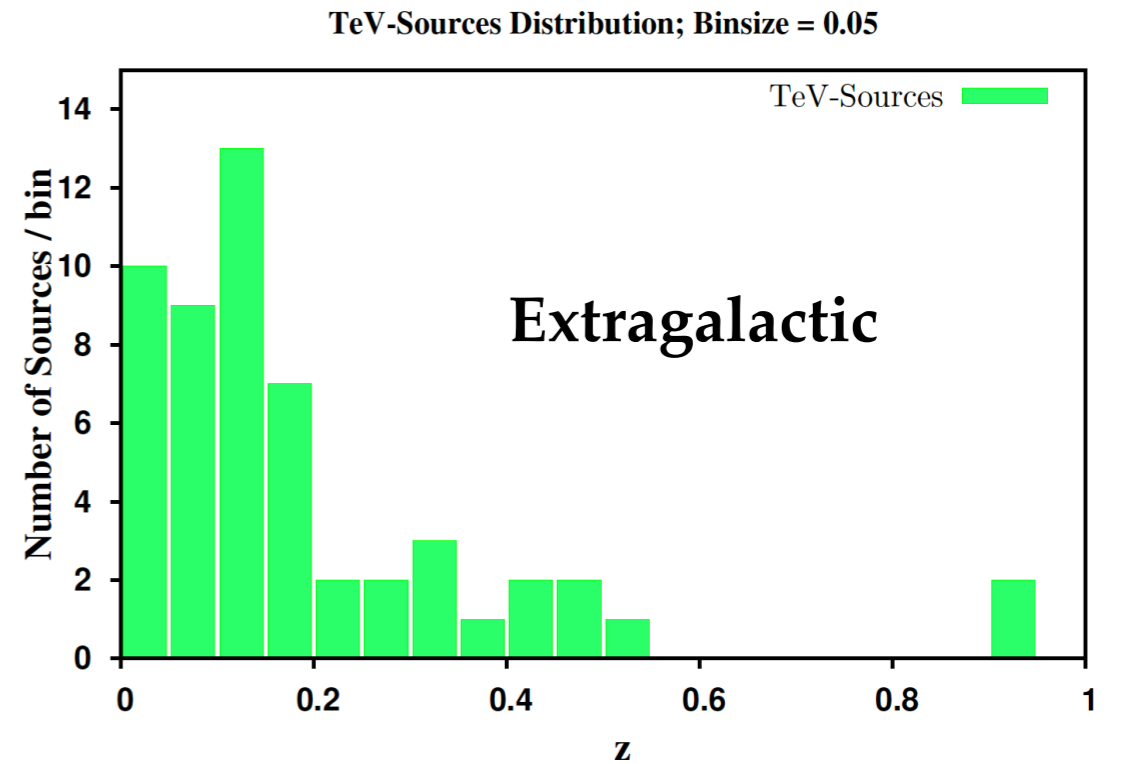


Catalog of TeV sources



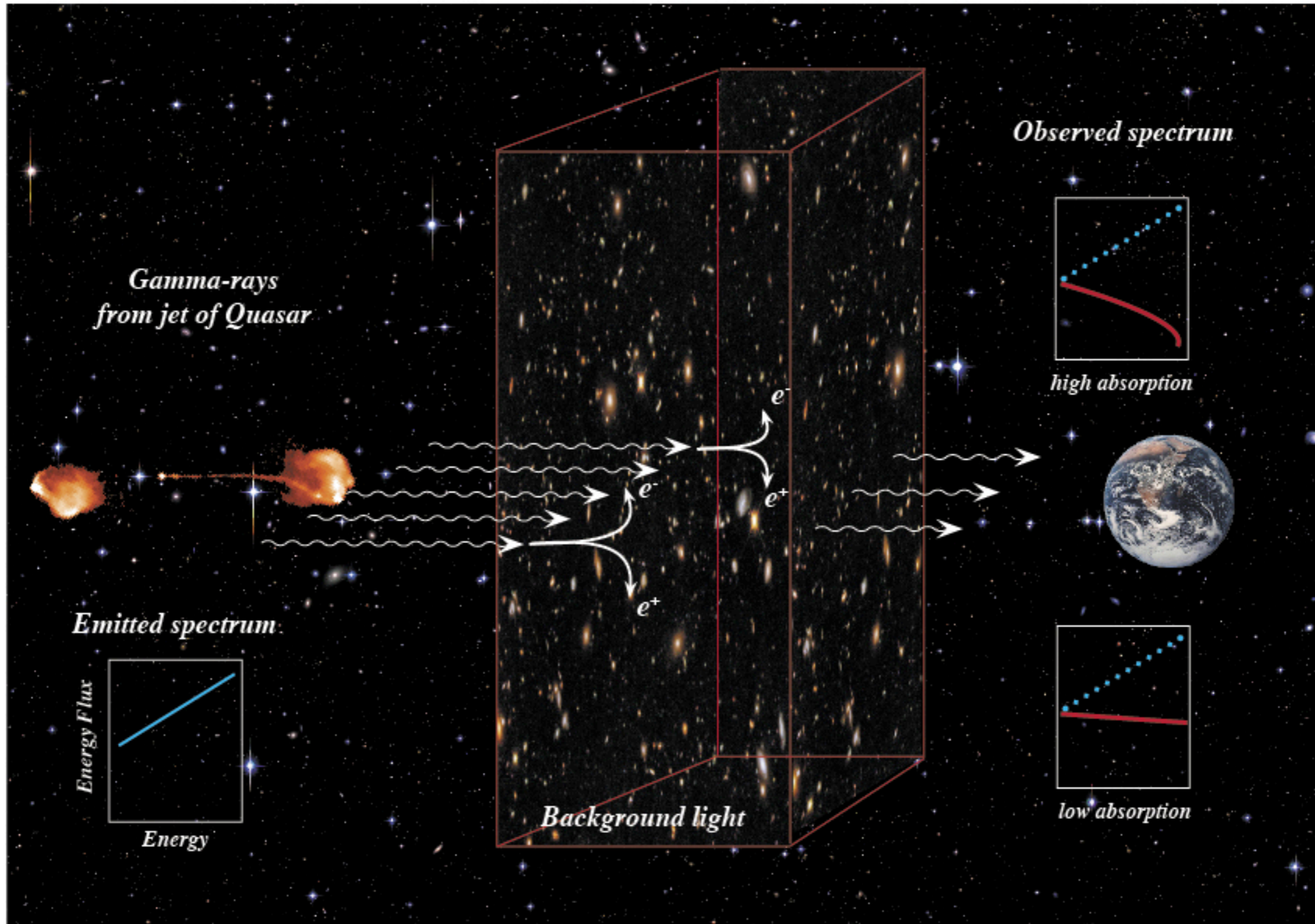
<http://tevcat2.uchicago.edu>

- 54 (6 FSRQ + 48 BL Lac) of these TeV emitters are extragalactic sources



Accounting for absorption effects in the GeV-TeV

Universe's opacity to VHE photons



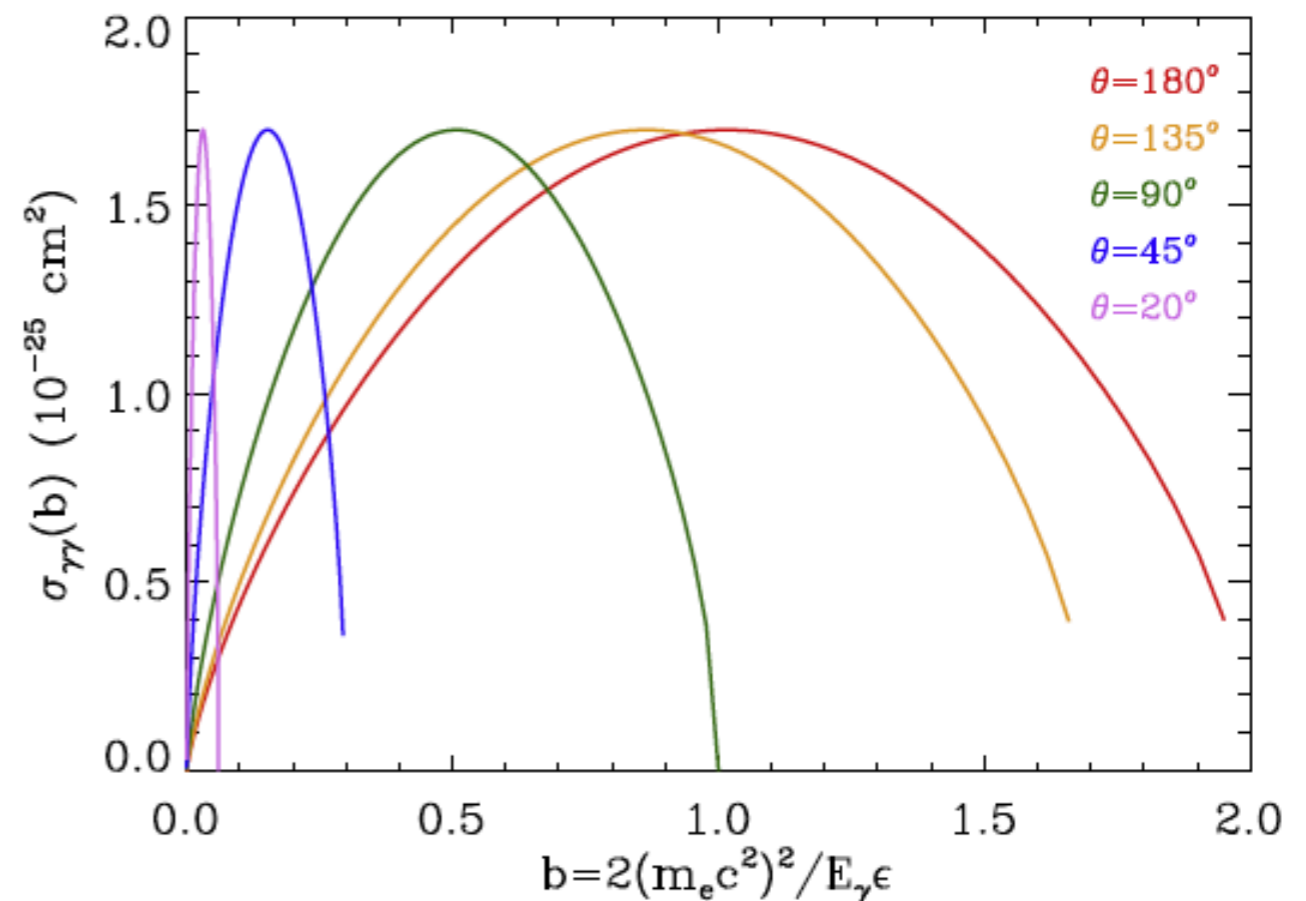
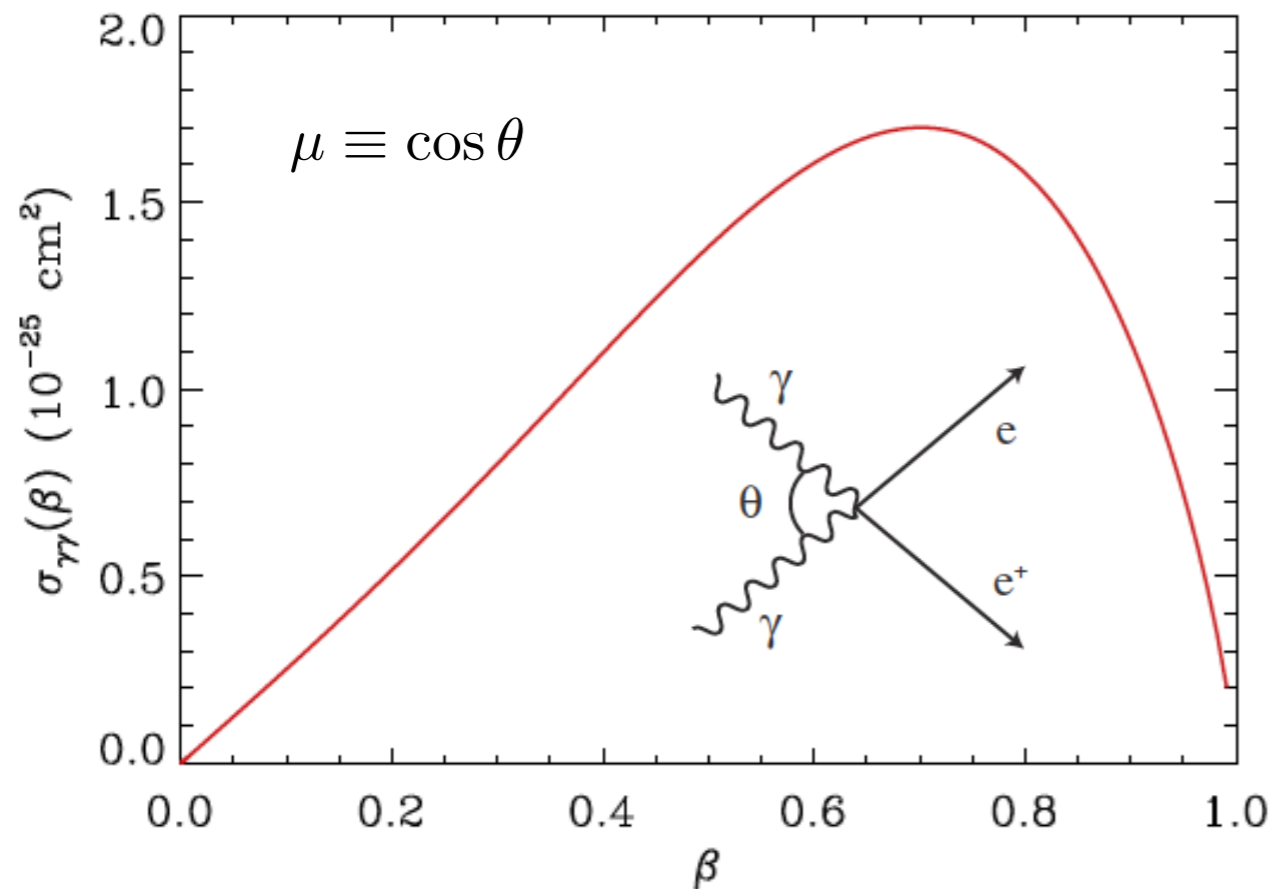
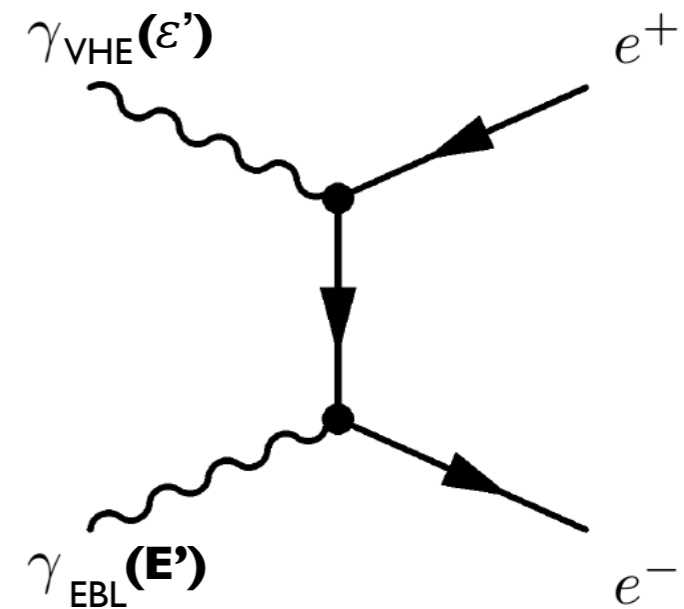
Cross-section for gamma-gamma scattering

Well understood QED process:

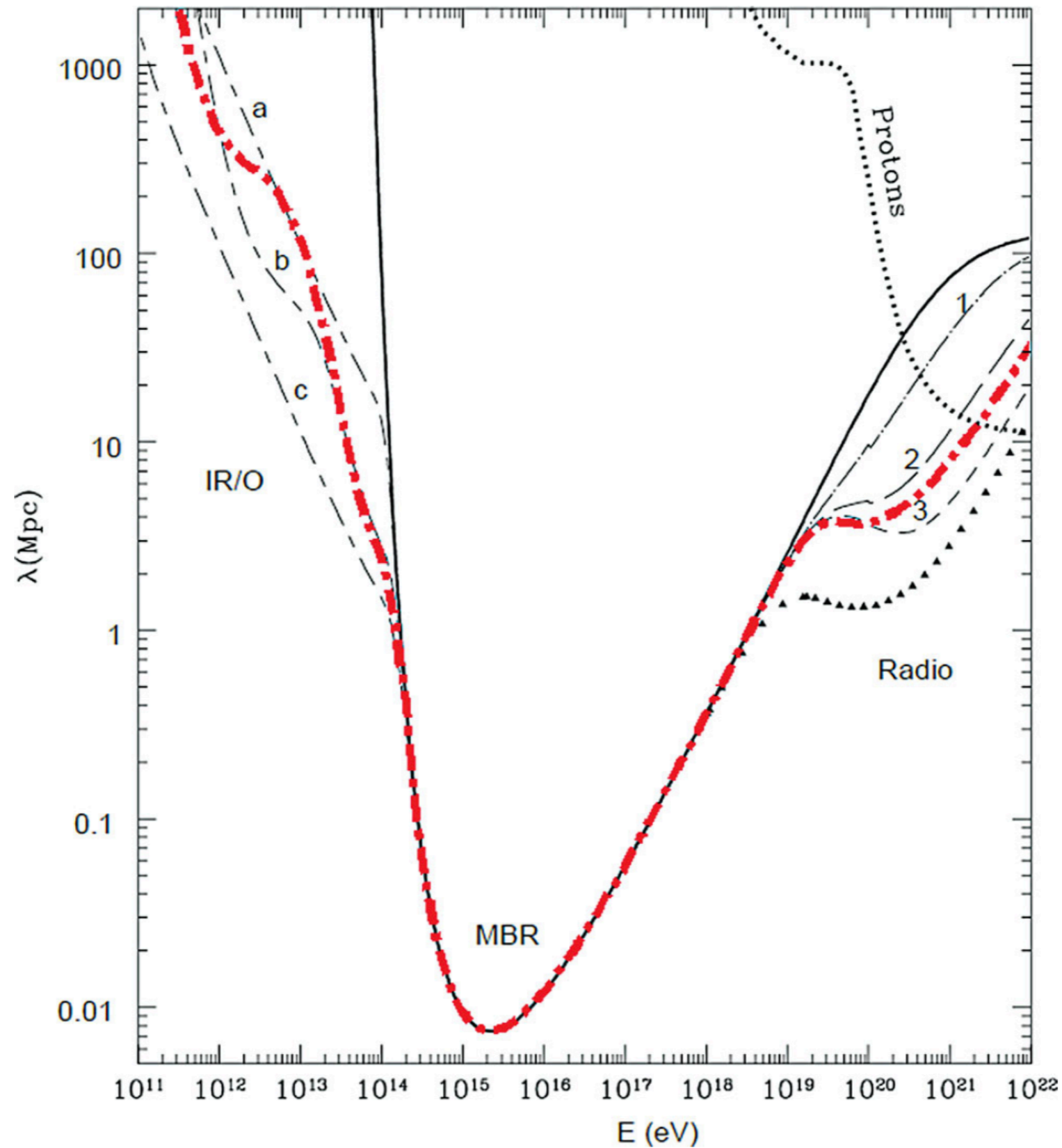
$$\sigma(E', \epsilon', \mu) = \frac{3\sigma_T}{16} (1 - \beta^2) \left[2\beta(\beta^2 - 2) + (3 - \beta^4) \ln \left(\frac{1 + \beta}{1 - \beta} \right) \right]$$

$$\beta = \sqrt{1 - \frac{2m_e^2 c^4}{E' \epsilon' (1 - \mu)}}$$

$$E'_{th} = \frac{2m_e c^2}{\epsilon' (1 - \mu)}$$

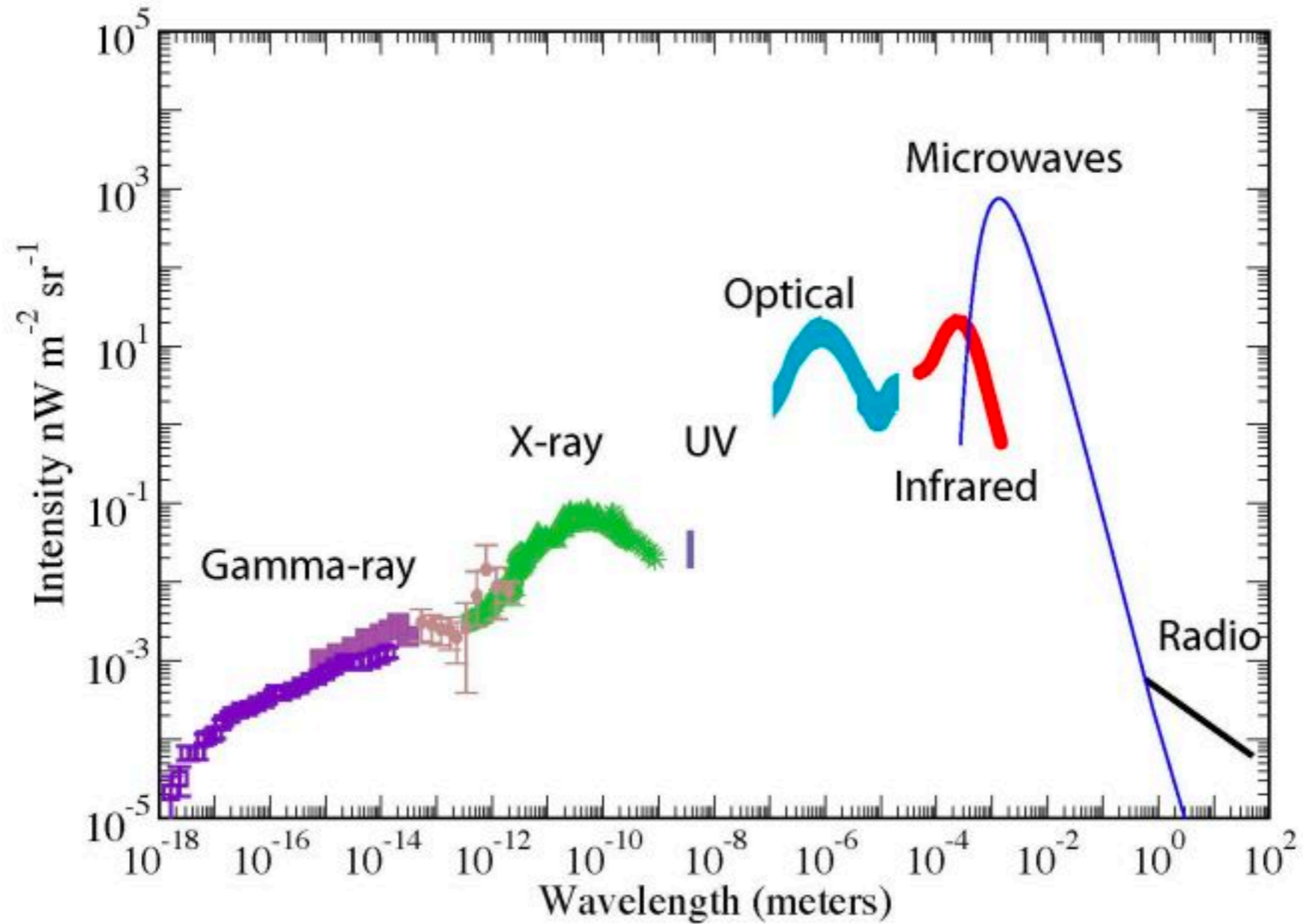


VHE photon mean free path



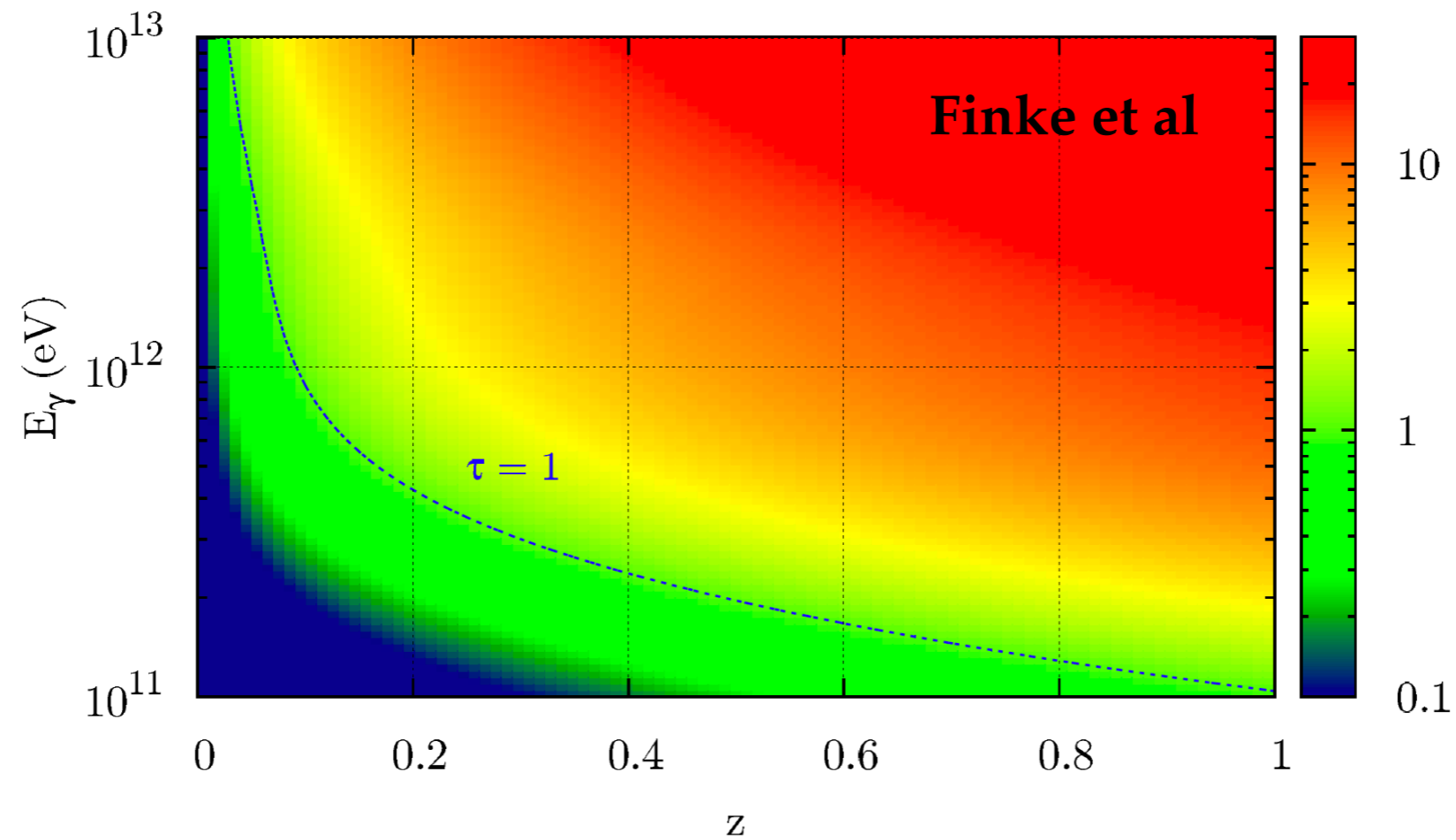
$$\lambda = \frac{1}{\int \sigma dn}$$

The extragalactic diffuse backgrounds



Optical depth

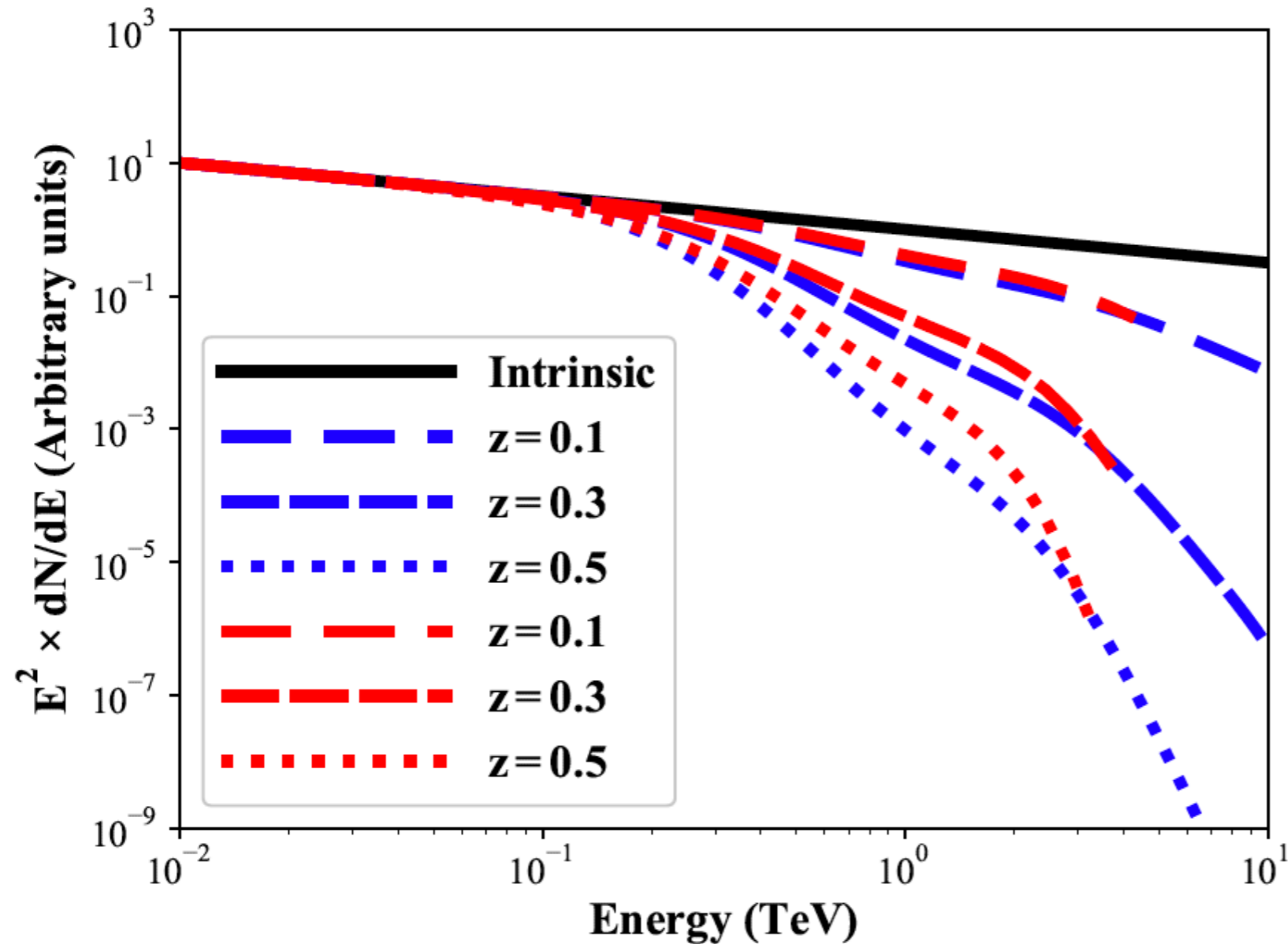
$$\tau_{\gamma\gamma}(\varepsilon, z) = c \int_0^z \frac{dt}{dz'} dz' \int_{-1}^1 (1 - \mu) \frac{d\mu}{2} \int_{E_{th}}^{\infty} \sigma(E', \varepsilon', \mu) n(E', z') dE'$$



Cosmic gamma-ray horizon (CGRH): $\tau=1$

Attenuation effects important for $\tau > 1$

Fingerprints of attenuation



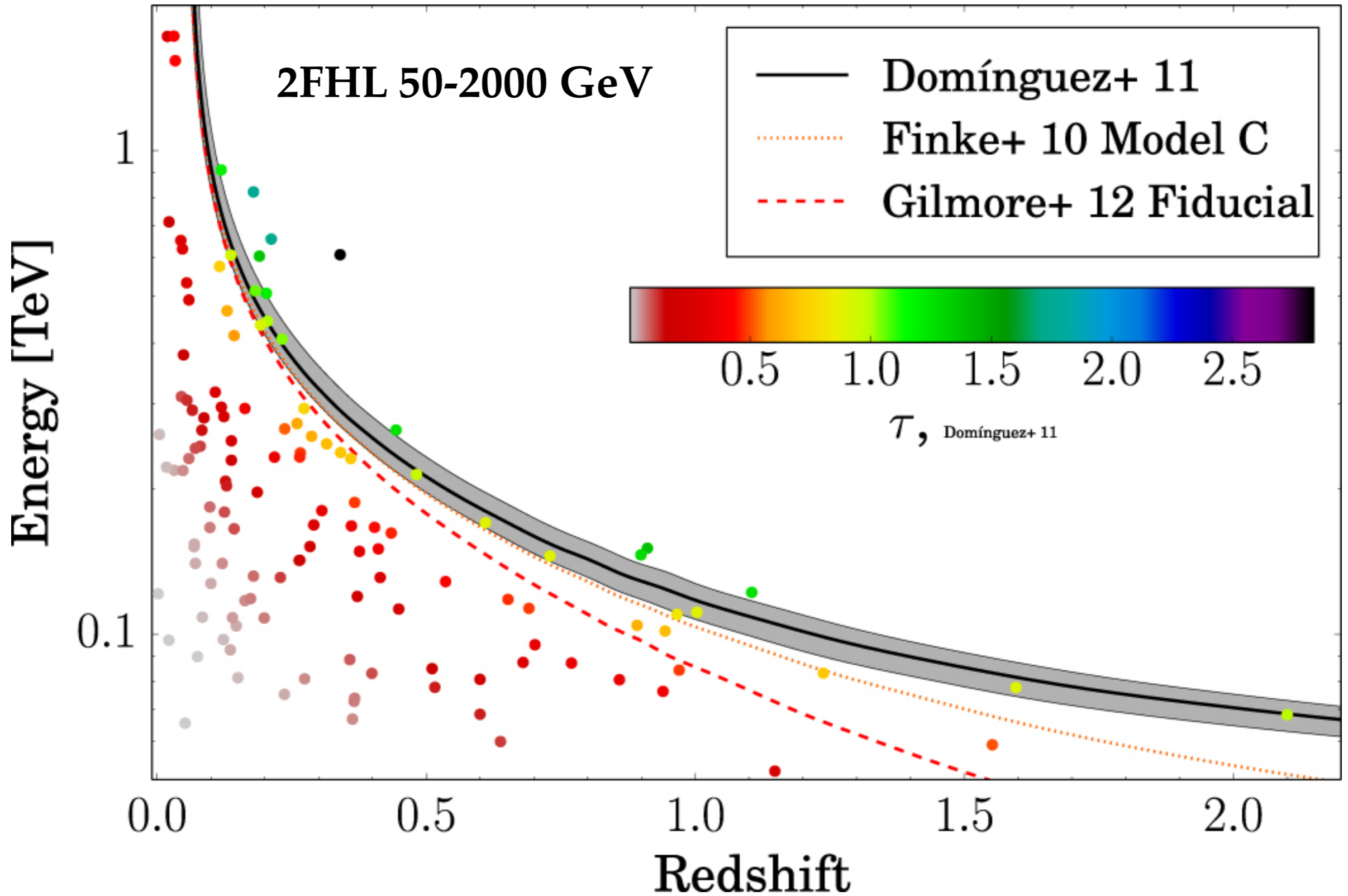
— Helgason et al

— Finke et al

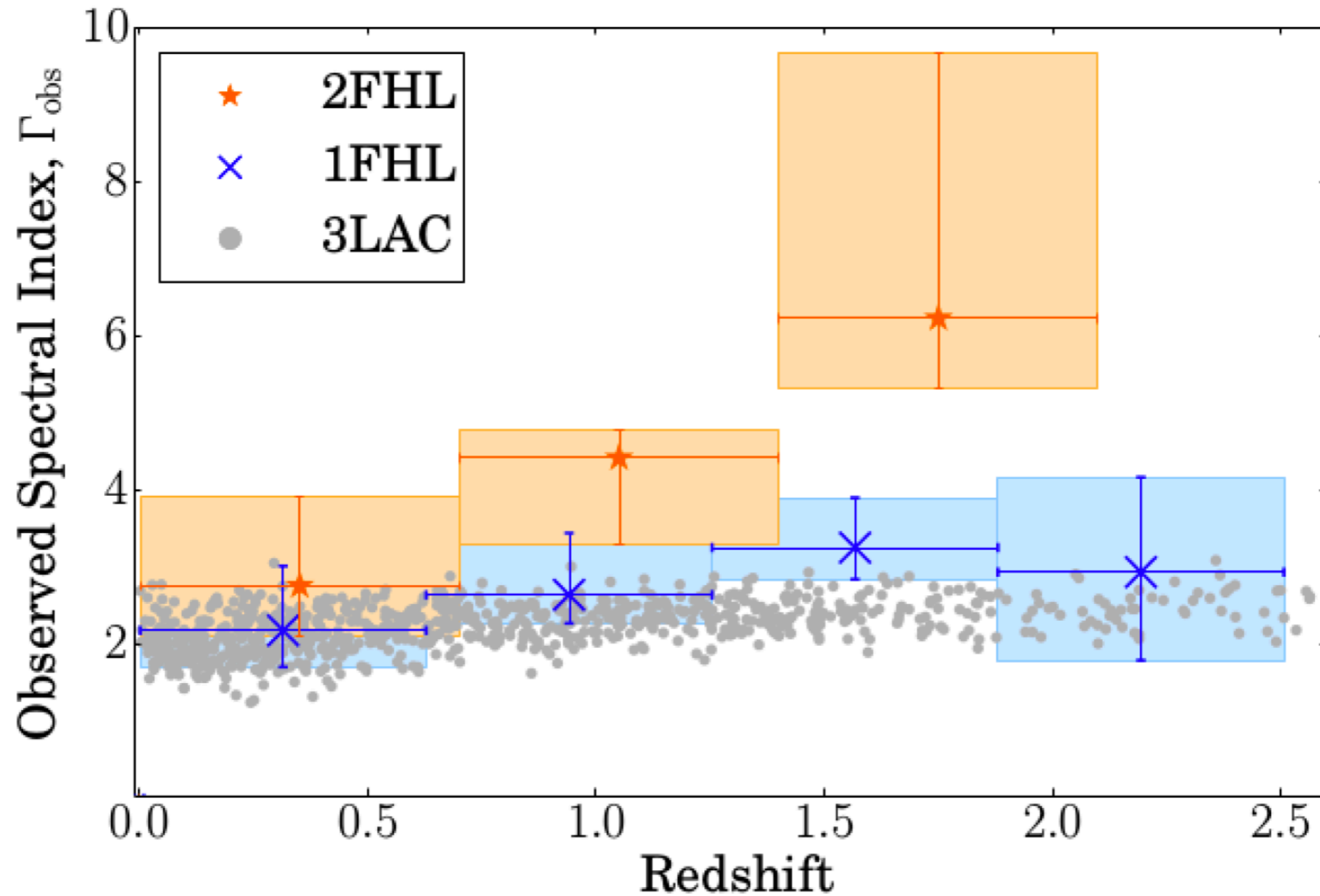
$$\Phi(E) = e^{-\tau} \Phi_0(E)$$

- Hypothetical source with intrinsic power-law spectrum $E^{-2.5}$
- Attenuation unimportant for energies below 100 GeV

The cosmic gamma-ray horizon (CGRH)



Spectral index “running”



2FHL: 50-2000 GeV

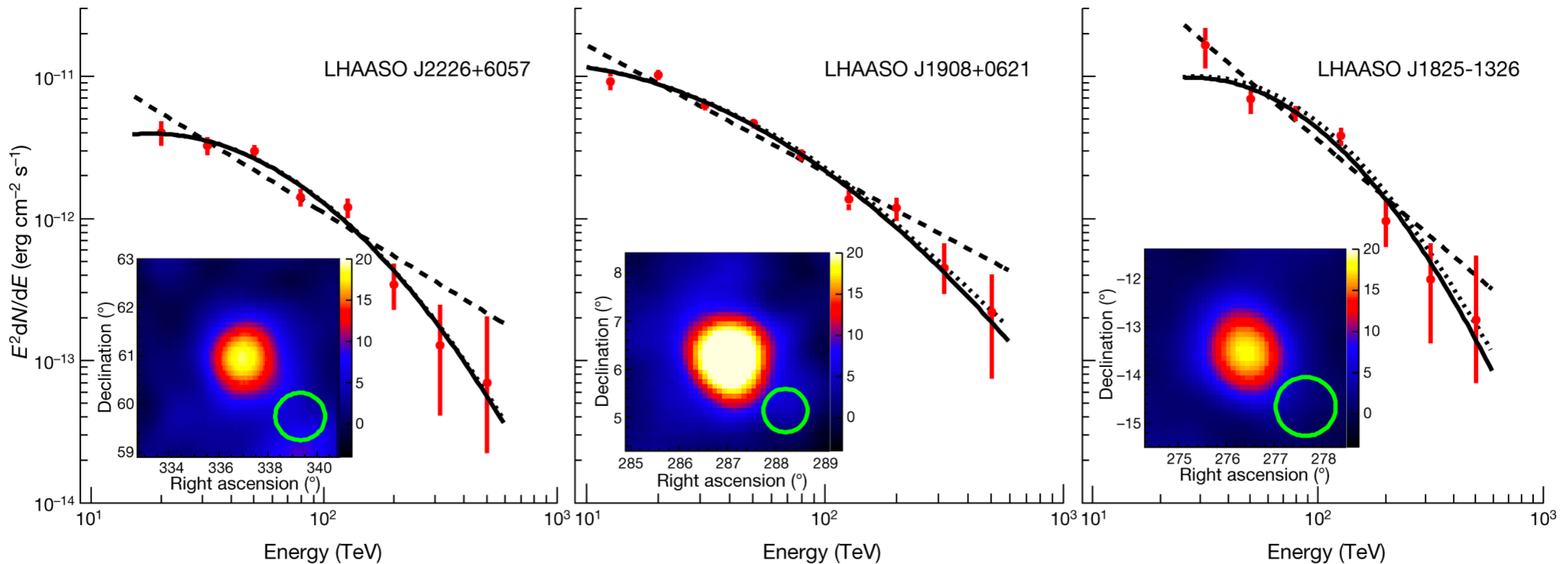
1FHL: 10-500 GeV

3LAC: 0.1-100 GeV

What do we see at the PeV energy scale?

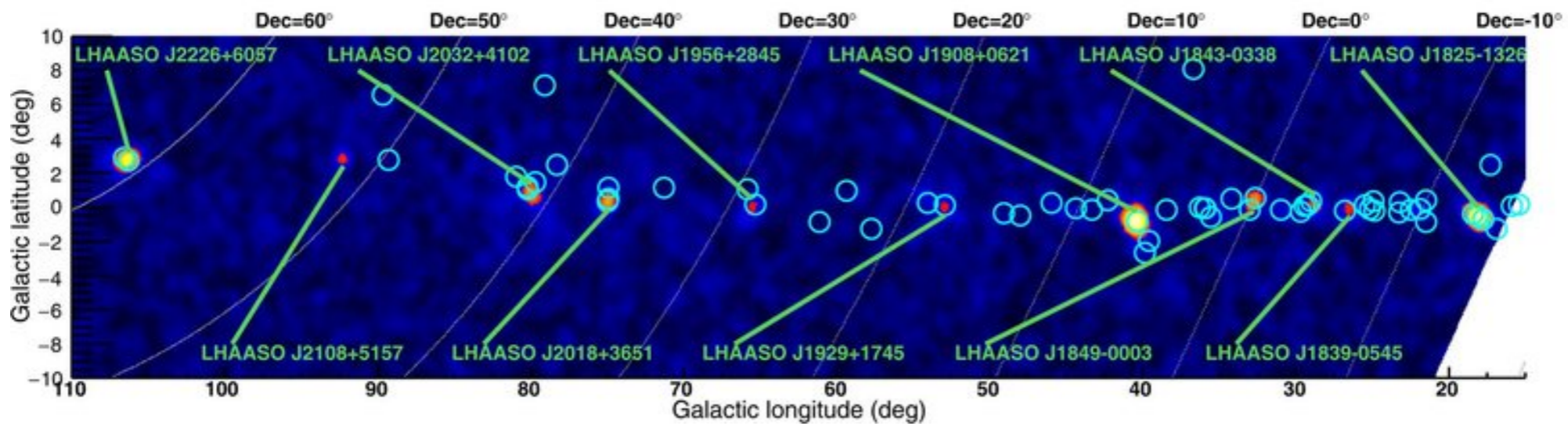
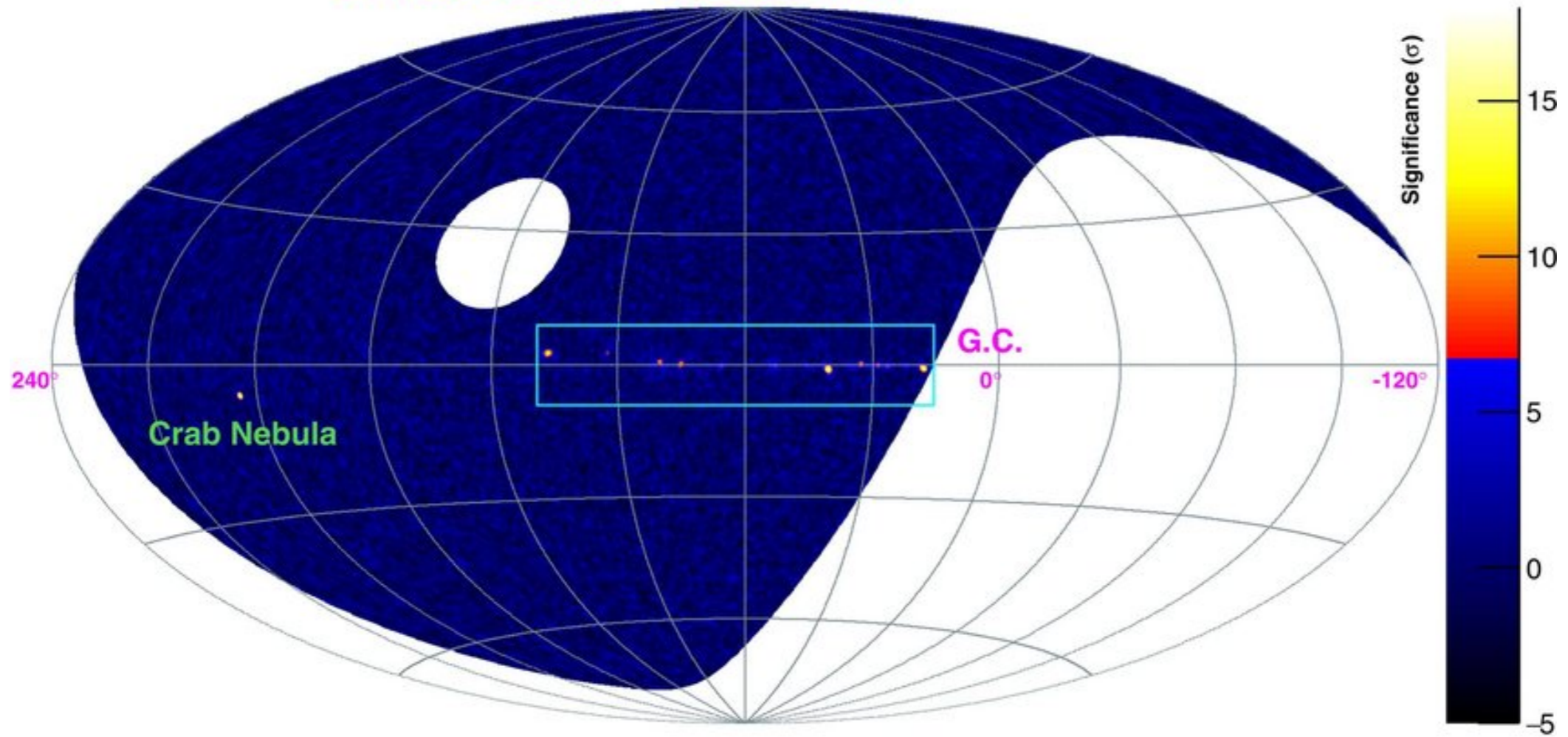
Ultrahigh-energy photons up to 1.4 petaelectronvolts from 12 γ -ray Galactic sources

LHASSO sources brighter than the Crab @ 100 TeV



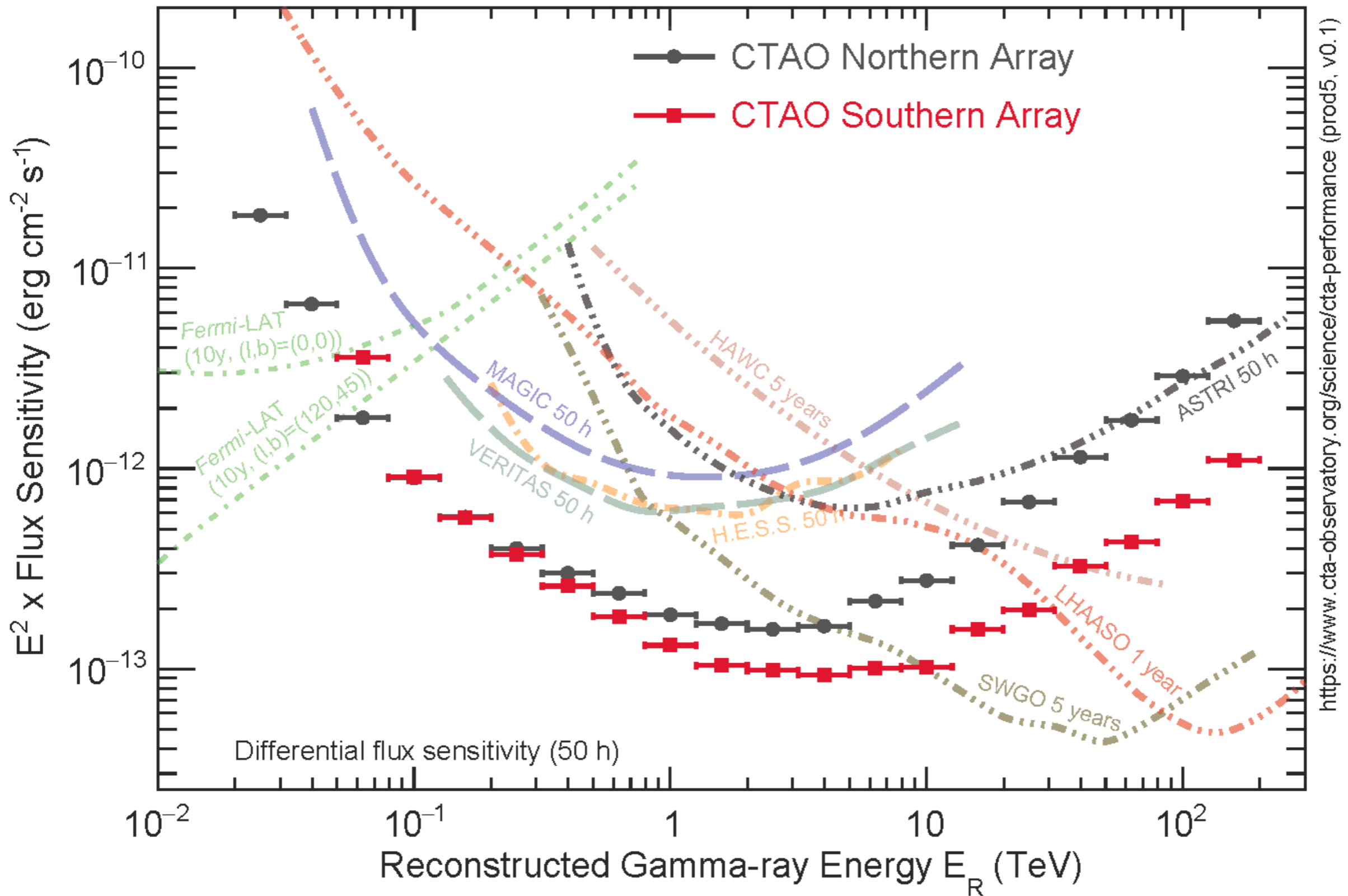
Zen Cao et. al. (LHAASO), Nature vol. 594, pag. 33–36 (2021)

LHAASO Sky @ >100 TeV



Zen Cao et. al. (LHASSO), Nature vol. 594, pag. 33–36 (2021)

Sensitivity curves



EBL and star formation rate (SFR)

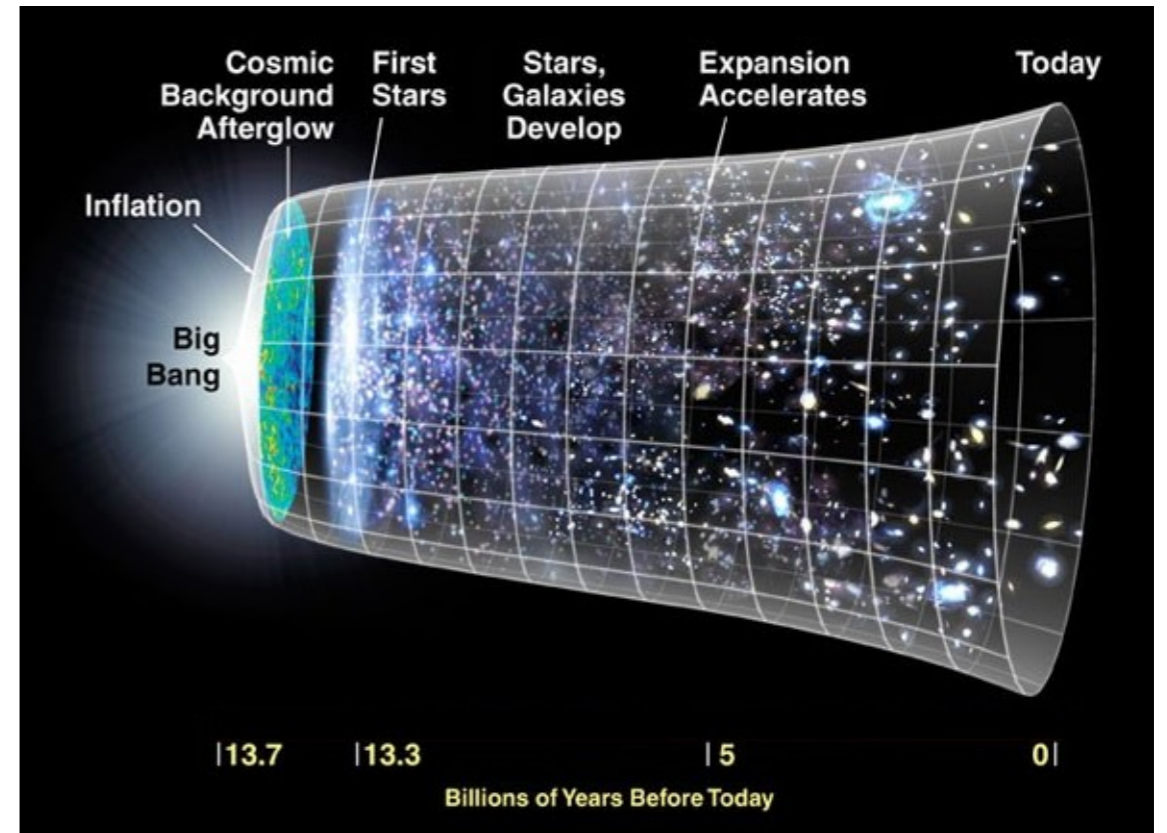
Comoving volume emissivity:

$$\epsilon_\nu(z) = \int L_\nu \phi(L_\nu, z) dL_\nu$$

Integrate over the whole SFR history:

$$n(E', z) = (1 + z)^3 \int_z^\infty \frac{\epsilon_{\nu'} / h}{h\nu'} \frac{dt}{dz'} dz'$$

- star light (UV / optical)
- dust emission (IR)
- AGN emission (accretion)
- First (pop III) and second (pop II) generation of stars (?)
- Exotic emissions (?)



For a Λ CDM model:

$$\left| \frac{dt}{dz} \right| = \frac{1}{H_0(1+z) \sqrt{(1+z)^3 \Omega_m + \Omega_\Lambda}}$$

Boltzmann equation for EBL

- Time evolution for the brightness I in physical coordinates:

EBL brightness [$\text{W m}^{-2} \text{Hz}^{-1} \text{sr}^{-1}$]

Emissivity [$L_{\odot} \text{Mpc}^{-3} \text{Hz}^{-1}$]

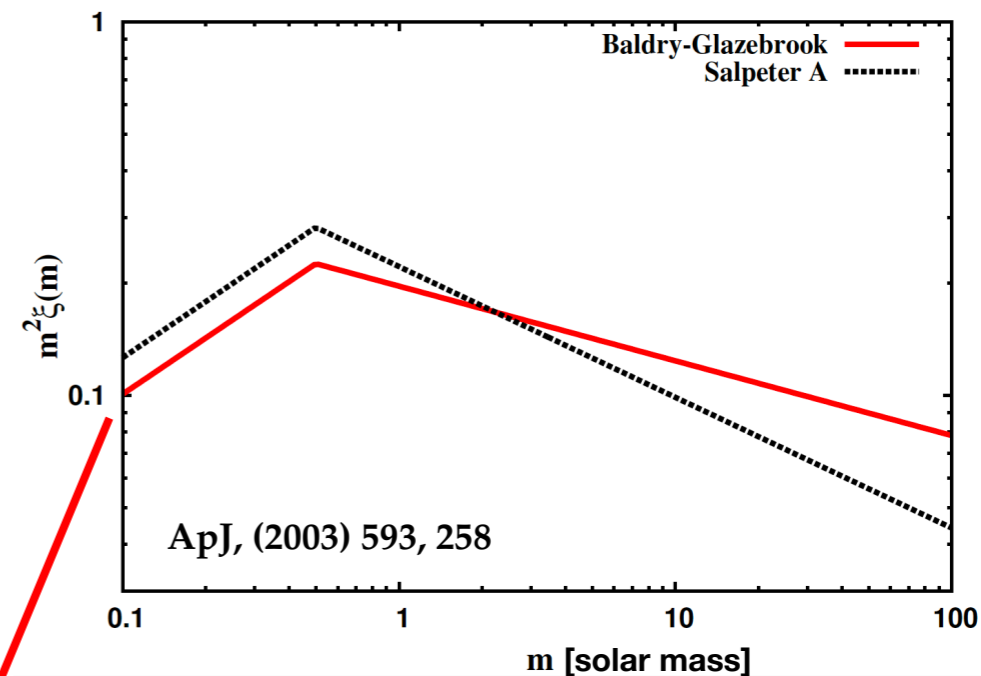
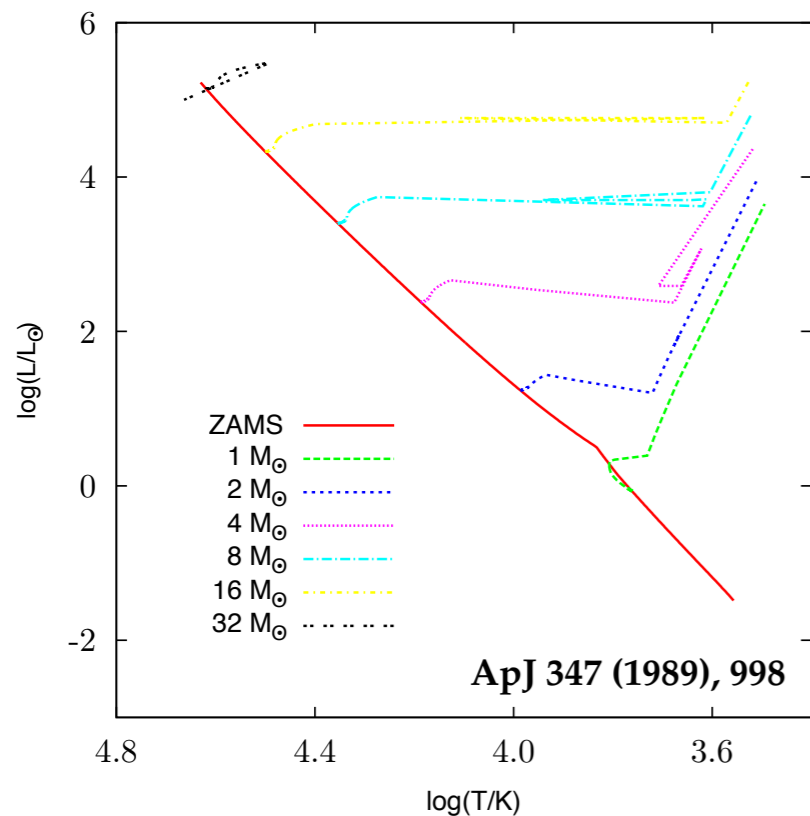
$$\frac{dI(t, \lambda)}{dt} = \underbrace{-3 \frac{\dot{a}}{a} I(t, \lambda)}_{\text{expansion}} + \underbrace{\frac{c}{4\pi} j(t, \lambda)}_{\text{source term}}$$

- Formal solution:

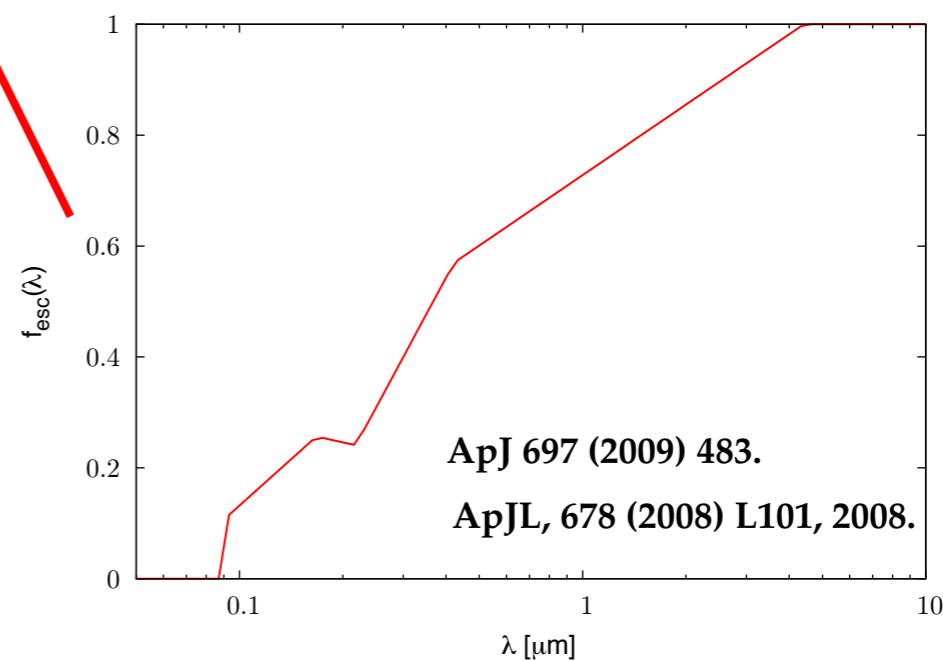
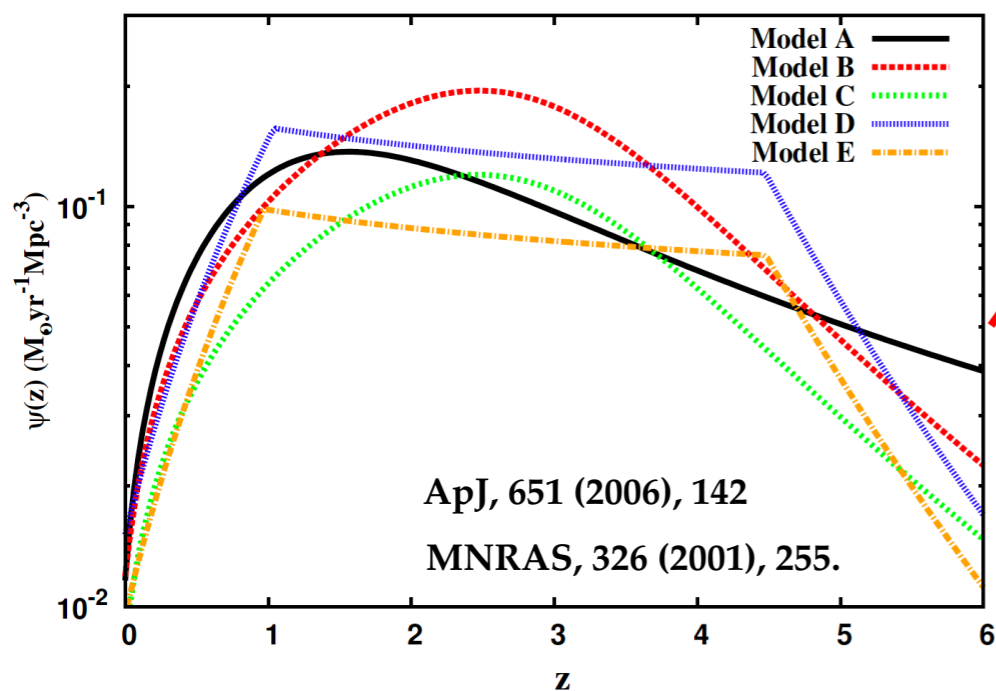
$$I(t, \lambda) = \frac{c}{4\pi} \int_0^t \frac{a^3(t')}{a^3(t)} j(t', \lambda') dt' = (1+z)^3 \frac{c}{4\pi} \int_z^{\infty} \underbrace{j_c(z', \lambda')}_{\text{Comoving emissivity}} \left| \frac{dt'}{dz'} \right| dz'$$

- Therefore, for a given cosmology, the EBL can be model by defining the coming emissivity $j_c(z, \lambda)$

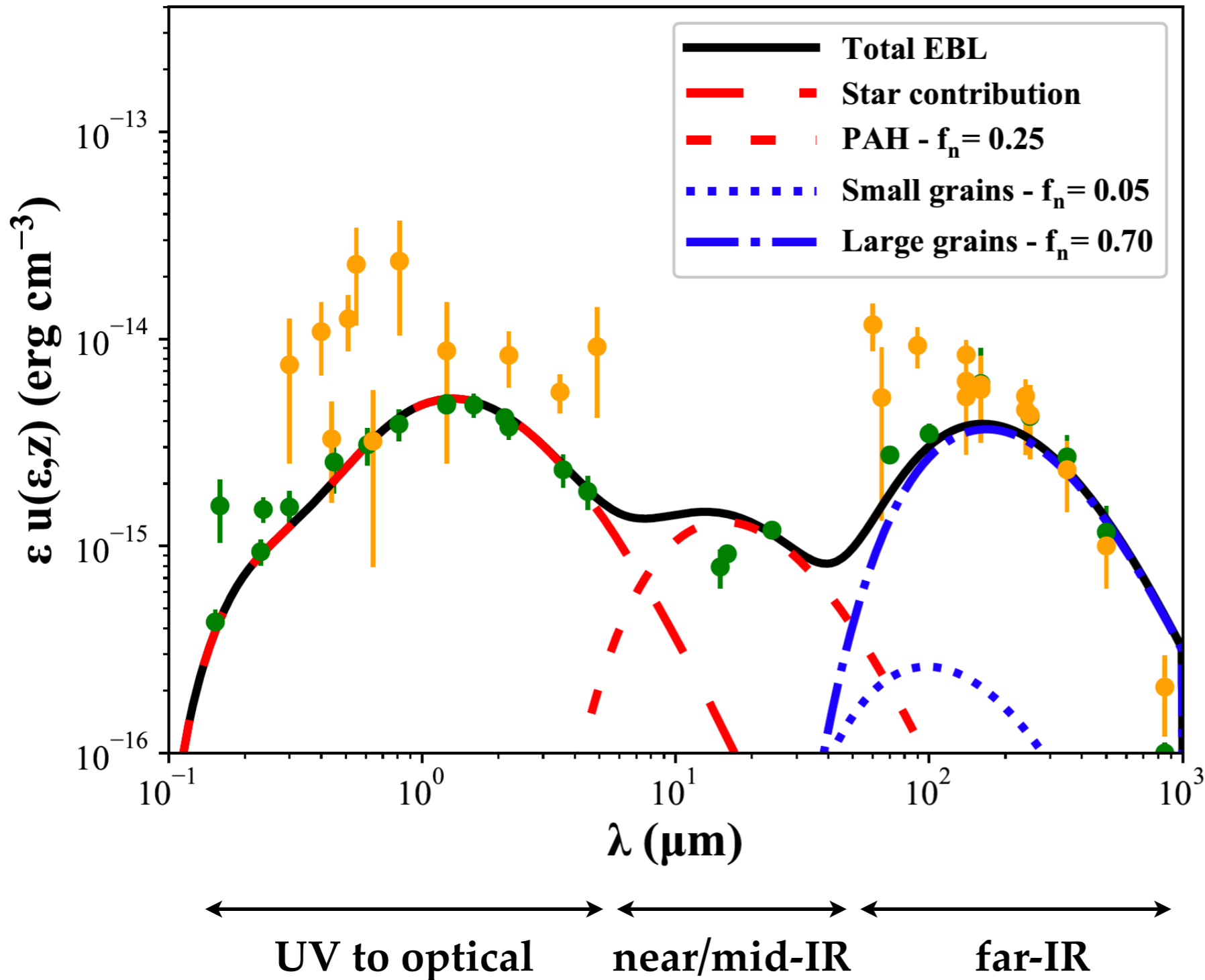
EBL model based on star+dust (Finke et al.)



$$I(t, \lambda) = (1 + z)^3 \frac{c}{4\pi} \int_z^{\infty} j_c(z', \lambda') \left| \frac{dt'}{dz'} \right| dz'$$



Energy density @ z=0 (Finke et al.)



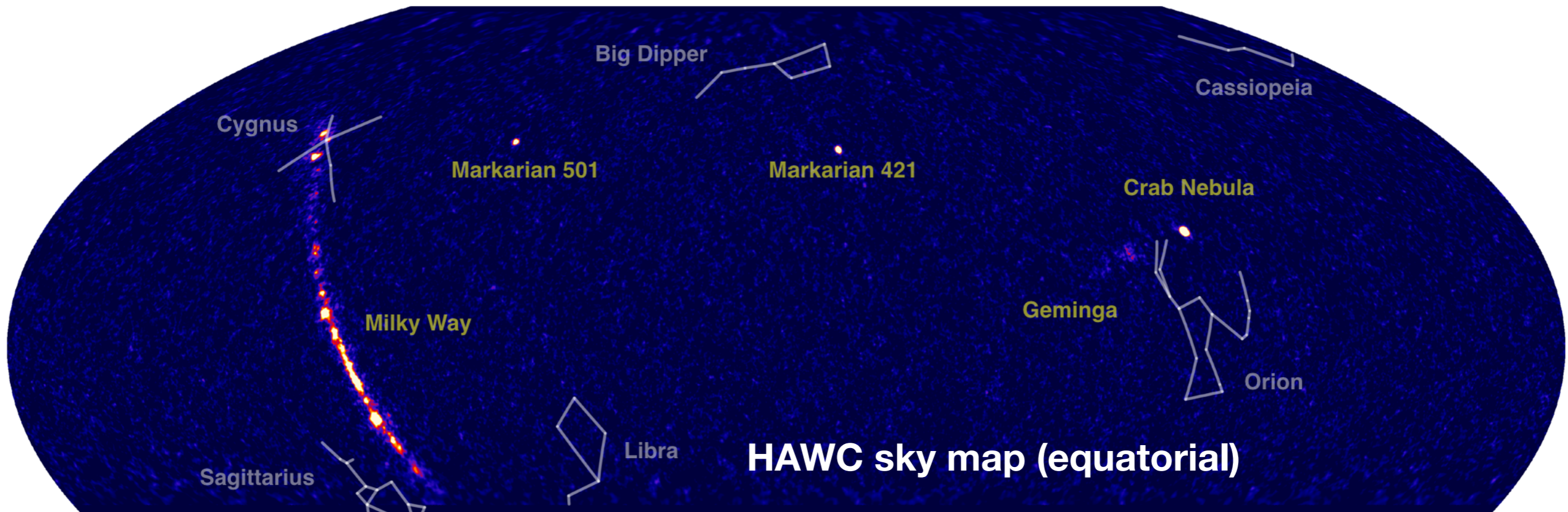
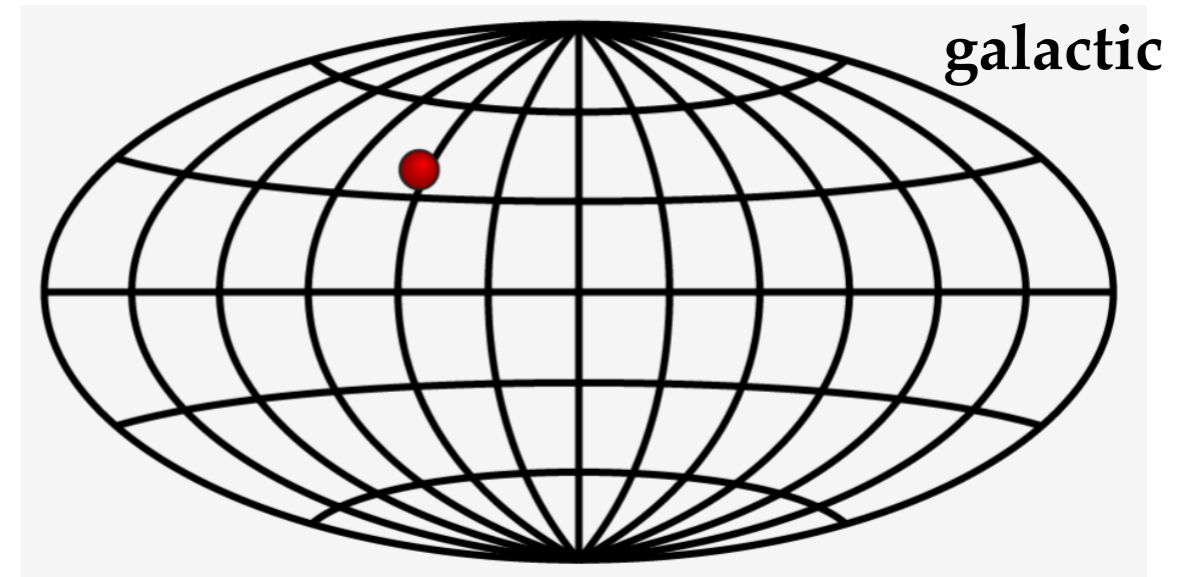
Component	I_{bol} ($\text{nW m}^{-2} \text{sr}^{-1}$)
Star	25.9
PAH	5.5
Small grains	1.1
Large grains	14.9
Total	47.4
CMB	1000.9

• About 5% of the CMB energy density

• Energy density very close to lower bound from galaxy counts

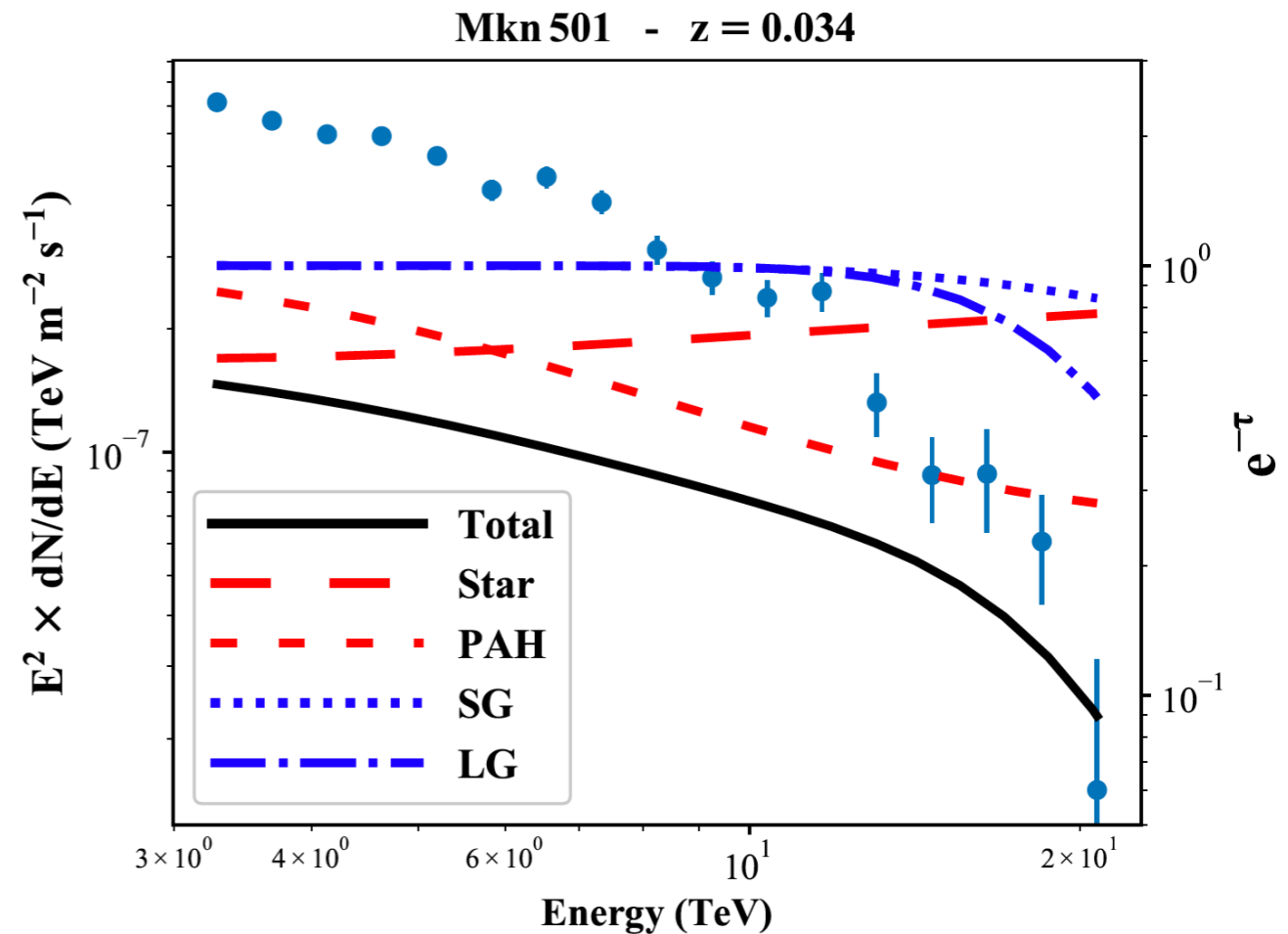
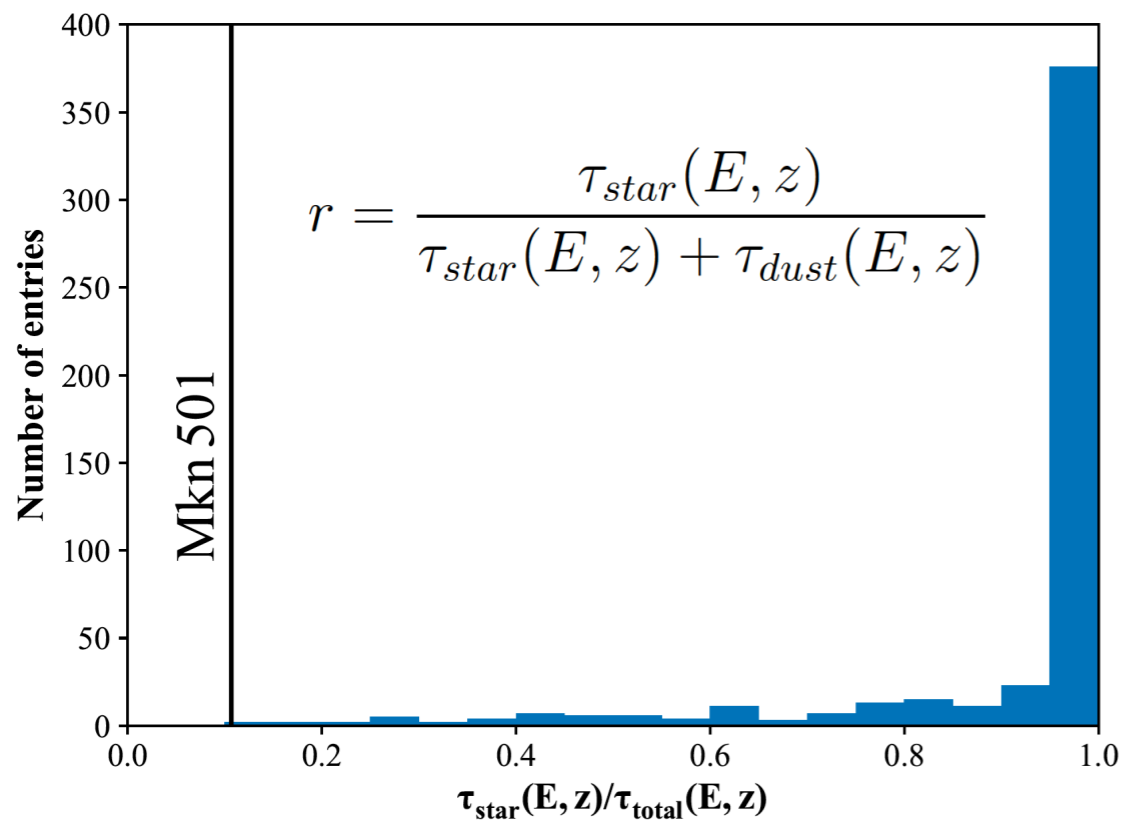
Case study: Markarian 501

- Blazar
- BL Lac type AGN
- $z=0.034$ (~ 140 Mpc)
- $(L_{\text{gal}}, B_{\text{gal}}) = (63.60, 38.86)$ deg
- High variability at TeV
- Violent flare seen by HEGRA in 1997



Case study: Markarian 501

- SED very well measured with emission extending up to 20 TeV
- High levels of attenuation predicted at the very end of Mkn 501 SED



Can we use the SED of Mkn 501 to constrain EBL model parameters?

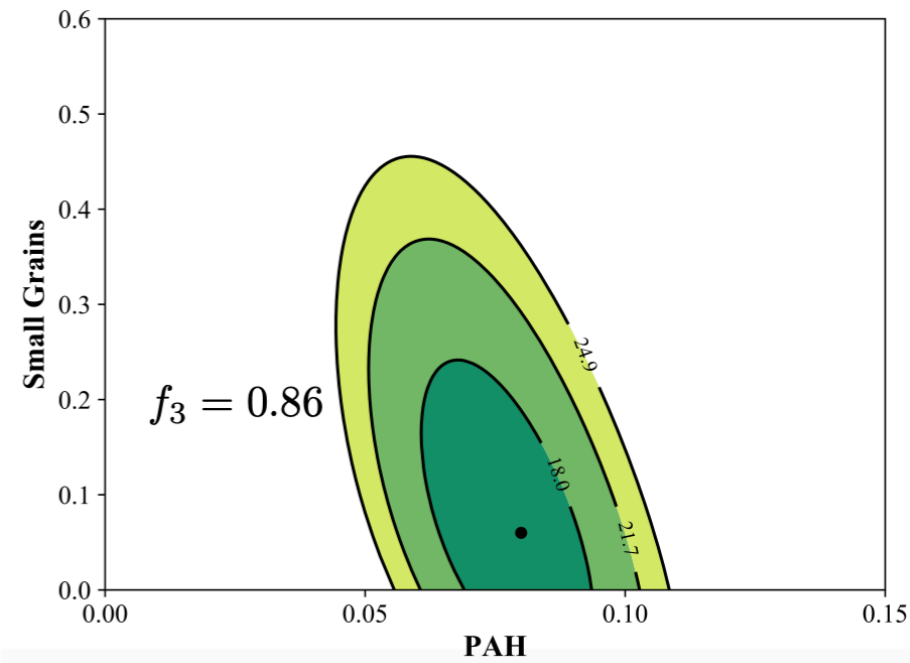
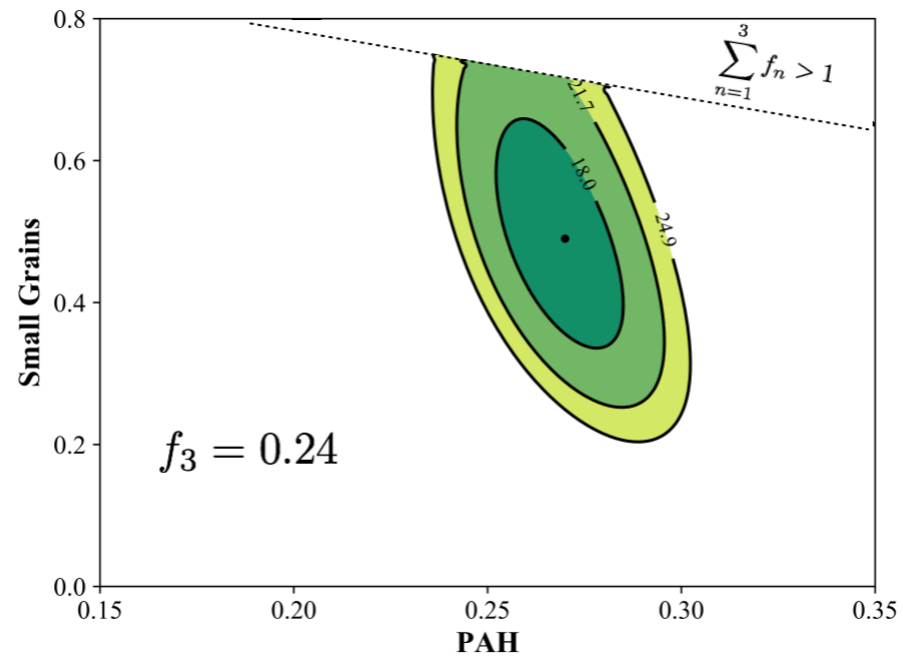
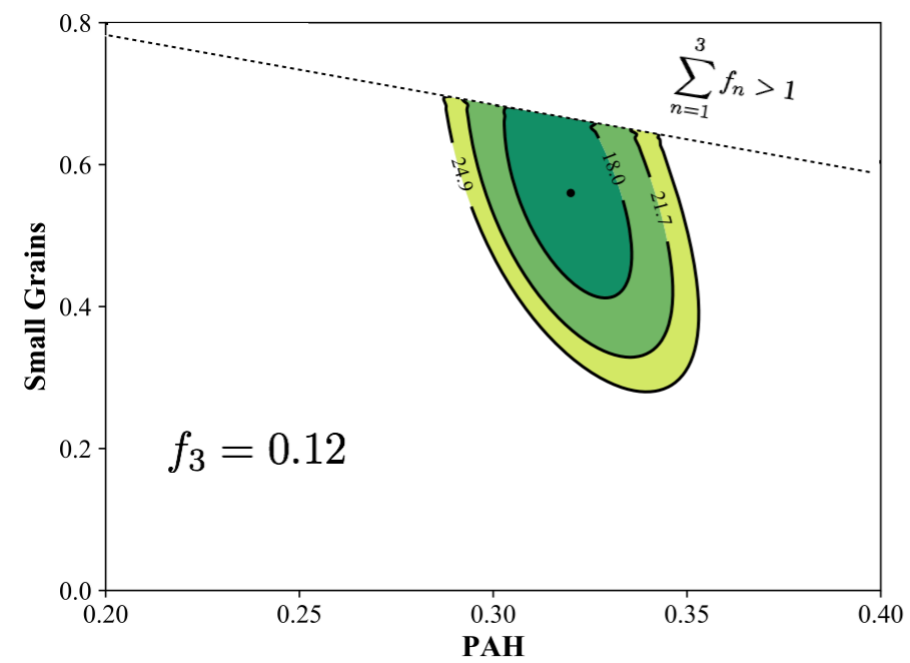
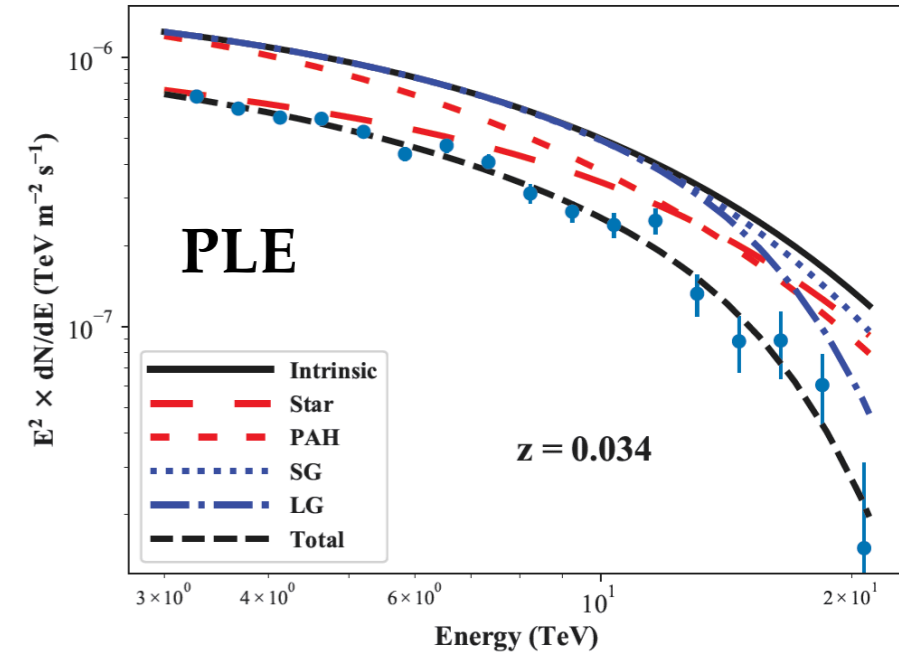
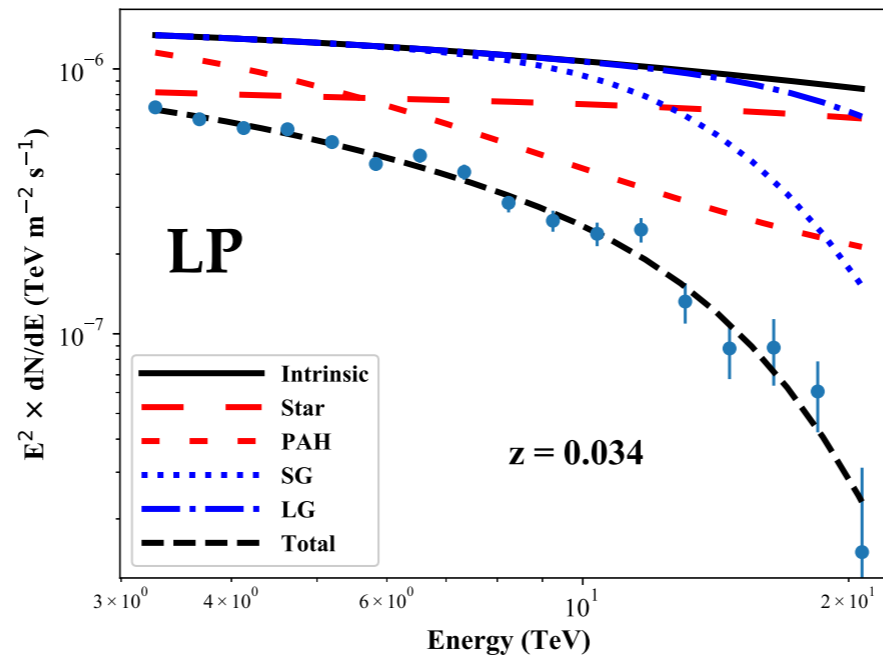
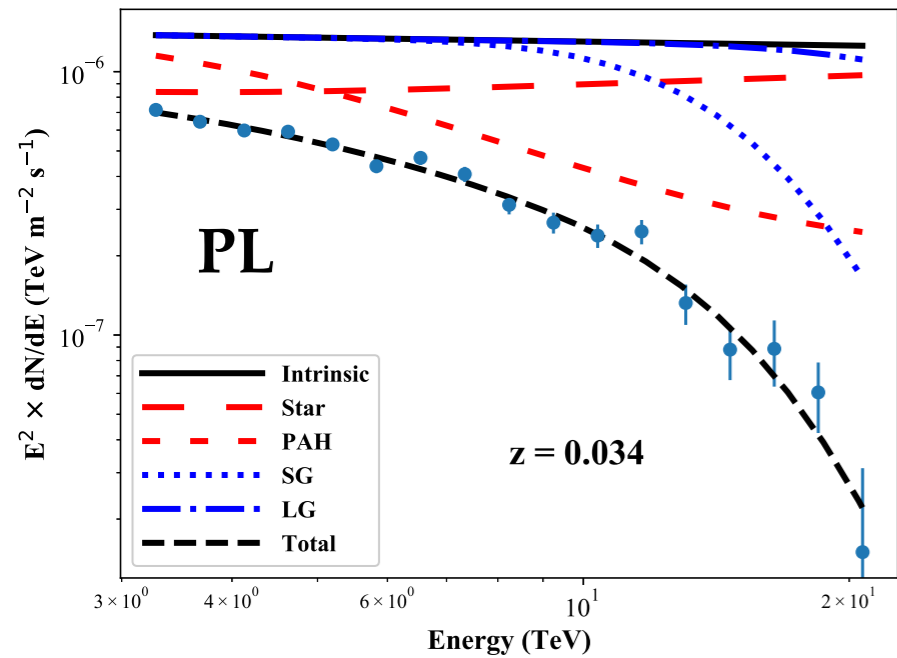
Analysis strategy

- Different flavors of intrinsic spectrum to assess this systematic uncertainty:

$$\Phi_0(E) = \begin{cases} N_0 \left(\frac{E}{E_0}\right)^{-\Gamma} & \text{(power-law)} \\ N_0 \left(\frac{E}{E_0}\right)^{-a-b \log(E/E_0)} & \text{(log-parabola)} \\ N_0 \left(\frac{E}{E_0}\right)^{-\Gamma} e^{-\left(\frac{E}{E_{\text{cut}}}\right)} & \text{(power-law with exponential cutoff)} \end{cases}$$

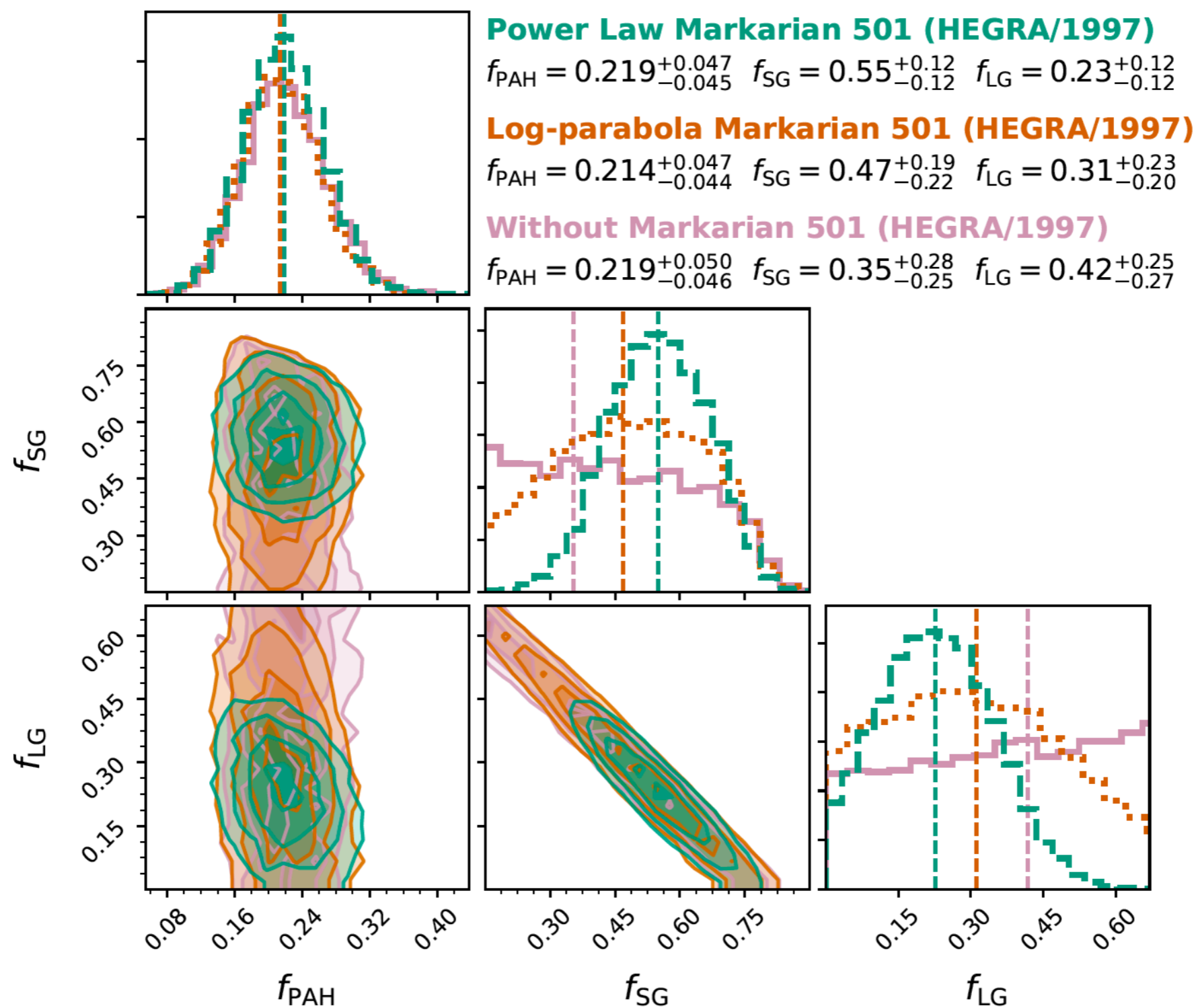
- $E_0 = 1$ TeV fixed to minimize correlations between parameters
- An EBL model based on star+dust blackbody contributions (Finke et al)
- Temperature of dust grains fixed a priori
- Relative grain contributions varied together with intrinsic spectrum parameters.
- Grain fractions will be subject to normalization condition: $\sum_i^3 f_n = 1$
- Fits will be performed with either 4 (PL) or 5 (LP/PLC)

MK 501 fit results



- Intrinsic spectrum parametrization is an important source of systematic uncertainty
- See, how important are PAHs to give the SED the correct inclination at low energies

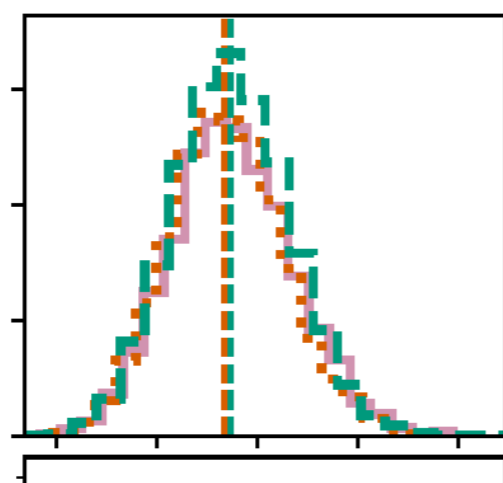
Breaking degeneracies with a combined fit



- Spectra of all 54 extragalactic TeVCat sources fitted simultaneously

M. G. Dantas Xavier et al, in prep.

Breaking degeneracies with a combined fit



Power Law Markarian 501 (HEGRA/1997)

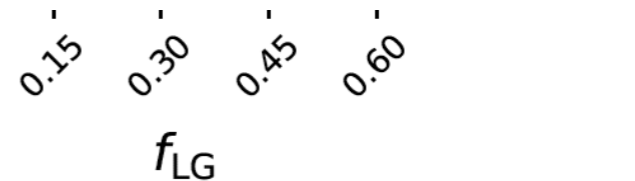
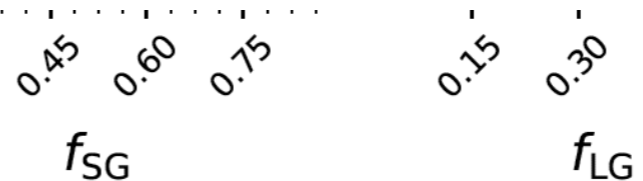
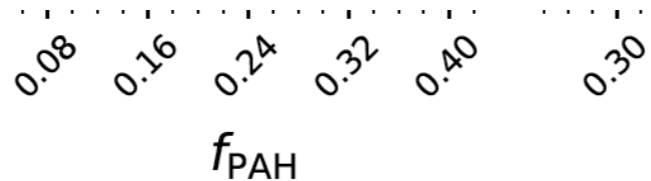
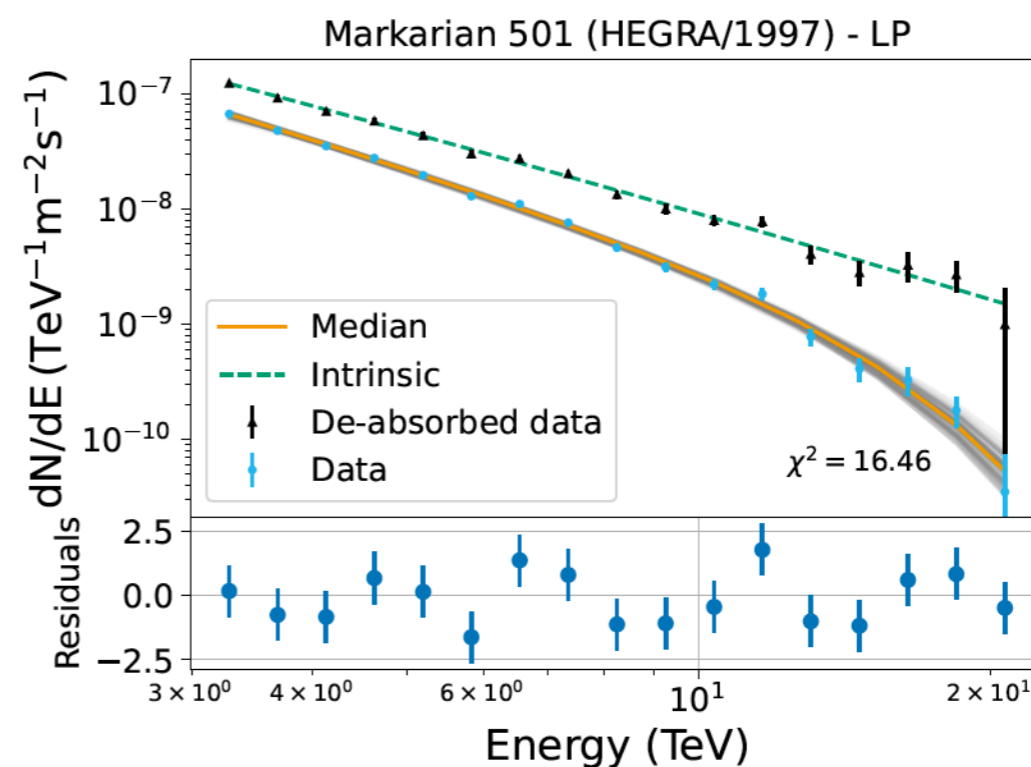
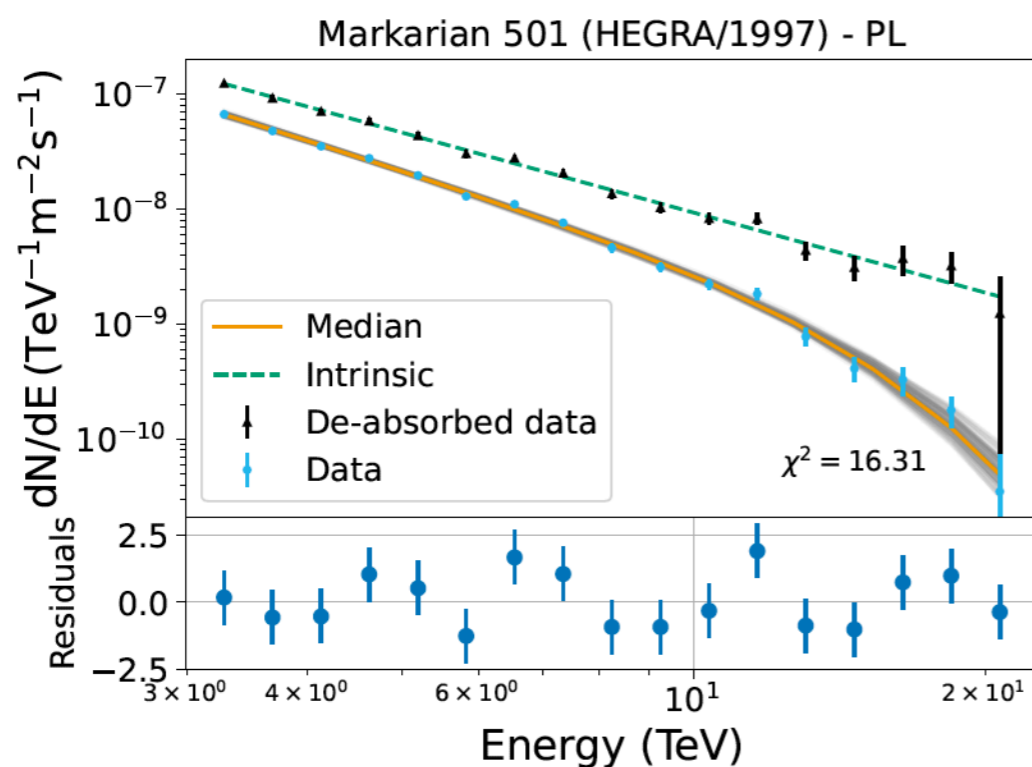
$$f_{\text{PAH}} = 0.219^{+0.047}_{-0.045} \quad f_{\text{SG}} = 0.55^{+0.12}_{-0.12} \quad f_{\text{LG}} = 0.23^{+0.12}_{-0.12}$$

Log-parabola Markarian 501 (HEGRA/1997)

$$f_{\text{PAH}} = 0.214^{+0.047}_{-0.044} \quad f_{\text{SG}} = 0.47^{+0.19}_{-0.22} \quad f_{\text{LG}} = 0.31^{+0.23}_{-0.20}$$

Without Markarian 501 (HEGRA/1997)

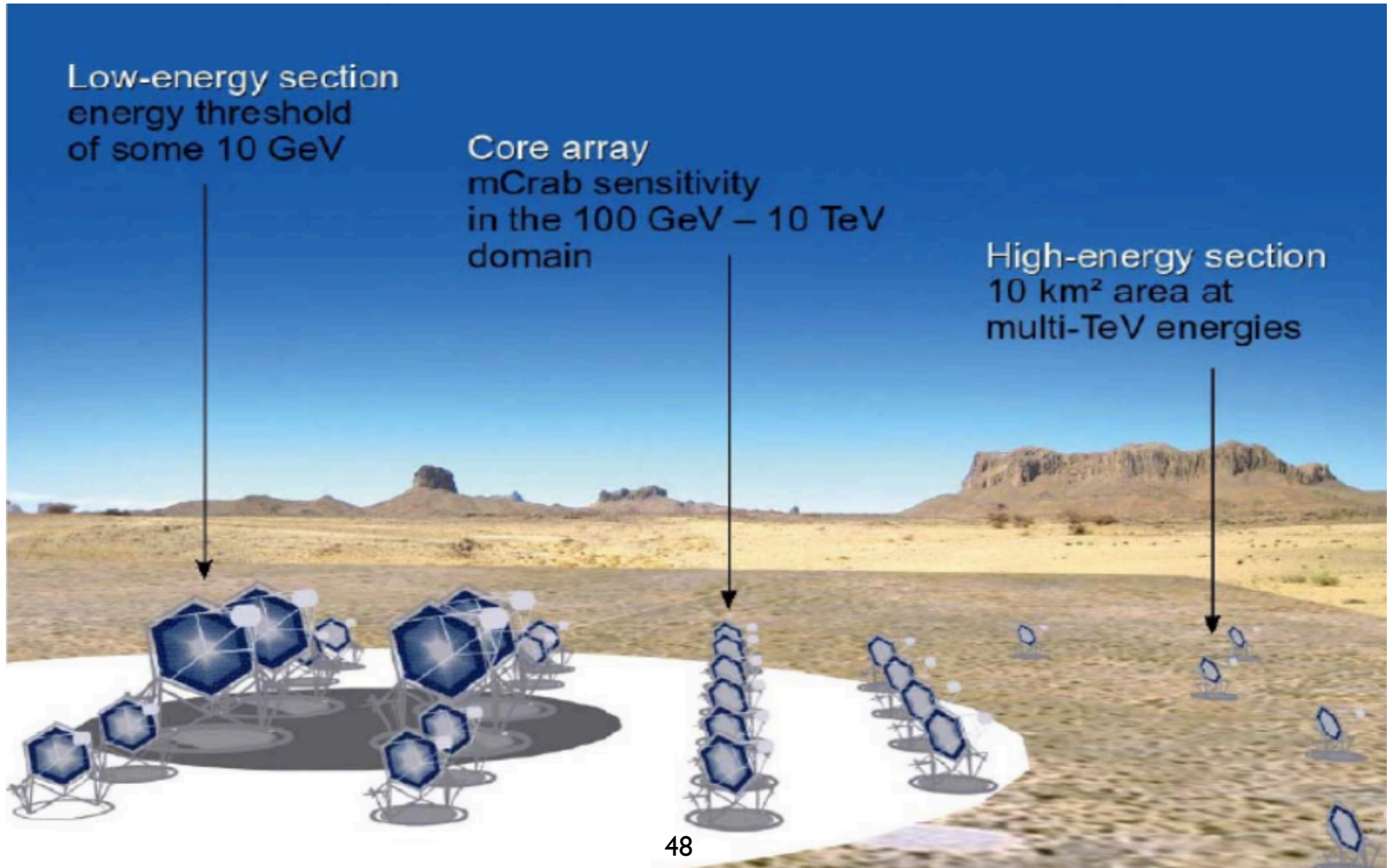
$$f_{\text{PAH}} = 0.219^{+0.050}_{-0.046} \quad f_{\text{SG}} = 0.35^{+0.28}_{-0.25} \quad f_{\text{LG}} = 0.42^{+0.25}_{-0.27}$$



The CTA extragalactic survey

The CTA concept

- improve sensitivity by one order of magnitude
- increase energy range (10 GeV to 100 TeV)
- larger FoV
- improve angular resolution
- flexibility in operation
- full sky coverage (one observatory in each hemisphere)



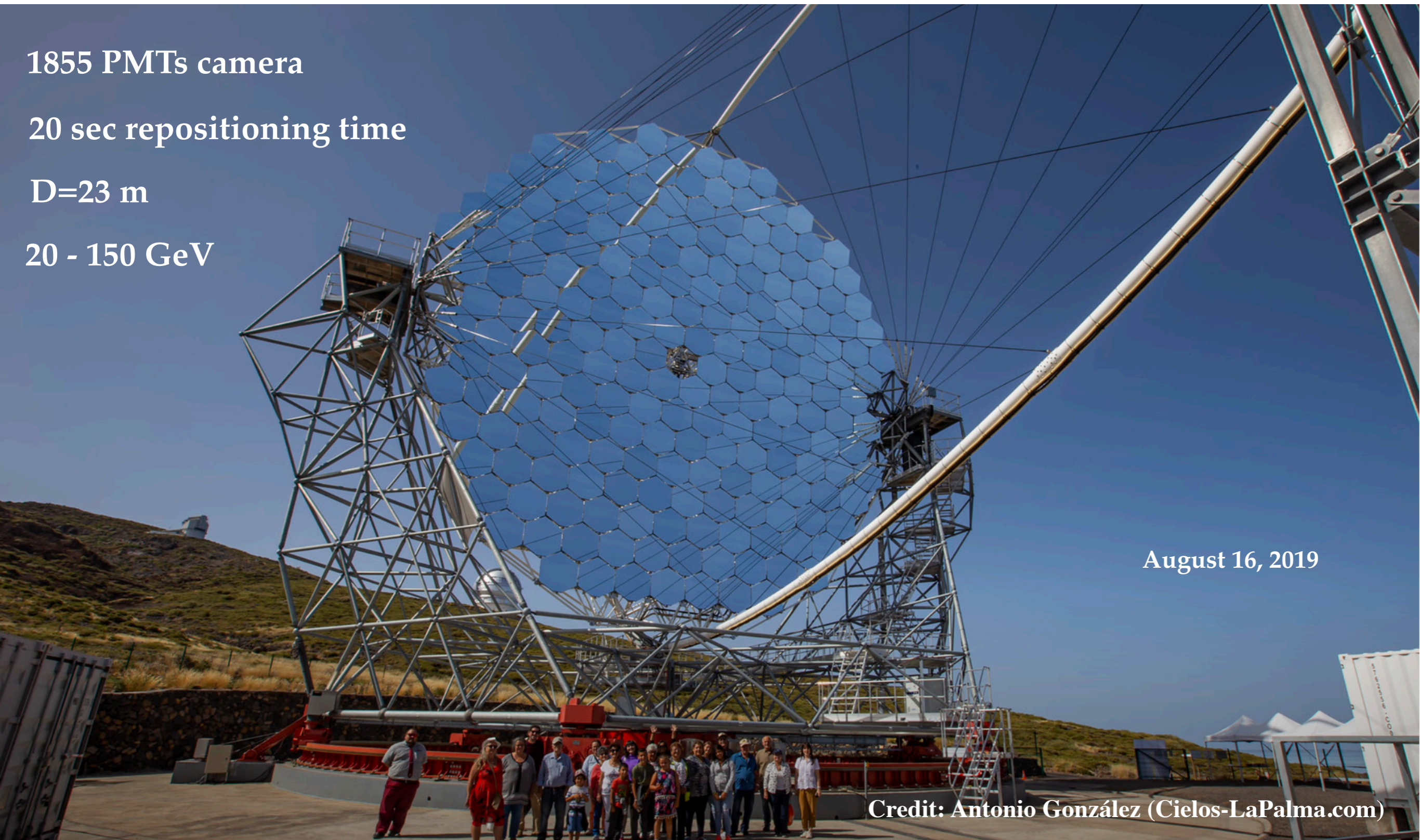
LST (Large Size Telescope)

1855 PMTs camera

20 sec repositioning time

$D=23$ m

20 - 150 GeV

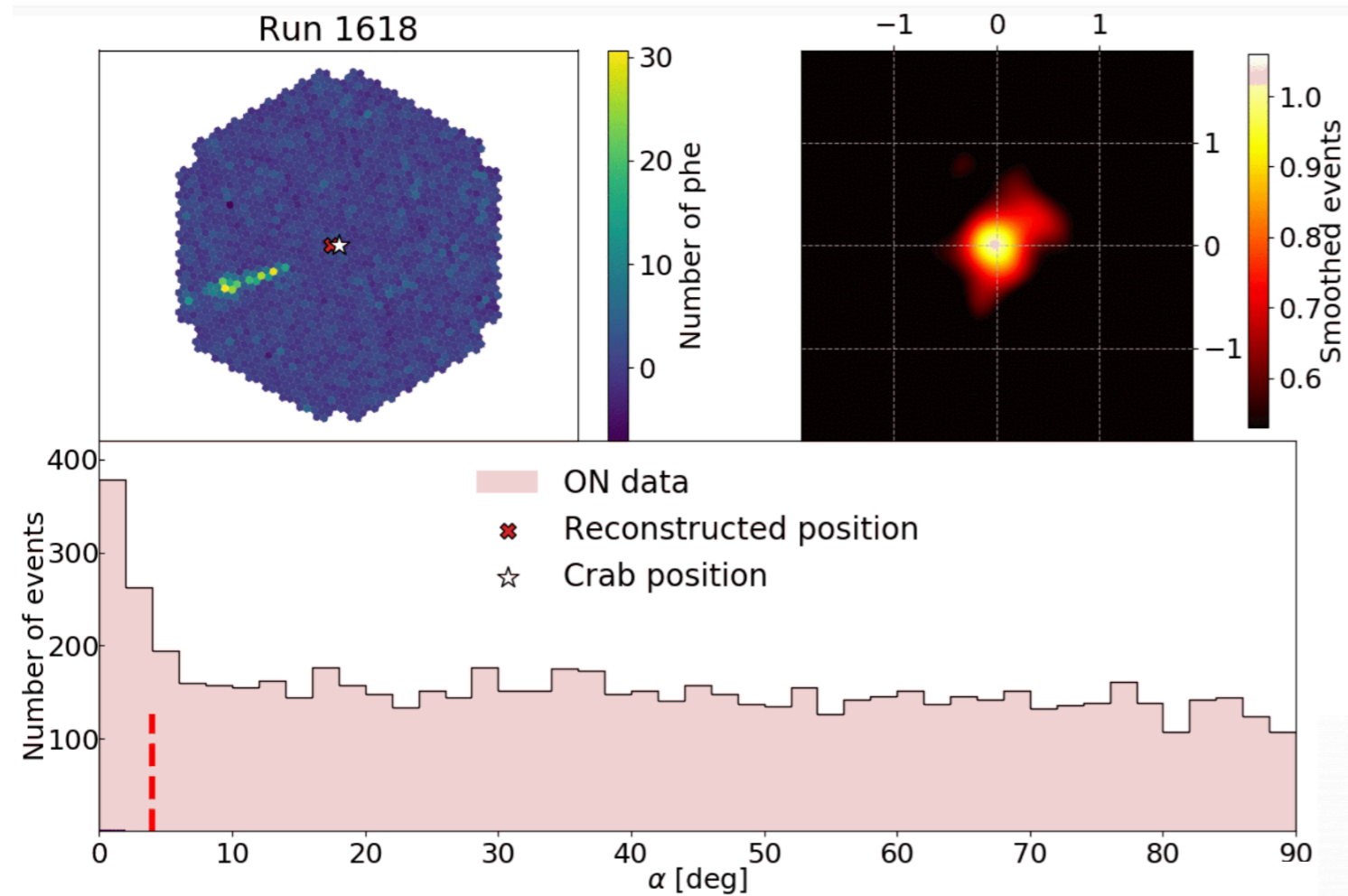


August 16, 2019

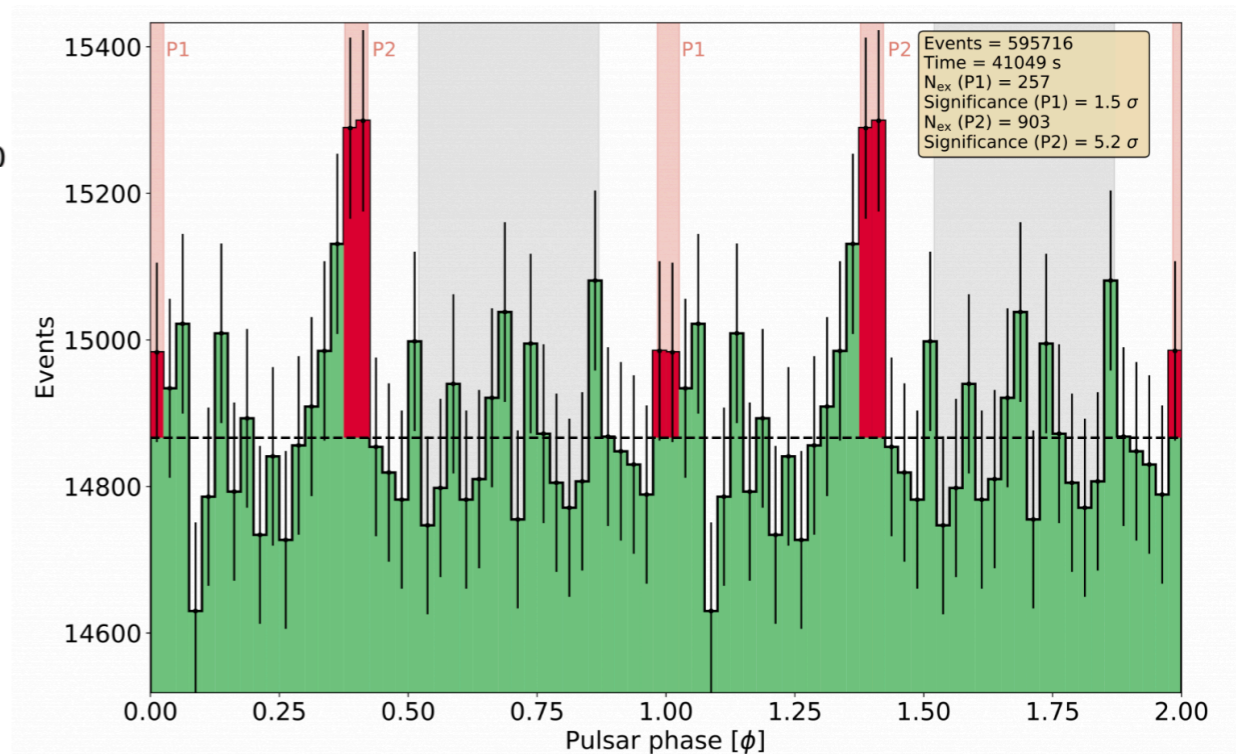
Credit: Antonio González (Cielos-LaPalma.com)

LST-1 first results

December 23, 2019 (269 min)



Jan. and Feb. 2020 campaign



- Detection of the **Crab Nebula** and the **Crab pulsar**

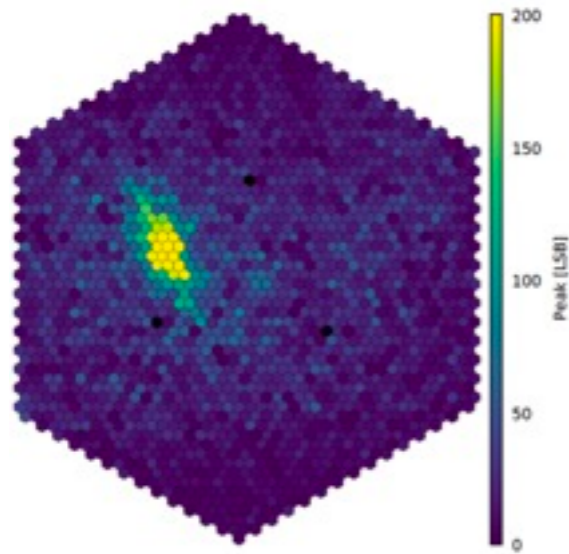
LST: Brazil, Bulgaria, Croatia, France, Germany, India, Italy, Japan, Poland, Spain and Switzerland

Credit: LST Collaboration

MST (Medium Size Telescope)

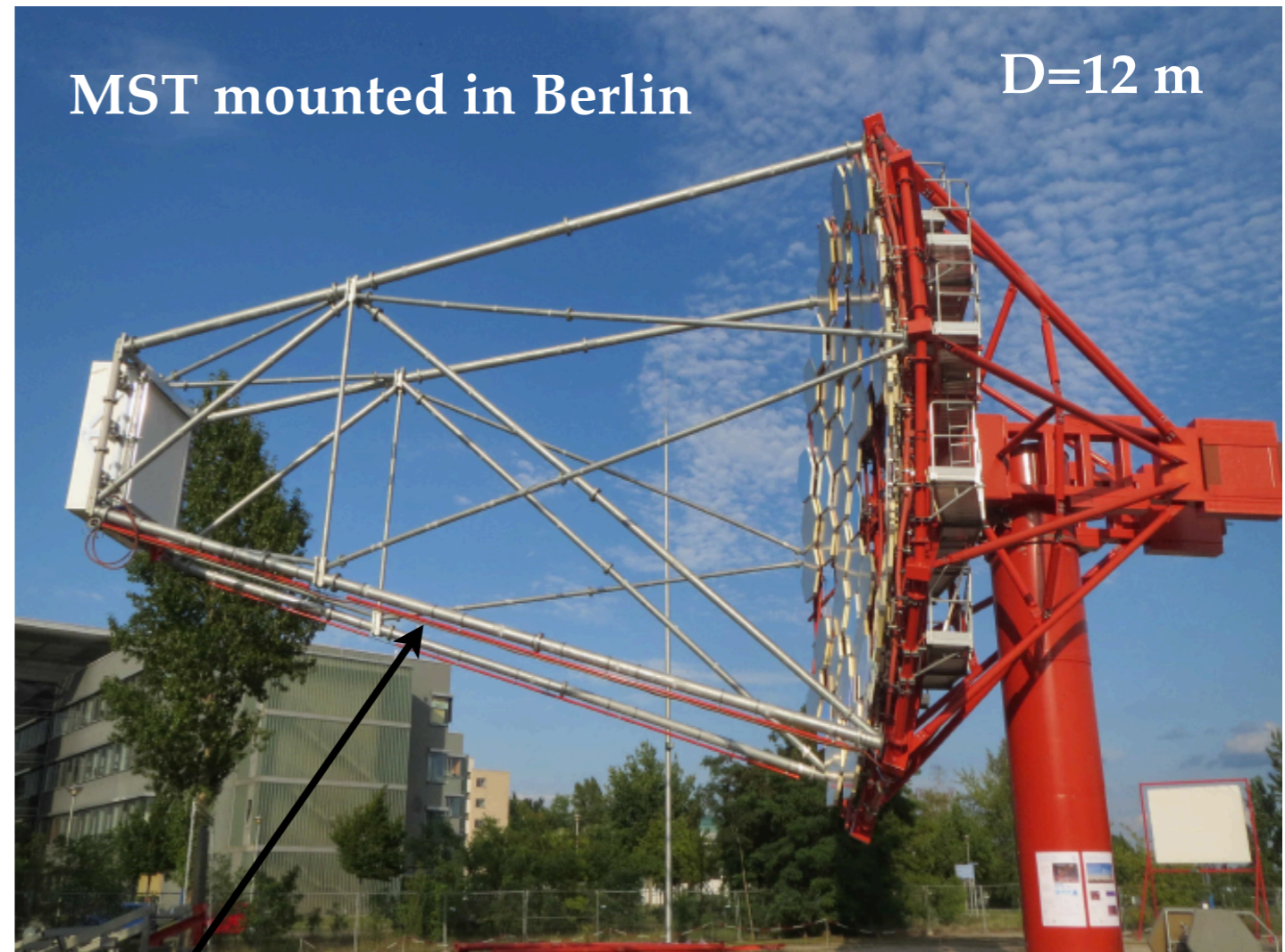
“CTA’s workhorses”

150 GeV - 5 TeV



First FlashCam
light on Sept. 2017

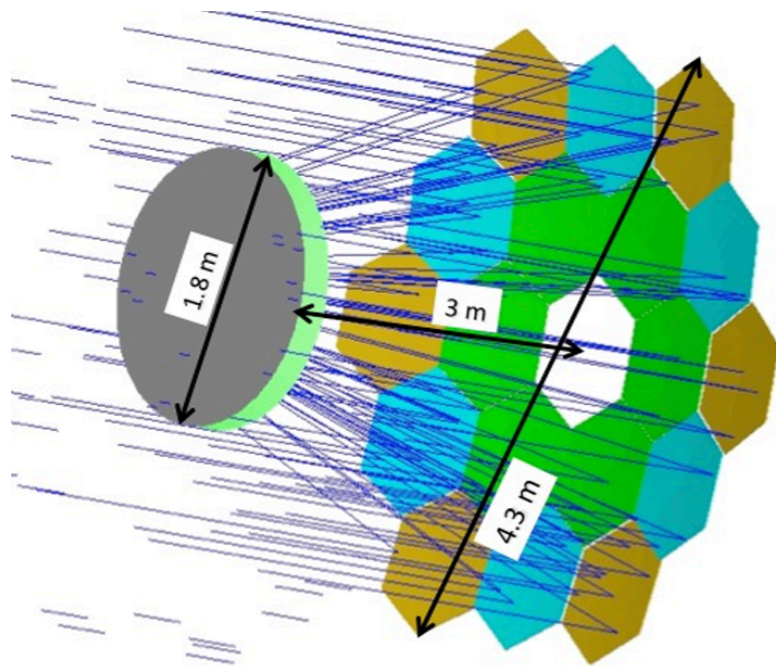
- Brazil (structure)
- Germany (mirror / structure / camera)
- France (mirror)
- Italy (mirror)
- Poland (mirror)
- Swiss (camera)



Camera Structure Support (CSS) developed at USP-São Carlos together with the Brazilian company Orbital Engenharia (São José dos Campos)

ASTRI SST (Small Size Telescope)

- Schwarzschild-Couder (dual mirror) design
- Fast SiPM based camera
- Primary segmented mirror $D=4.3$ m
- Secondary monolithic mirror $d=1.8$ m
- Prototype installed Serra La Nave (Etna volcano surroundings)



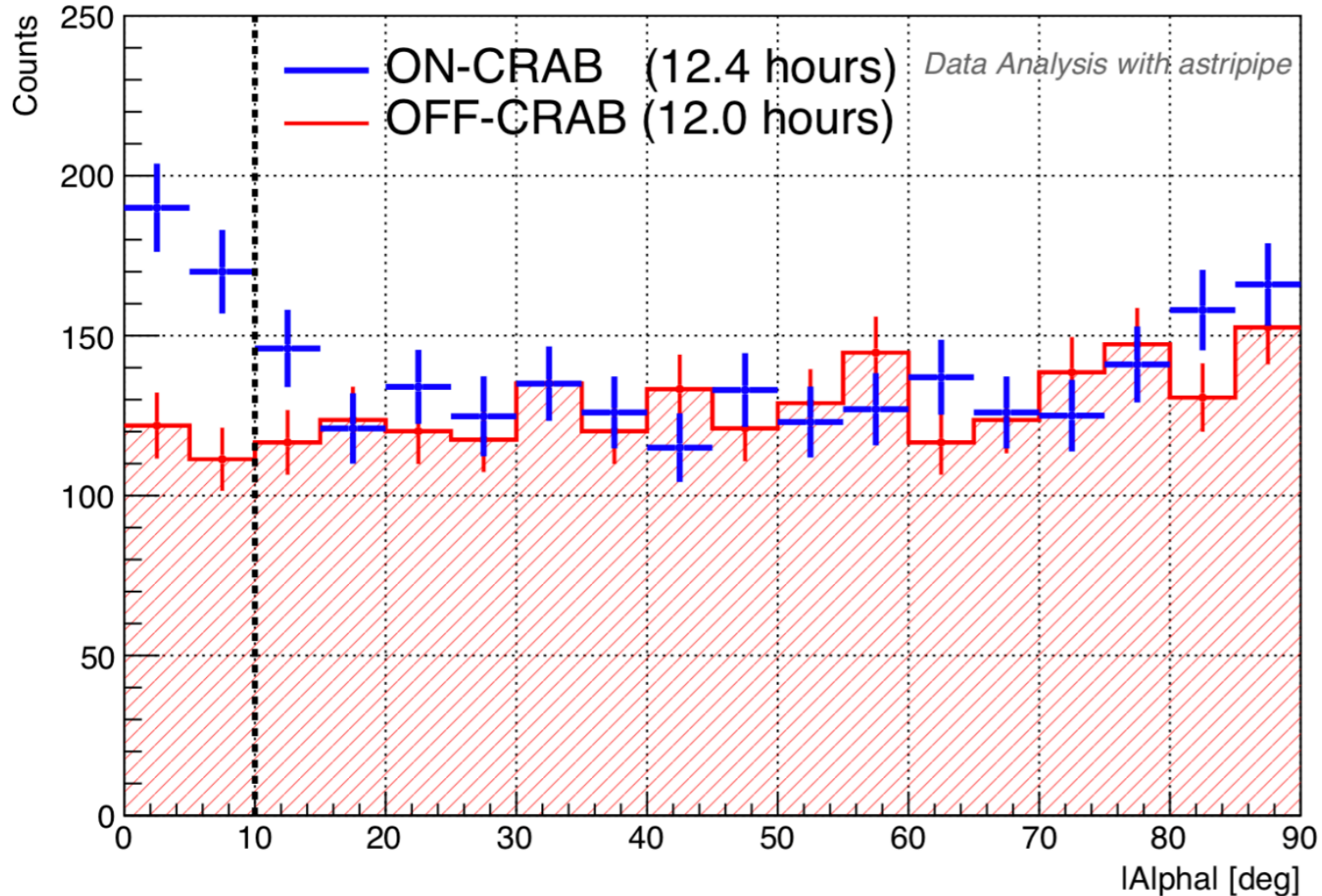
INAF / Italian Universities

IAG-USP / FAPESP

North West University of South Africa

ASTRI-HORN first results

ASTRI SST-2M prototype, December 2018



A&A 634, A22 (2020)
<https://doi.org/10.1051/0004-6361/201936791>
 © ESO 2020

**Astronomy
&
Astrophysics**

First detection of the Crab Nebula at TeV energies with a Cherenkov telescope in a dual-mirror Schwarzschild-Couder configuration: the ASTRI-Horn telescope

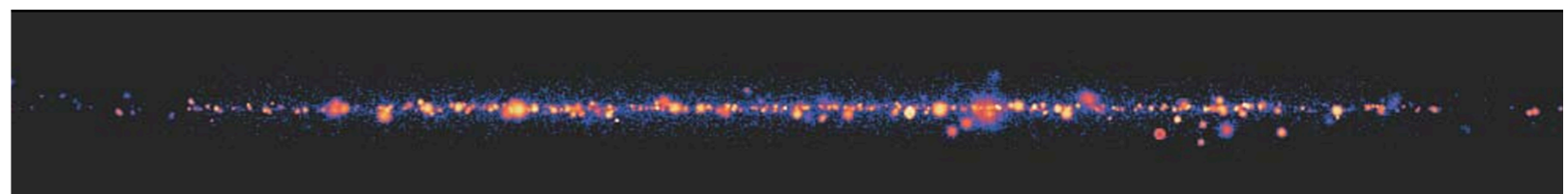
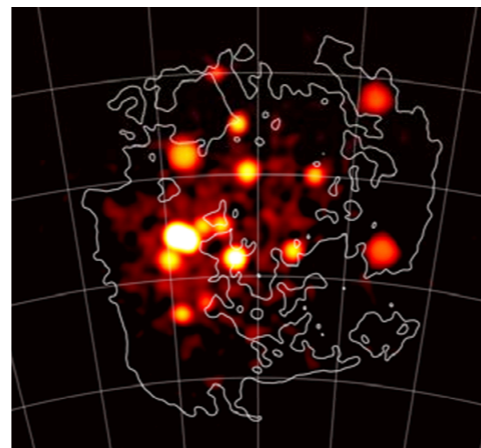
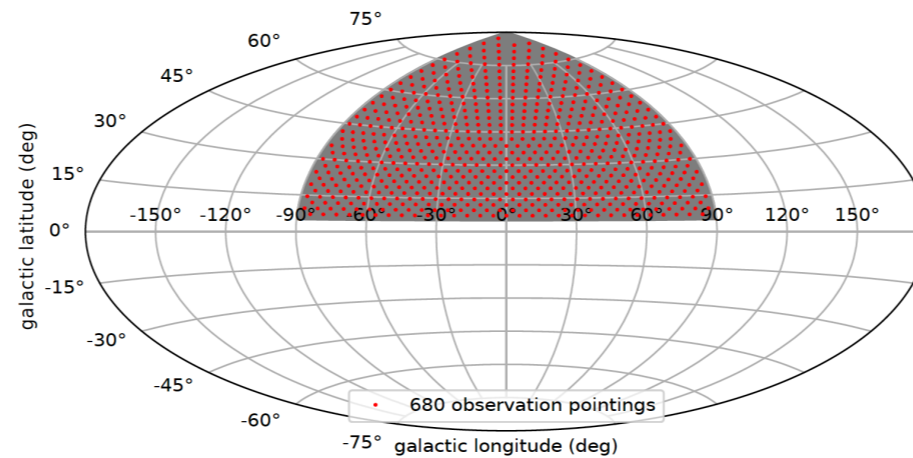
S. Lombardi^{1,2,*}, O. Catalano^{3,*}, S. Scuderi^{4,*}, L. A. Antonelli^{1,2}, G. Pareschi⁵, E. Antolini⁶, L. Arrabito⁷, G. Bellasai⁸, K. Bernlöhr⁹, C. Bigongiari¹, B. Biondo³, G. Bonanno⁸, G. Bonnoli⁵, G. M. Böttcher¹⁰, J. Bregeon¹¹, P. Bruno⁸, R. Canestrari³, M. Capalbi³, P. Caraveo⁴, P. Conconi⁵, V. Conforti¹², G. Contino³, G. Cusumano³, E. M. de Gouveia Dal Pino¹³, A. Distefano⁴, G. Farisato¹⁴, C. Fermino¹³, M. Fiorini⁴, A. Frigo¹⁴, S. Gallozzi¹, C. Gargano³, S. Garozzo⁸, F. Gianotti¹², S. Giarrusso³, R. Gimenes¹³, E. Giro¹⁴, A. Grillo⁸, D. Impiombato³, S. Incorvaia⁴, N. La Palombara⁴, V. La Parola³, G. La Rosa³, G. Leto⁸, F. Lucarelli^{1,2}, M. C. Maccarone³, D. Marano⁸, E. Martinetti⁸, A. Miccichè⁸, R. Millul⁵, T. Mineo³, G. Nicotra¹⁵, G. Occhipinti⁸, I. Pagano⁸, M. Perri^{1,2}, G. Romeo⁸, F. Russo³, F. Russo¹², B. Sacco³, P. Sangiorgi³, F. G. Saturni¹, A. Segreto³, G. Sironi⁵, G. Sottile³, A. Stammera¹, L. Stringhetti⁴, G. Tagliaferri⁵, M. Tavani¹⁶, V. Testa¹, M. C. Timpanaro⁸, G. Toso⁴, G. Tosti¹⁷, M. Trifoglio¹², G. Umamã⁸, S. Vercellone⁵, R. Zanmar Sanchez⁸, C. Arcaro¹⁴, A. Bulgarelli¹², M. Cardillo¹⁶, E. Cascone¹⁸, A. Costa⁸, A. D'Ài³, F. D'Ammando¹², M. Del Santo³, V. Fioretti¹², A. Lamastra¹, S. Mereghetti⁴, F. Pintore⁴, G. Rodeghiero¹⁴, P. Romano⁵, J. Schwarz⁵, E. Sciacca⁸, F. R. Vitello⁸, and A. Wolter⁵

Crab Nebula detected at 5.4 sigma significance

Science with the CTA

<https://arxiv.org/abs/1709.07997>

- Dark matter program
- Galaxy clusters
- Active Galactic Nuclei
- Extragalactic survey
- Star forming systems
- Transients
- LMC survey
- Galactic plane survey
- PeVatrons
- Galactic center
- Fundamental Physics (LIV)



Forecasts for the CTA x-gal survey

- **Intrinsic spectrum parameterization: power-law**
- **Sources with redshifts, luminosities and spectral indices drawn from the Ajello's AGN luminosity function and extrapolated to the TeV range**
- **Observations following the extragalactic survey of the CTA KSP**
- **IRFs from prod3b-v1 (omega) and prod5 (alpha)**
- **Cosmic ray background rate after gamma/hadron separation cuts**
- **Detections threshold: $TS > 25$ for a power-law spectrum**

OMEGA CONFIGURATION (118 telescopes)

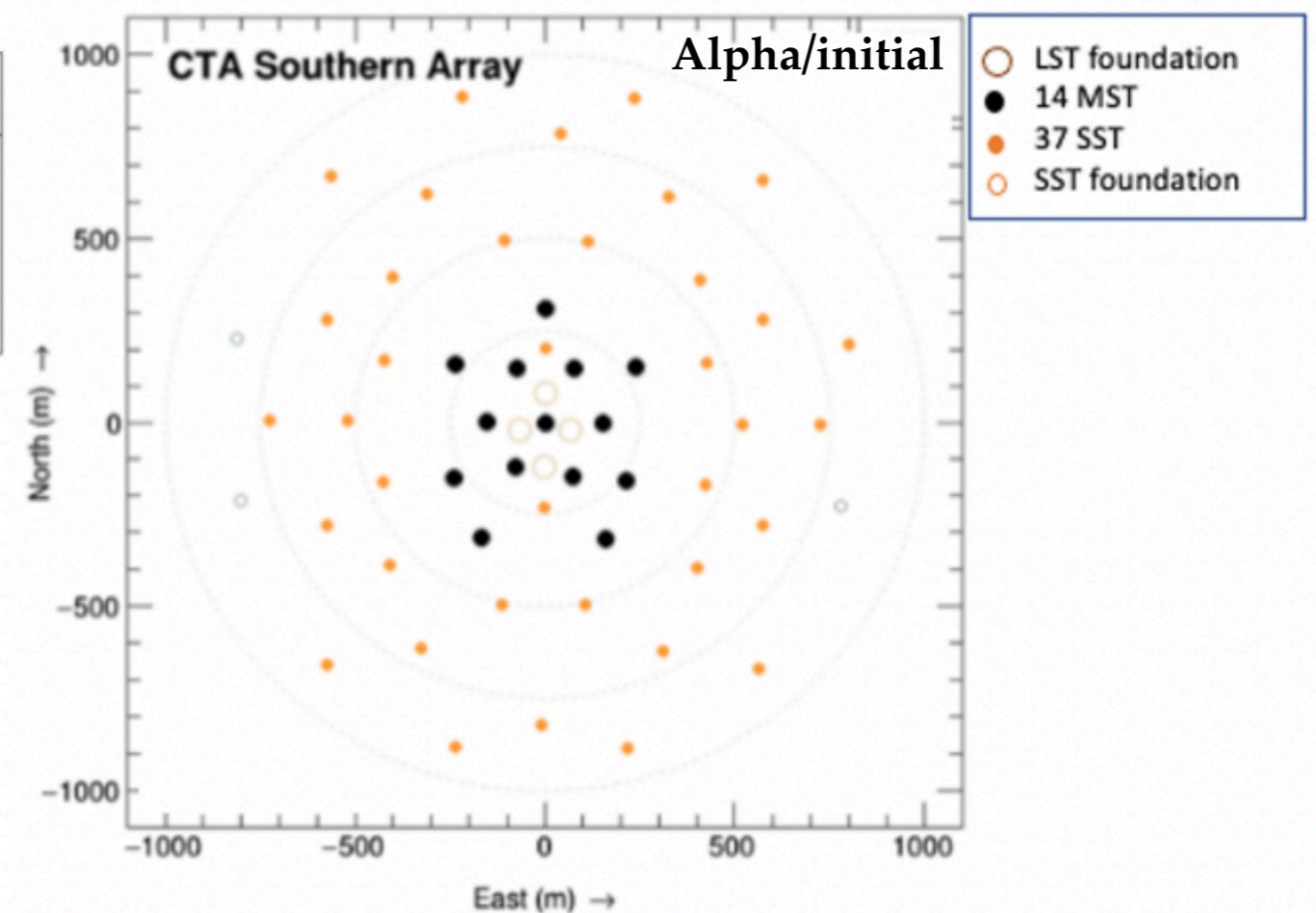
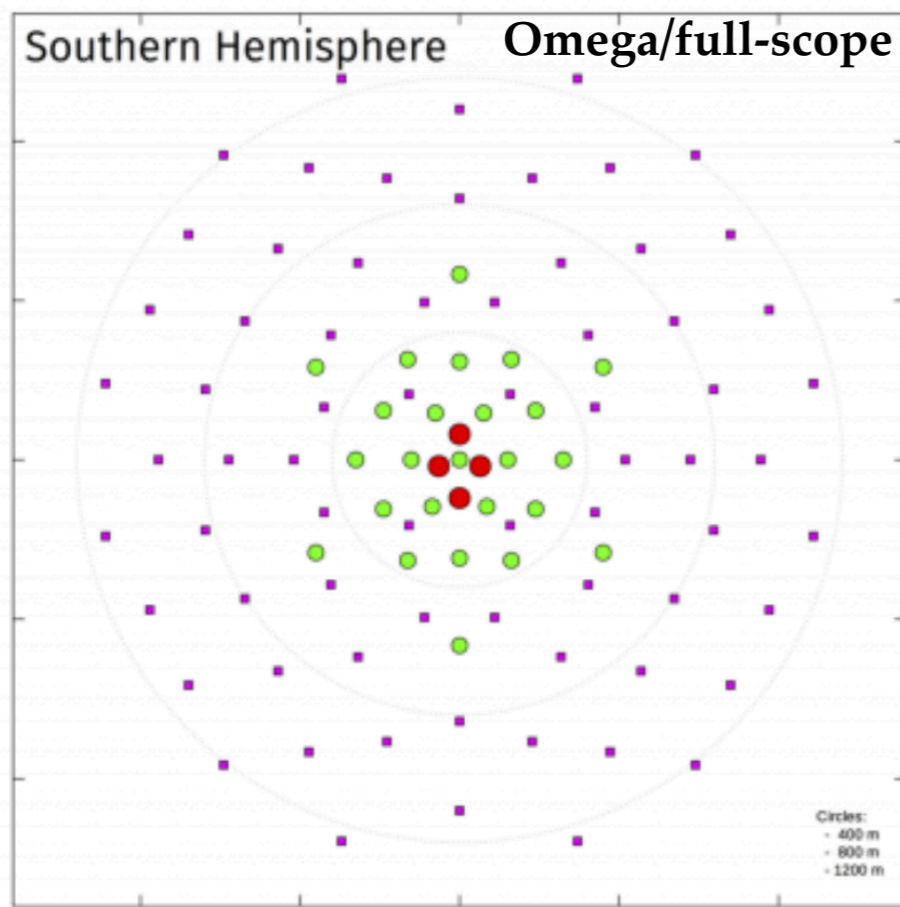
Southern Hemisphere: 4 LSTs, 25 MSTs, 70 SSTs (covered area: $\sim 4 \text{ km}^2$)

Northern Hemisphere: 4 LSTs, 15 MSTs (covered area: $\sim 0.6 \text{ km}^2$)

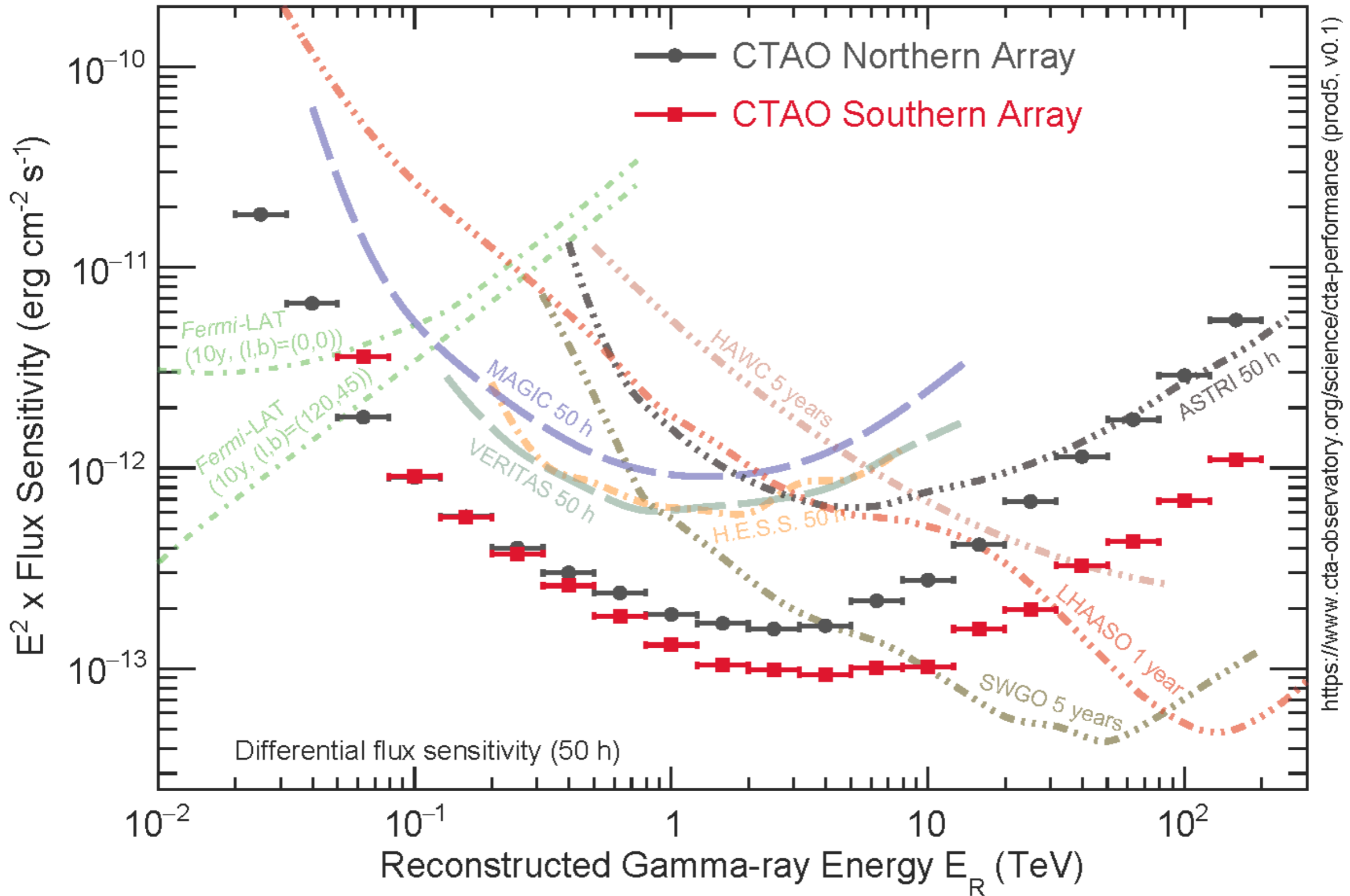
ALPHA CONFIGURATION (64 telescopes)

Southern Hemisphere: 14 MSTs, 37 SSTs (covered area: $\sim 3 \text{ km}^2$) (150 GeV - 300 TeV)

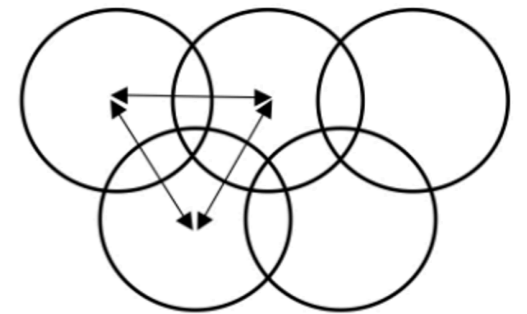
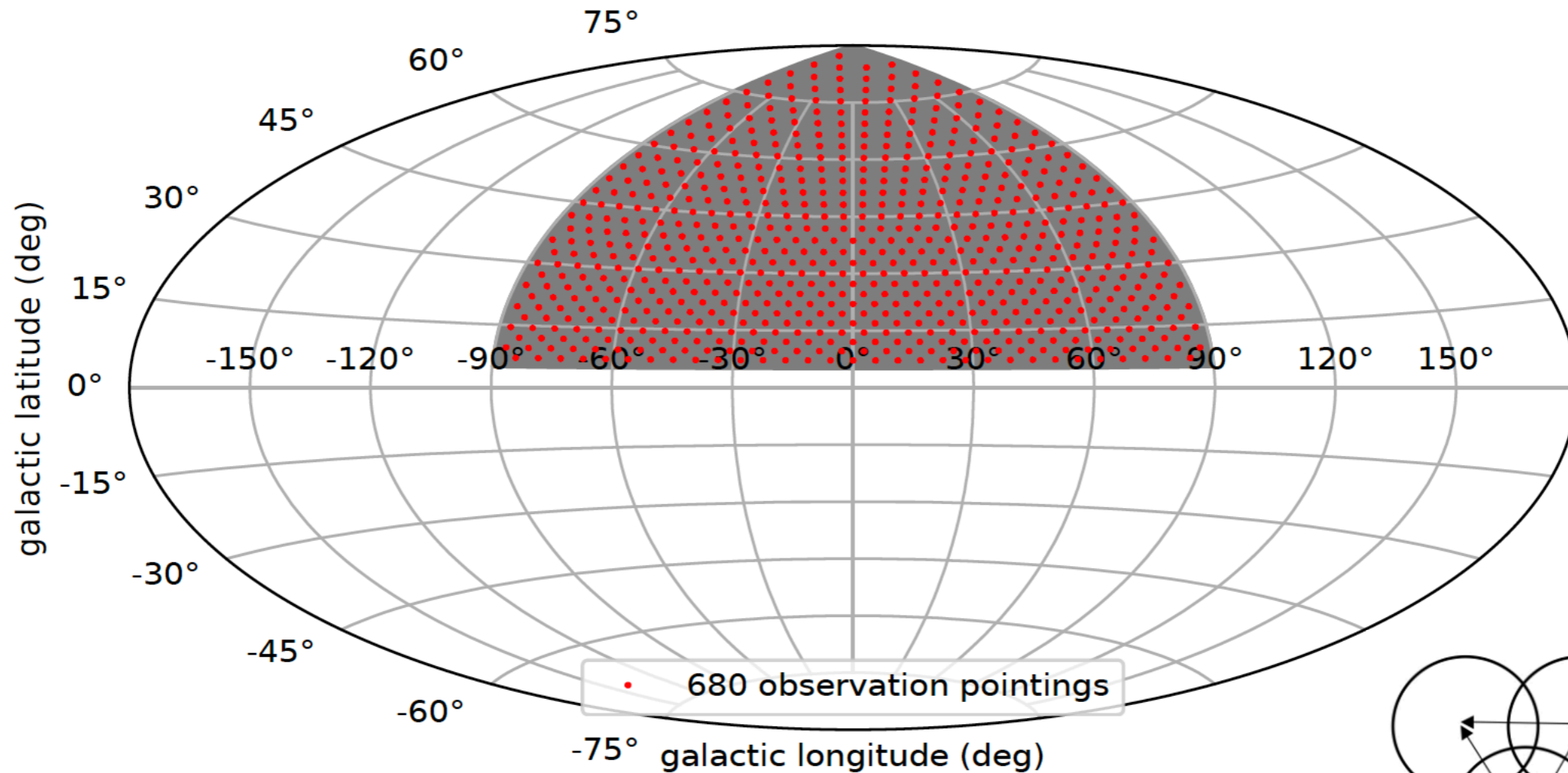
Northern Hemisphere: 4 LSTs, 9 MSTs (covered area: $\sim 0.25 \text{ km}^2$) (20 GeV - 5 TeV)



Alpha configuration sensitivity



EGAL survey observation strategy



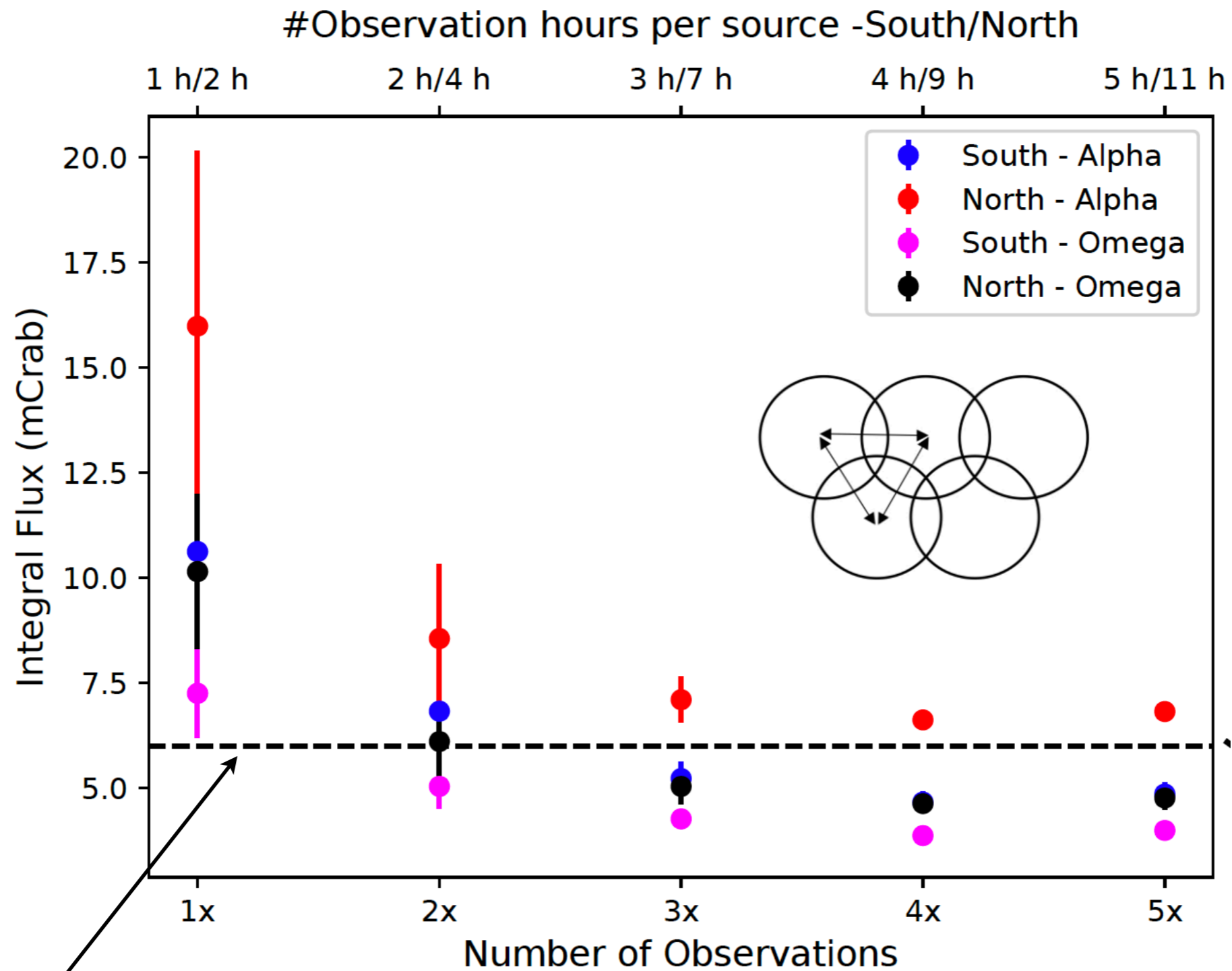
- One of the Key Science Projects (KSP)
- 25% of the sky ($B > 5 \text{ deg}$ $-90 < L < 90$)
- 1000 hours of observations ($\sim 400 \text{ h}$ [S] + $\sim 600 \text{ h}$ [N])



2.21 h / pointing [N]

0.98 h / pointing [S]

EGAL survey sensitivity (alpha)

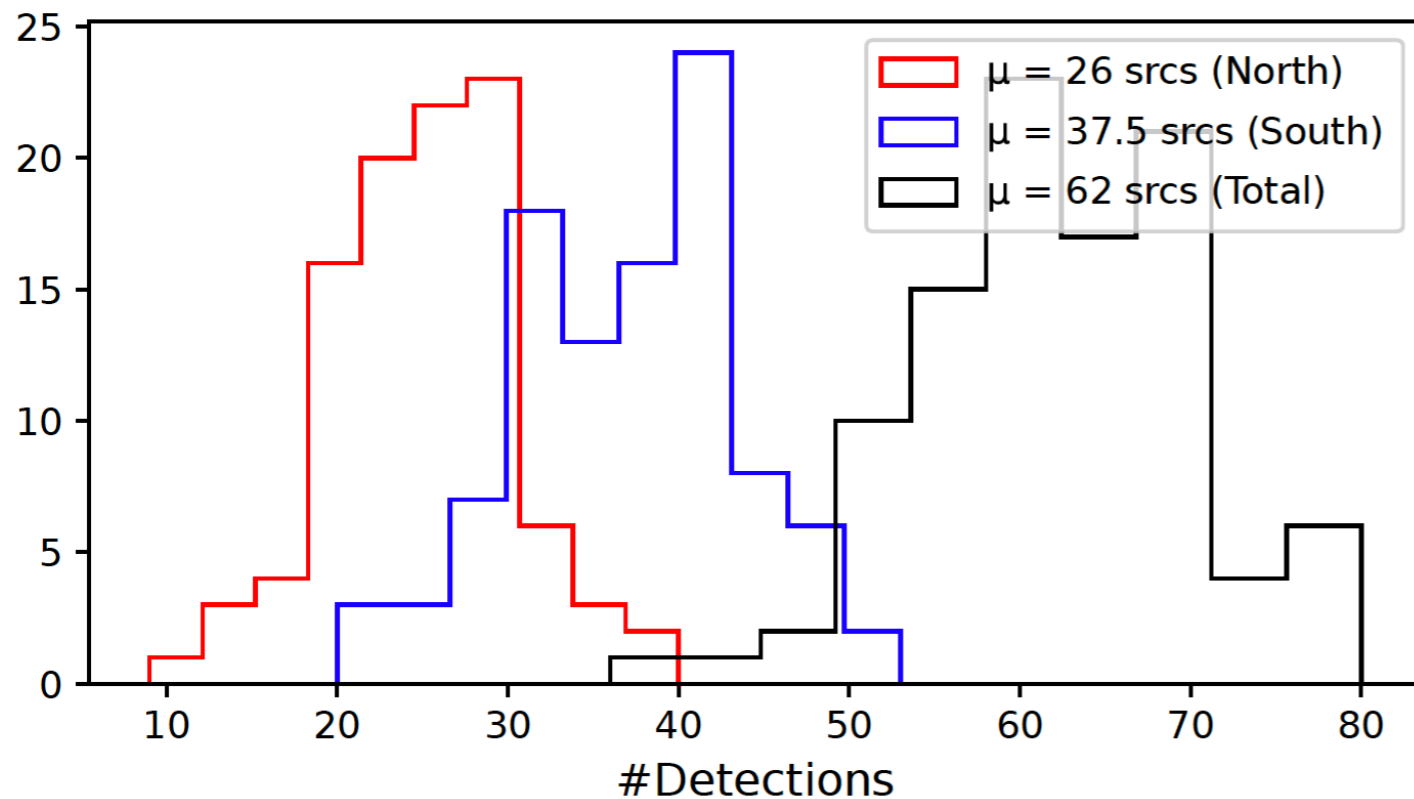
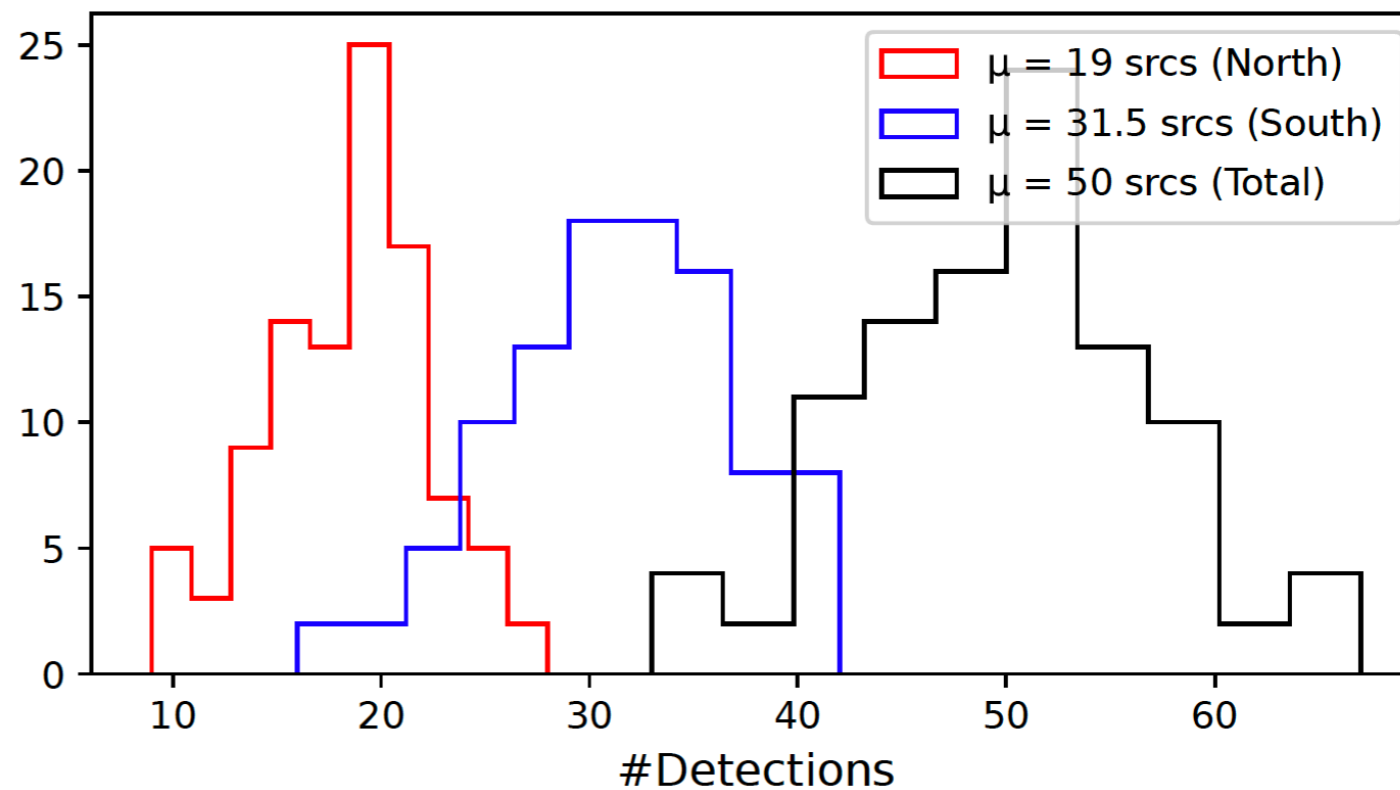
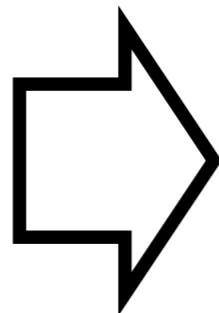


Target sensitivity

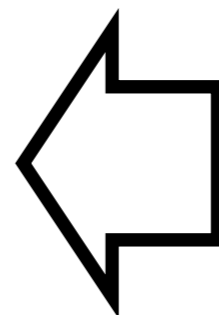
Expected number of new detections

PRELIMINARY

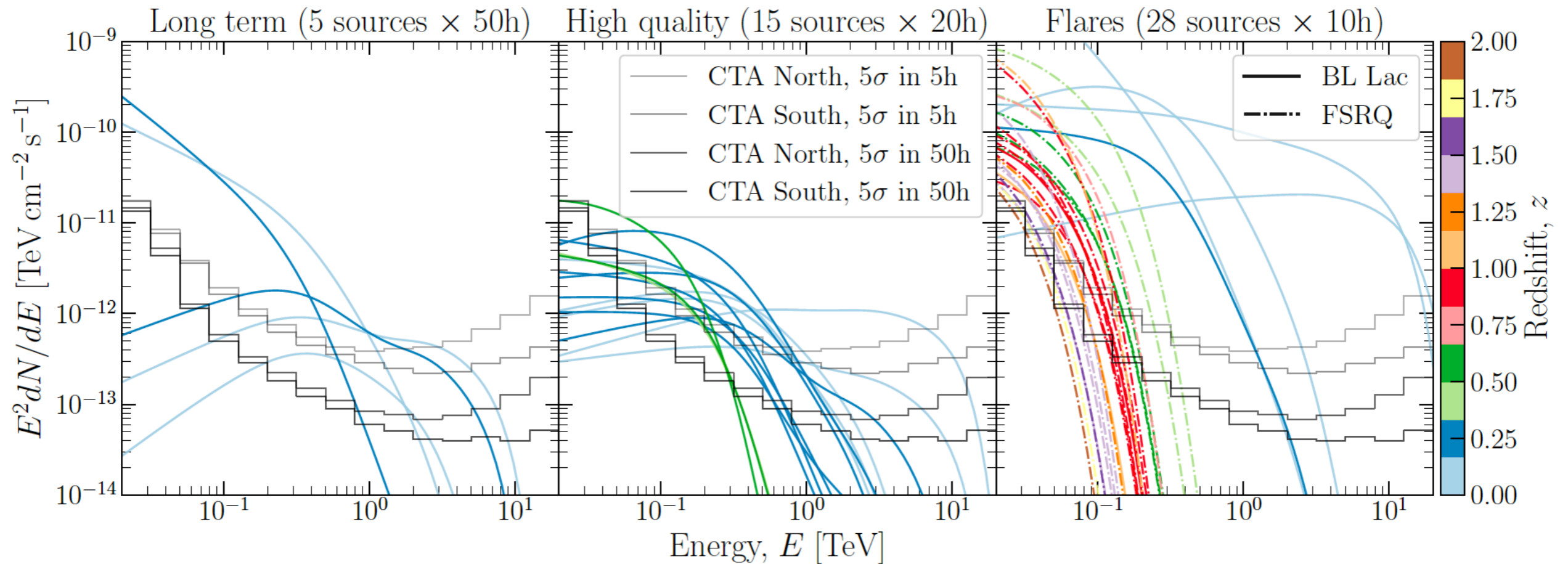
ALPHA



OMEGA

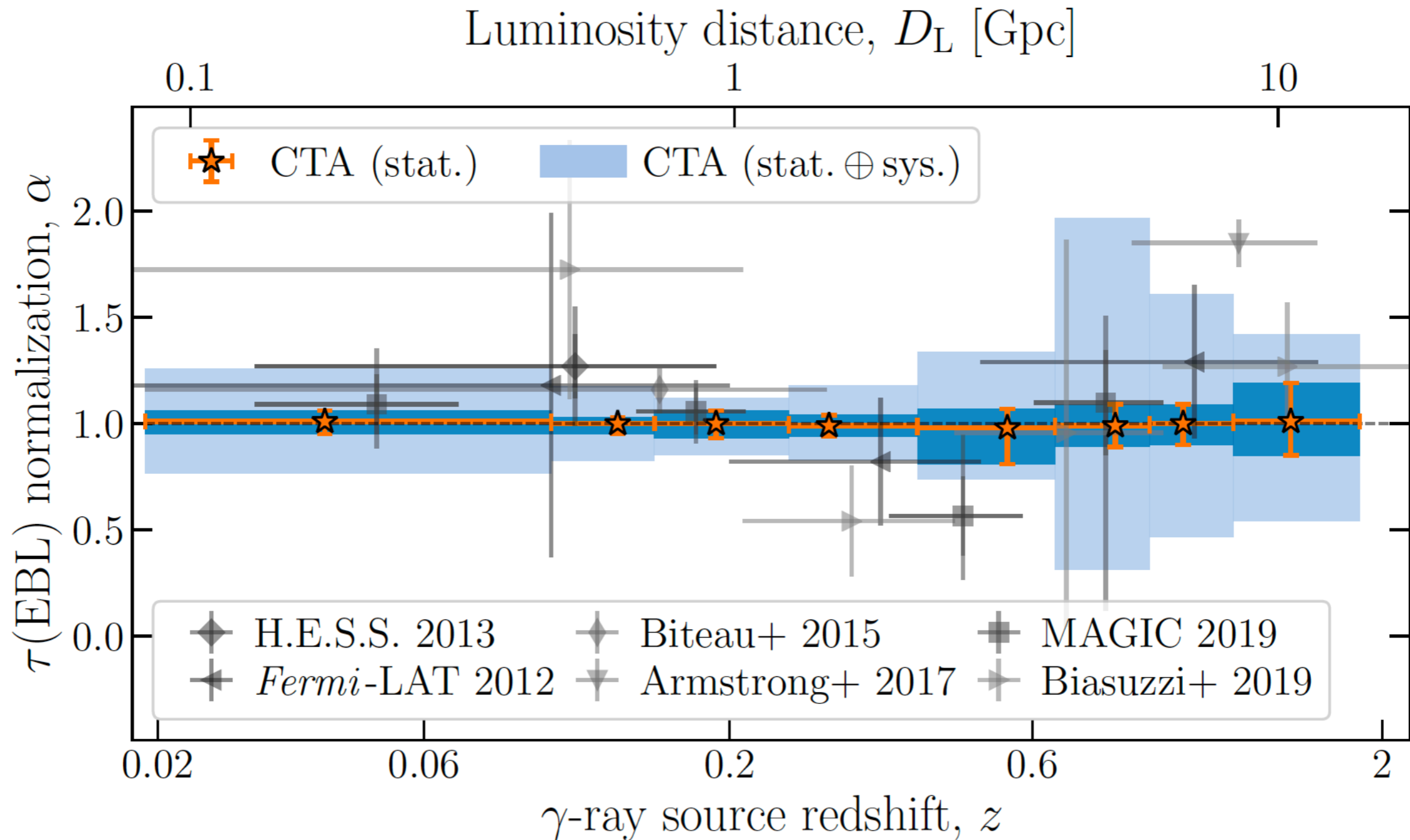


Constraining EBL with CTA

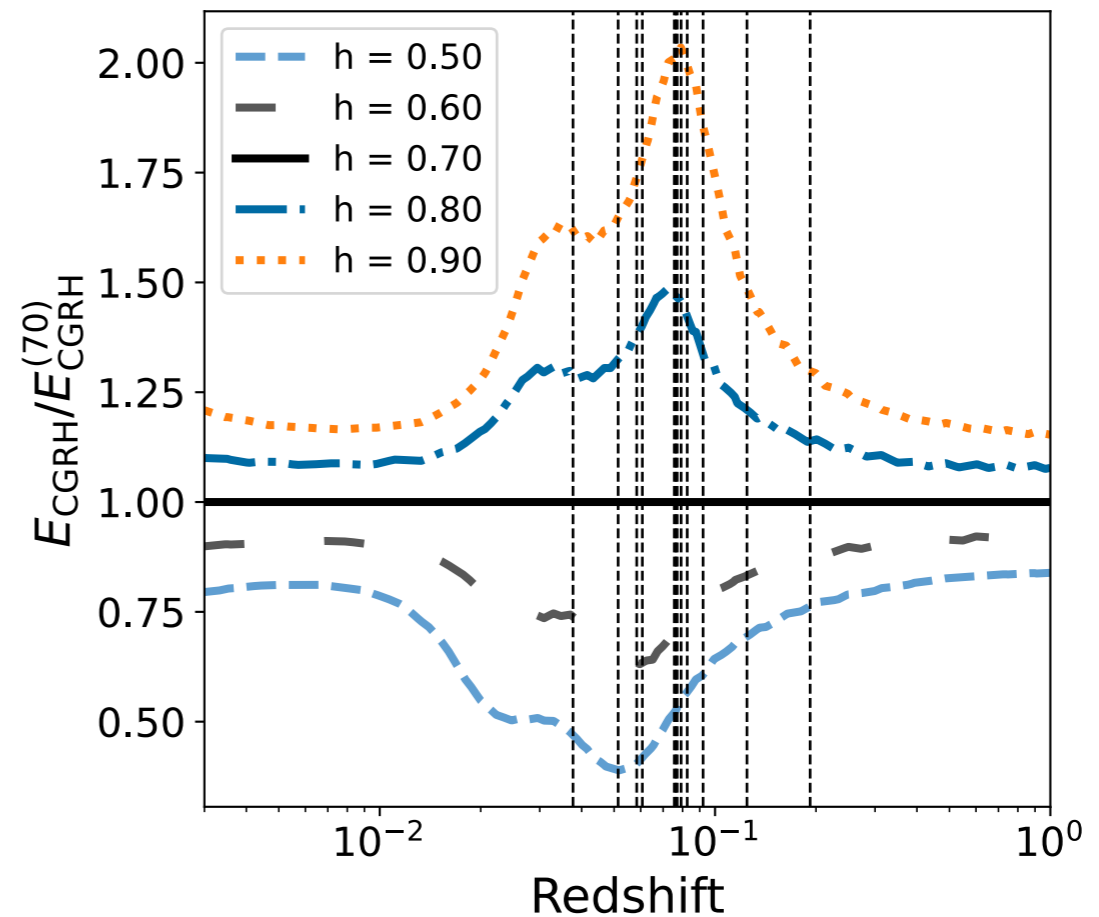
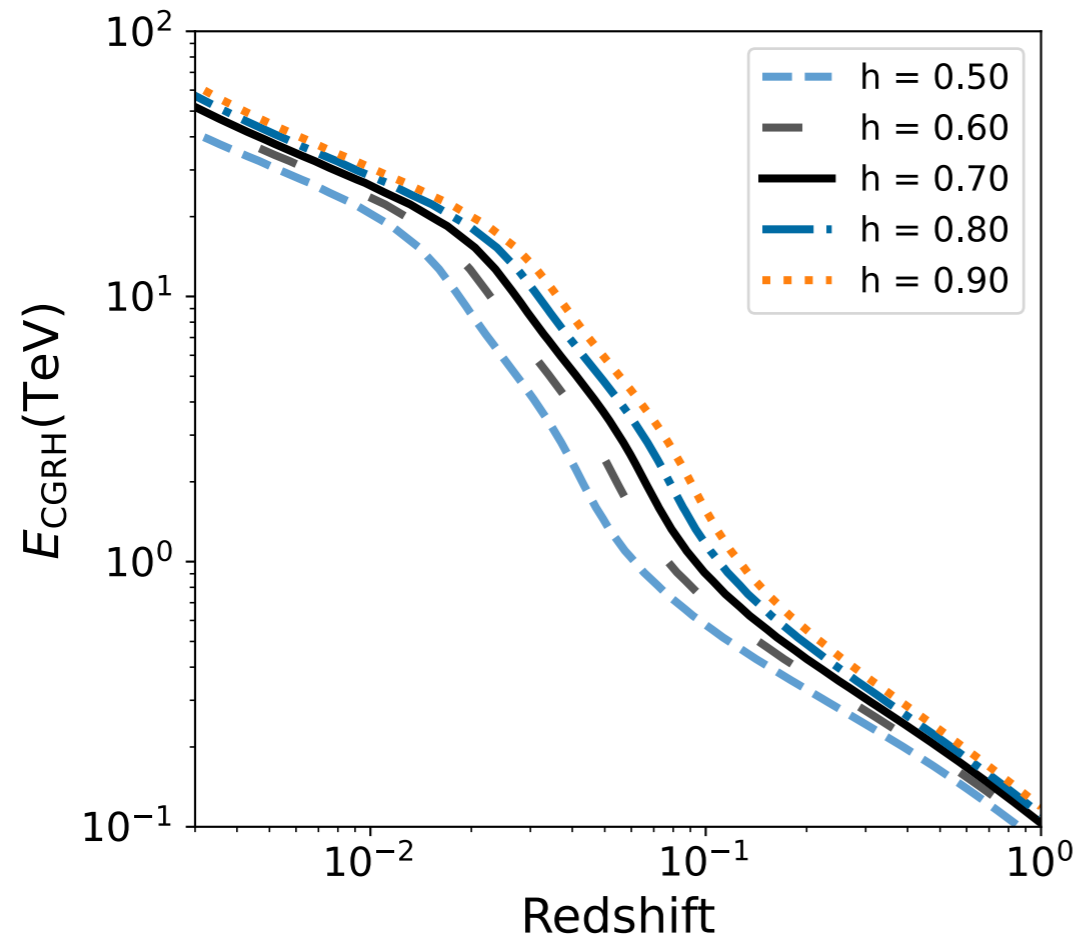


- $\text{TS} > 25$ for $E(\tau=1)$
- Class dependent intrinsic cutoff at comoving energies: $E_{\text{cut}} = 100 \text{ GeV}$ (LSP/ISP), $E_{\text{cut}} = 1 \text{ TeV}$ (HSP), and $E_{\text{cut}} = 10 \text{ TeV}$ (EHSP).
- Only sources with well determined redshift (spectral lines, $\text{Ly}\alpha$)

Constraining EBL with CTA



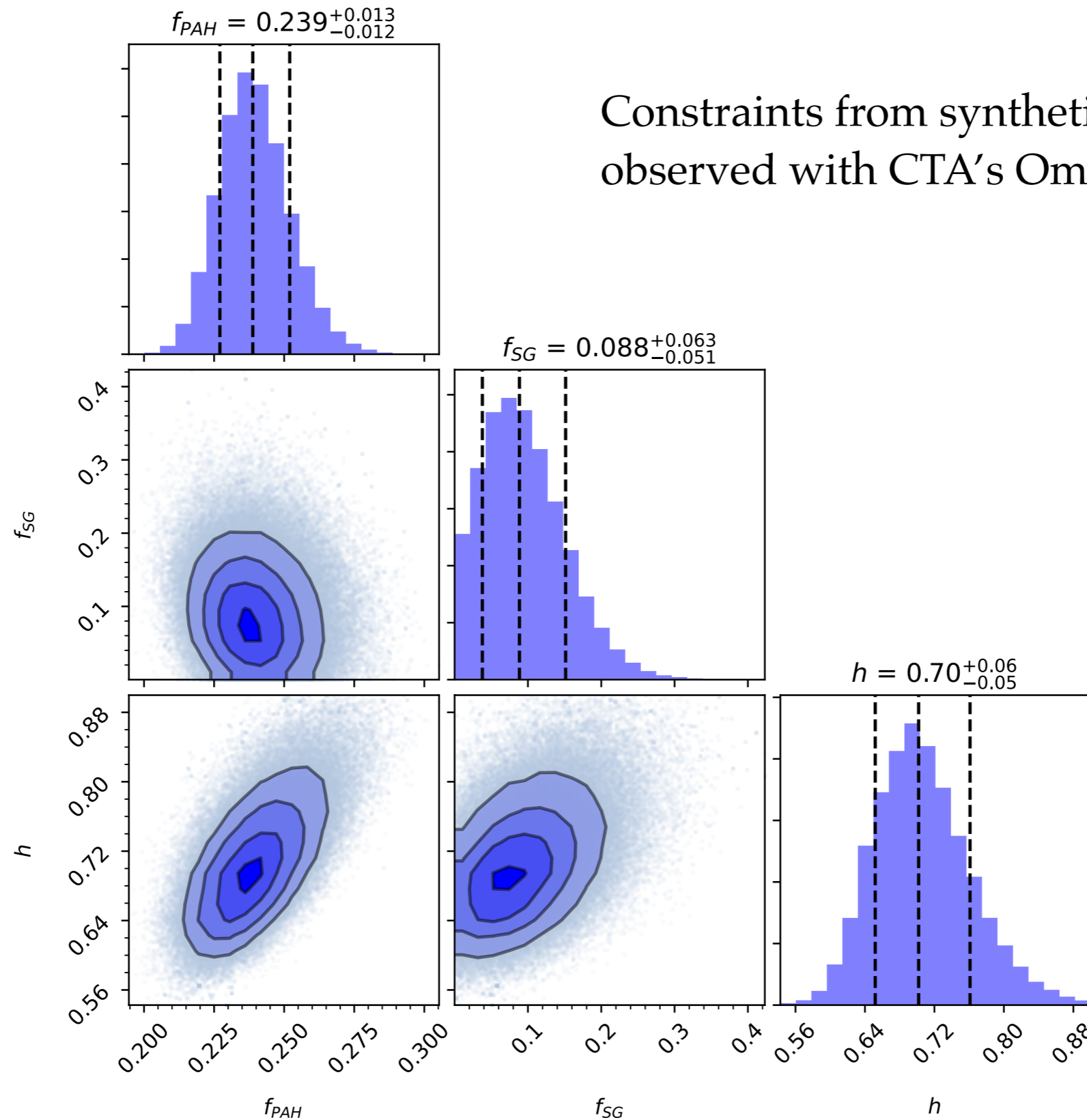
Sensitivity to the Hubble constant



2 competing effects:

- Change in the star light emissivity (positive correlation with H_0)
- Change in dt/dz (negative correlation)

Sensitivity to the Hubble constant



Thank you for the
attention!